The Potential of Internal Combustion Engines Using Methanol as Fuel in the Energy Transition

Prins, D.M.

Award date:
2021

The Potential of Internal Combustion Engines Using Methanol as Fuel in the Energy Transition

Master Thesis Report

Master:	Innovation Sciences, Sustainable Energy Technology
Department:	Industrial Engineering & Innovation sciences, Mechanical Engineering
Research group:	Technology, Innovation & Society, Power & Flow

Student:	D.M. Prins
Identity number:	0899754
Thesis supervisors:	Prof. Dr. F. Alkemade, Dr. Ir. L.M.T. Somers
Company Supervisor:	Michel Voorwinde

Examination committee:

SET	IS
Dr. Ir. L.M.T. Somers	Prof. Dr. F Alkemade
Dr. Ir. N.C.J. Maes	Dr. E.M. Mas Tur
Dr. Ir. F.C.A. Veraart	Dr. Ir. L.M.T. Somers

Date: 04-08-2021

TU/e EINDHOVEN UNIVERSITY OF TECHNOLOGY

Declaration concerning the TU/e Code of Scientific Conduct for the Master's thesis

I have read the TU/e Code of Scientific Conduct[I].

I hereby declare that my Master's thesis has been carried out in accordance with the rules of the TU/e Code of Scientific Conduct

Date 8/4/21

Name Dylan Martin Prins

ID-number 0899754

Signature 

Insert this document in your Master Thesis report (2nd page) and submit it on Sharepoint

[I] See: http://www.tue.nl/en/university/about-the-university/integrity/scientific-integrity/
The Netherlands Code of Conduct for Academic Practice of the VSNU can be found here also.
More information about scientific integrity is published on the websites of TU/e and VSNU

Version 202007

Abstract

The transport sector plays a major role in the energy transition and accounts for 21% of the worldwide energy use. It is responsible for a large part of the GHG and pollutant emissions. A lot of attention is paid to electrification, but this is not a short term option for all heavy duty applications due to its low energy density. Sustainable methanol may provide a solution for these challenging applications. Methanol can be produced sustainably from a variety sources and it could be used in the current engine pool and infrastructure after relatively minor modifications.

To find out which applications cannot be electrified, and require a fuel like methanol, a comparison is made of the performance of electric pilot cases to diesel, methanol and LNG and calculations are performed to compare the energy storage size and weight. The analysis shows that a large share of the road transport can be electrified with the exception of long haul heavy duty trucks. For the agriculture sector it is only possible to electrify small tractors and in the inland shipping electrification is limited to short distance point-to-point shipping for the foreseeable future. All other application will require a higher energy density fuel like methanol.

Methanol is a high octane fuel and the easiest engine retrofit solution is to add methanol through port fuel injection and ignite it with a direct injection of diesel. The performance of this retrofit solution is assessed by performing CFD simulation in CONVERGE on a digital twin of the PACCAR MX-13. Both the conventional diesel set-up and the methanol-diesel dual fuel set-up are optimized through a design of experiment approach followed by a genetic algorithm optimization of the resulting regression models. The results show an increase in efficiency and a reduction in PM emissions. The relative NOx emissions varied depending on the optimization criteria, while CO, UCH and formaldehyde emissions increased. Where the diesel operation primarily faced an efficiency-NOx trade-off, the methanol-diesel operation was mainly challenged by the maximum pressure rise rate. Neither the diesel or methanol-diesel operation met the Stage V emissions limit without aftertreatment. Other combustion strategies, requiring more extensive retrofits or new engines may be able to perform better using methanol.

Besides the technical challenges and opportunities there are also socio-economic challenges and opportunities. These are investigated specifically for the inland shipping sector. This is done through mapping of the methanol and inland shipping innovation ecosystem and the value blueprint. The multi-level perspective framework is used to analyze the dynamics between different parts of the system and the different alternative fuels. The theoretical framework of Walrave et al. (2018) combines innovation ecosystems theory, the multi-level perspective and strategic niche management and is used to gain insight how this could be managed. There are relatively few barriers for methanol, but the biggest challenge is the lack of opportunities compared to the alternatives. Only biomethanol appears to offer a competitive solution. The biggest challenge for biomethanol is the very small supply and the fact that it is only price competitive with other sustainable fuels or with the current HBE-subsidy for renewable fuels. It is difficult to overcome this challenge as there is a lot of uncertainty due to the many alternative alternatives. Experimentation, collaboration and subsidies are required to overcome this uncertainty.

Biomethanol may provide a solution as a fuel in heavy duty applications, especially in the agricultural machinery and the inland shipping sector. However, the technical and socio-economic analyses show that there are almost no opportunities for a quick solution. The biomethanol supply chain still largely needs to be developed and it there is no great incentive yet to convert to methanol engines. Methanol has chances to play a role in the medium term. Nonetheless, it shows long term potential as well using increasingly advanced aftertreatment or fuel cell technology.

Preface

Working on this thesis during the Covid-19 pandemic has been a peculiar time and it did not leave thesis unaffected. Especially the technical part of this thesis has changed as the original plan was to do experimental research on an engine set-up.

I would like to express my gratitude towards my university supervisors Floor Alkemade and Bart Somers. Thank you for your patience and feedback. It has been marathon, but you were there the entire time.

Next to them, I would like to thank my company supervisor Michel Voorwinde, of Bovag Energy Systems and Revision. Thank you for helping me to get in touch with the right people and for your feedback on my work. I am especially grateful for the many Friday morning calls to discuss my work and progress. These calls helped me to stay motivated throughout my thesis.

Lastly, I would like to express the utmost gratitude towards my parents. They have supported me not only throughout my thesis, but my entire life. Without you I would never be where I am now.

Table of Contents

Abbreviations

AHRR	Apparent heat release rate
AIHRR	Apparent integrated heat release rate
AMR	Adaptive mesh refinement
ANN	Artificial neural networks
ATDC	Crank angle degrees after top dead center
BTDC	Crank angle degrees before top dead center
CAD	Crank angle degrees
CI	Compression Ignition
CO	Carbon monoxide
DoE	Design of Experiments
EM	Ecosystem model
EVP	Ecosystem value proposition
GA	Genetic Algorithm
GCWR	Gross Combined Weight Rating
GIE	Gross indicated efficiency
HBE	Hernieuwbare brandstofeenheden
HD	Heavy duty
HRR	Heat release rate
ICE	Internal combustion engine
IHRR	Integrated heat release rate
IMEP	indicated mean effective pressure
IOC	International oil company
ISCO	Indicated specific CO
ISFORM	Indicated specific formaldehyde
ISNOx	Indicated specific NOx
ISPM	Indicated specific PM
ISUHC	Indicated specific
KPI	Key performance indicator
LES	Large eddy simulation
LHV	Lower heating value
LTC	low temperature combustion
MD	Medium duty
MEF	Methanol energy fraction
MLP	Multi-level perspective
MPRR	Maximum pressure rise rate
MSW	Municipal Solid Waste
NOC	National oil company
NOx	Nitrogen oxides
NTC	No-time counter
RANS	Reynolds Averaged Navier Stokes
RCCI	Reactivity controlled compression ignition
RON	Research octane Number

SI	Spark ignition
SNM	Strategic niche management
SOI	Start of injection
SOx	Sulfur oxides
SQ	Sub question
TTW	Tank-to-wake
UHC	Unburned hydrocarbons
WTT	Well-to-tank
WTW	Well-to-wake

Symbols

γ	Ratio of specific heats
ω	Engine speed
η	Efficiency
E_{req}	Required energy
E_{frac}	Energy fraction
p	pressure
V	Volume
Q_a	Apparent heat release
Q_c	Heat release
Q_{HL}	Heat loss
m_{fuel}	Fuel mass
SS_{reg}	Sum of squares regression
SS_{tot}	Sum of squares total
SS_{res}	Sum of squares residuals
y_i	Measured value
$\hat{y}_i$	Predicted value

List of Figures

List of Tables

Chapter 1: Introduction

The world is in the middle of an energy transition, a pathway towards a clean and renewable energy system. The transport sector plays a crucial part as it accounts for 21% of the world's energy consumption and this is only expected to increase towards 2050 (BP, 2020; U.S. Energy Information Administration, 2020). However, this is not the only challenge the transport sector is facing. It is also responsible for more than 67% of all NO_x emissions and roughly 10% of the total emissions of pollutants (European Environmental Agency, 2019).

Electrification is potentially the most efficient way to reduce both carbon and local emissions in transport. Electric engines do not have any tailpipe emissions, so its drivetrain does not produce any local emissions and if electricity is produced in a sustainable manner it is also carbon neutral. A second reason is the fact that battery electric drivetrains have the highest efficiency when considering the conversion of 1 kWh of electricity to work produced by the drivetrain (Curran et al., 2014; International Energy Agency, 2015). Good progress is being made with the electrification of light duty vehicles but some applications are more challenging. According to forecasts, electrification will not be a solution in the foreseeable future for all applications in the agriculture, road transport and inland shipping sector (Dominković et al., 2018; European Commission, 2017). Hydrogen fuel cells are posed as the solution for these applications. However, this technology is lagging in technological maturity and infrastructure. Therefore, it is no option for short term implementation (DNV GL, 2019; Geertsma & Krijgsman, 2019). A Methanol-fueled internal combustion engine (ICE) may provide a solution for these challenging applications. To investigate for which applications methanol may provide a solution the performance of electrical pilot cases are compared to the performance of the common alternative, diesel engines. This analysis is conducted for the road transport, agriculture and inland shipping sector.

Methanol is one of the most traded chemicals and offers several advantages (DNV GL, 2019). One of the key advantages of methanol is that it can be produced from different sources: fossil, biomass and synthetic. This makes it a scalable and potentially carbon neutral solution. Next to that, methanol is a liquid above -97,6 °C which means it can use the current infrastructure (Chakarov, 2011). With an energy density of 16 MJ/l, the required volume will double compared to diesel. While this may seem to be a disadvantage, it is of a similar order compared to its alternatives and it is larger than batteries and compressed or liquid hydrogen. The advantage of methanol as an ICE fuel is the low emissions of critical pollutants. It can even be applied to the current engine pool with small modifications of the engine (Dierickx et al., 2018). On the long term methanol can also be used in fuel cells, either directly or as a hydrogen carrier. Methanol could be a promosing fuel for internal combustion engines (ICE) that can be implemented quickly. Nonetheless, there are challenges of both technical and socio-economic nature.

For the opportunities and challenges of methanol the scope narrows down to the inland shipping sector with primary focus on the aftermarket of inland shipping vessels. For inland shipping vessels it is especially important to provide a solution or the existing vessels because of their long lifetime. Trucks and tractors have an expected lifetime of 10 years (Dan Meszler et al., 2018; Petrov & Trendafilov, 2011), while inland shipping vessels have an average age of 20-50 years (Panteia, 2013). Solutions that require a new engine would therefore diffuse very slowly in the inland shipping sector. The fact that inland shipping sector engines have long lifetimes and are extensively revised also provides opportunities for retrofitting. Trucks and tractors have very tightly packed drivetrains as the vehicle is partly designed around the drivetrain. Ships generally have more room for adjustments to the engine.

When looking at the challenges on the technical side, modifications to the engine are still needed as most heavy duty (HD) applications use compression ignition (CI) engines. Methanol is in principle a fuel for spark ignition (SI) engines, due to its high octane number and its low tendency to knock (Wang et al., 2019). It already has an extensive track record in SI automotive engines (Bromberg & Cheng, 2010) and HD SI engines are commercially available (K. Zhao, 2019). However, the Dutch heavy duty market uses almost exclusively CI engines and conversion to SI is difficult. It requires

major adjustments and parts of the engine need to be rebuild. Next to that, it will lower the efficiency of the engine as CI engines are more efficient than SI engines due to their higher compression ratio (Moirangthem, 2016).

There is far less experience with methanol in CI engines. Nonetheless, there are multiple strategies to convert (CI) engines to methanol operation. Dierickx et al. (2018) discuss several options. The first option is to inject methanol with an ignition improver like MD95 (Ellis, 2017) or diesel. However, ignition improvers often contain toxic and or carcinogenic compounds and diesel and methanol have a limited miscibility. This limits the diesel substitution to a few percent.

Another option is to convert the engine to dual fuel operation. This be can be achieved in two ways: dual direct injection (through two separate injectors or one dual injector), or port fuel injection (PFI). The advantage of the first method is the control over the methanol air mixing, adding another method for controlling the combustion (Verhelst et al., 2019). However, the downside of the dual direct injection approach is the difficult conversion of the engine. MAN uses separate injection in their 2-stroke marine engines (MAN Diesel & Turbo, 2014), but this is difficult to achieve with smaller high speed engines due to the limitied space in and around the cylinder head. The problem with dual injectors is the lack of a universal retrofit solution increasing the modification costs (Maritiem Kennis Centrum et al., 2018).

The PFI approach mixes the methanol with the intake charge and ignites it with a direct diesel injection. This is the easiest option to implement as it only requires a low pressure injector that is connected to the engine intake which is generally easily accesable. The disadvantage of this approach is lack of control over the mixing, since PFI will result in a premixed methanol-air mixture. This could lead to knock or too high pressure rise rates at high loads and a too lean mixture at low loads, approaching the flammability limits (Verhelst et al., 2019).

The results of methanol PFI look promising. Dierickx et al. (2019) achieved up to 70% methanol operation in a Penta D7C marine engine. Dual fuel operation resulted in a 12% efficiency increase and a decrease in nitrogen oxides (NOx) and particulate matter (PM) emissions of 60% and 77%, respectively. The simulations of Li et al. (2013) in a light duty engine even suggest that Euro 6, the latest light duty vehicle emissions norm, may be achieved without aftertreatment. Even though the results in literature look promising, there is still more research to be done. The optimization of methanol-diesel PFI engines focuses mostly on optimizing a single variable or system. For example Liu et al. (2015) focus on solely the injection pressure. There have been multivariable studies like Li et al. (2013), but these are conducted on light duty engines. A multivariable optimization of heavy duty diesel-methanol PFI engines is yet to be conducted. In the EU formaldehyde emissions are not regulated as it not a problem with diesel. However, there are indications that it might become a problem with methanol combustion and it is identified as a research gap by Verhelst et al. (2019). If the Stage V emission norm, the latest emission norm for inland shipping, can be achieved without excessive increase in formaldehyde emissions it would save investments in expensive aftertreatment systems.

Besides the technical challenges there are also socio-economic challenges to the introduction of methanol as an ICE fuel. The first challenge is the integration of methanol as a fuel, which requires re-alignment of actors. The upstream supply chain changes from the petroleum sector to the chemical sector. Next to that, methanol may be compatible with the current infrastructure, but it still requires dedicated bunkering or storage capacity. The second challenge is the feedstock used for production. The current production of methanol is mainly based on fossil sources. For methanol to contribute to the reducting in carbon emissions it should be produced from biomass or synthetically. This requires a transition within the methanol industry. Lastly, methanol is expected to increase costs compared to conventional fuels (Maritiem Kennis Centrum et al., 2018).

Methanol could be implemented rather easily, but it still has pathbreaking elements. It requires a transition from oil or gas based fossil sources to renewable sources, challenging the locked-in fossil

regime (Coenen et al, 2015; Upham et al, 2014). While it might be possible for methanol to contribute to the energy transition, this transition pathway is also characterized by large uncertainties, requiring re-alignment of technologies, actors and institutions.

Since methanol requires modifications of the current engine pool and infrastructure, success in the market place is dependent on the internal alignment of the current innovation ecosystem (Adner, 2012). Innovation ecosystem theory states that this could be achieved through mapping and orchestrating the ecosystem (Adner et al., 2013). However, since methanol has path-breaking elements, internal alignment of the ecosystem might not be enough (Walrave et al., 2018). Different suppliers will be necessary to supply sustainable methanol and the barrier of a cost increase has to be overcome will methanol as an ICE fuel be adopted (McGill et al., 2013). Thus, there needs to be a change in selection criteria. If these challenges are not properly managed the innovation will fail. Walrave et al. (2018) have created a framework that combines the multi-level perspective (MLP) and strategic niche management (SNM) with innovation ecosystem theory to manage pathbreaking innovations.

Current literature on the adoption of methanol and similar alternative fuels is limited to the analyses of technical performance (DNV GL, 2019), supply chain analyses (Zomer et al., 2020), assessment of stakeholder support (Hansson et al., 2019; Turcksin et al., 2011) and best practices. This thesis will provide an overview of the technical and socio-economic challenges and opportunities and how these could be managed through the framework of Walrave et al. (2018)

1.1 Research Questions

The aim of this thesis is to determine the role of the ICE using methanol as a fuel in the energy transition. This is investigated through the following research questions:

RQ: "What is the potential of methanol as an ICE fuel in the energy transition and under what conditions can this potential be realized?"

This research question is answered through the following sub questions (SQ):

SQ1: "For which heavy duty applications does methanol provide a solution?"

The first sub question investigates to what applications within the road transport, agriculture and inland shipping sector cannot be electrified and provide a potential market for methanol. It will do so by comparing the performance of electrical pilot cases to the performance of the common alternative, diesel engines. After this broad overview, the focus will narrow down to the inland shipping sector for sub questions 2 and 3.

SQ2: How can a retrofit ICE be optimized to realize the potential of methanol?

The second sub question analyzes the performance with regard to the efficiency and emissions of methanol-diesel HD PFI engine. It provides insight in the potential of methanol as a fuel for retrofit engines and whether it can substitute aftertreatment systems.

SQ3: What are the opportunities and barriers for different stakeholders in the methanol innovation ecosystem and how can these be exploited or overcome?

The final sub question investigates the socio-technical challenges and opportunities of methanol in the innovation ecosystem. It analyzes the dynamics between the different parts of the system and between the alternatives. The theoretical framework is used to gain insight how these challenges can be managed and overcome.

1.2 Outline

The following chapters show how the research questions are answered. Chapter 2 provides background information on the three SQs and Chapter 3 outlines the methodology followed to answer

the SQs. Chapter 4 answers SQ1 showing which applications are most suitable for methanol. Chapter 5 focusses on SQ2 by comparing the results of diesel benchmark simulations to methanol dual fuel simulations. Chapter 5 and 6 adress the SQ3. Chapter 5 discusses the innovation ecosystem and barriers and opportunities, while Chapter 6 shows how these could be managed. Chapter 7 discusses all the results and Chapter 8 provides an overview of the conclusions.

Chapter 2: Background Information

This chapter discusses the literature and theory behind the research questions. It follows the structure of the report, providing background to each of the three sub questions. It starts with the discussion of the general transition roadmaps. Then, the literature review of different combustion methods and the influence of engine variables are discussed. Lastly, an explanation is given of the innovation ecosystem, the MLP and SNM theory and how these are used in the framework of Walrave et al. (2018).

2.1: Roadmaps

Sustainability can be achieved in multiple ways and it can differ between different applications. In the Dutch climate agreement (Dutch Government, 2019) the goal is set to use synthetic and biofuels up to 2030 and to try to introduce electric alternatives where possible. In the second period up to 2050 the goal is to reach dominance of electric drivetrains. This is a lot more ambitious than the prediction of the U.S. Energy Information Administration (2020) for the United States which expects fossil fuels to remain dominant through 2050.

To gain an understanding of the positioning of different energy sources within time and between modalities roadmaps of different energy sources are discussed. When looking at 2050 the expectations are that battery electric drivetrains will be used for lighter transport and hydrogen FCs will be used for heavier and long range applications (Fuel Cells and Hydrogen Joint Undertaking (FCH), 2019). The exception is the shipping and aviation sector, in which synthetic fuels are considered the only option. Figure 2.1 shows that higher load and longer distance applications are more attractive for FCEV. It is also likely that these applications will make use of ICE, while FCEV is still in the development phase.

Hydrogen trucks have a technology readiness level (TRL) of just 3-7 requiring another 3-10 years for the technology to be market ready. This means that some hydrogen trucks currently are in the pilot phase, which is indeed the case (WaterstofNet, 2020). It can still take years before large scale production will start and even at that point it can still take decades for the technology to gain a majority share of the market. In line with Gigler & Weeda (2018), a market share of around 20-25% is expected in 2050 (FCH, 2019). Gigler and Weeda (2018) also investigated other modalities and considered that inland vessels are still in the exploration phase and it is expected to take more than 10 years for the technology to be ready for large scale commercialization. In most scenarios mass market readiness of FC technology will not be reached until 2030 or 2035, while for freight ships this can even be beyond 2045.

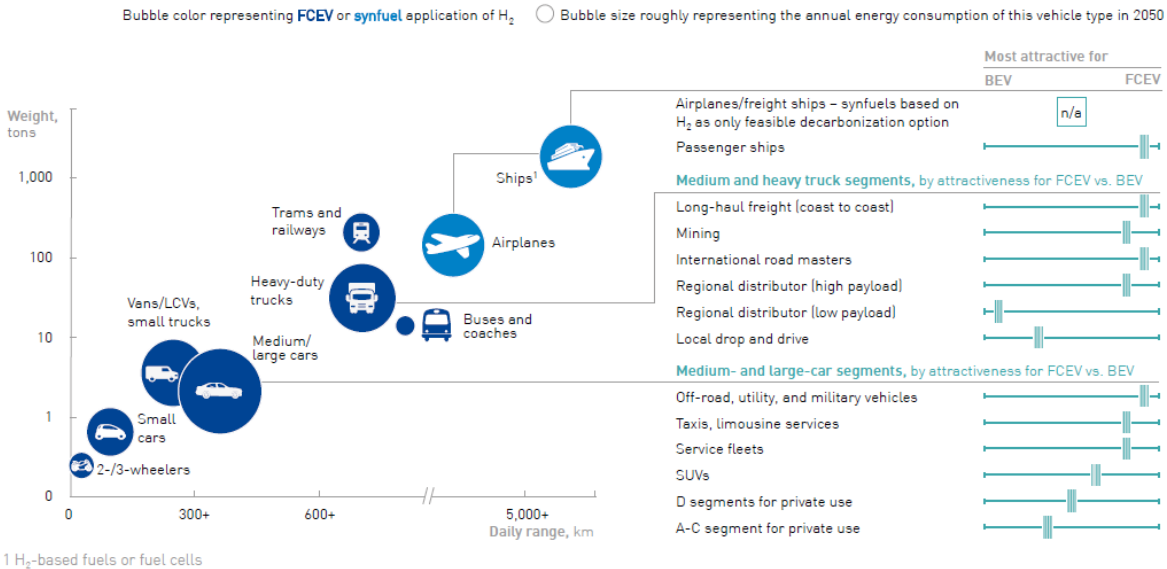

Figure 2. 1: Attractiveness of BEV and FCEV for different applications (FCH, 2019)

2.1.1: Electrification

Electrification is expected to be limited to mainly light duty application, due to its challenges regarding the batteries and infrastructure. On the battery side there is a clear trend of decreasing battery prices. In 2010 battery prices were 500-1200 $/kWh, while today prices below 100 $/kWh are reported (BloombergNEF, 2020). However, the battery prices are not expected to remain a large challenge. The major challenge is the low energy density compared to conventional fuels, because weight and space are crucial for the performance of many transport modalities As can be seen in figure 2.2, even the theoretical energy density of currently used batteries is low compared to the 12.6 kWh/kg of diesel (World Nuclear Association, 2018). Even the higher electric drivetrain efficiency cannot compensate this factor 10 difference. The energy density of batteries is improving, but not at an exponential rate like computing power does (Cao et al., 2020; Lundgren et al., 2017). While there are batteries with theoretical energy densities above 1000 Wh/kg, it will take decades before these energy densities are reached in practice (Cao et al., 2020).

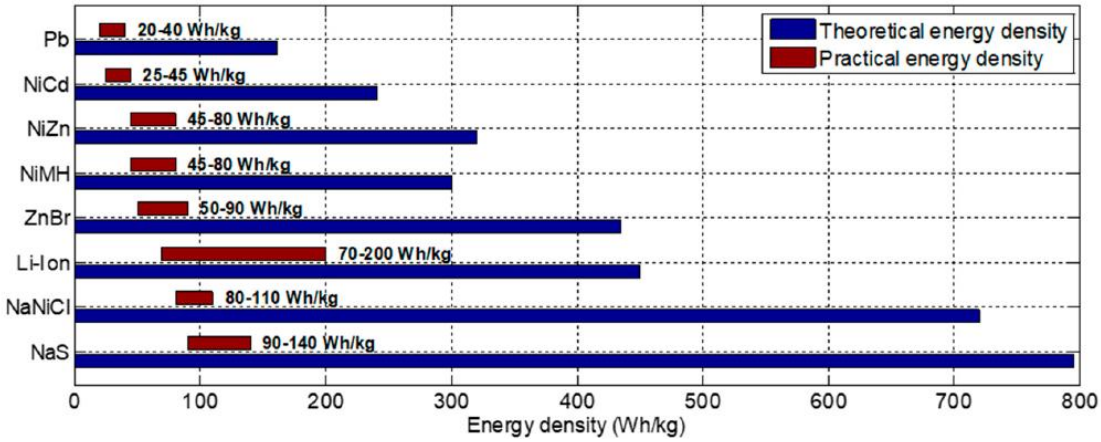

Figure 2. 2: Theoretical and practical energy density of batteries (Lajunen et al., 2018).

According to the European Roadmap Electrification of Road Transport (ERTRAC et al., 2017) the battery electric drivetrains will probably never fully replace the ICE when considering the current standard of performance. Automatization of vehicles could help to downsize vehicles making it easier to electrify them. However, that technology is not ready and full replacement of the vehicle park can take decades. ERTRAC et al. (2017) expect an increase in performance in every aspect of electric transportation and they see options to enable electrification of all road transport options by 2030. Though, this would not only require a fully distributed charging network but also dynamic wireless charging. This requires major investments and it would reduce the system efficiency of electric vehicles (CORDIS, 2019).

It is expected that the life cycle costs for electric and diesel HD trucks will come close to CONVERGEnce in most 2050 scenarios (Jadun et al., 2017). When looking specifically at the Netherlands, Moraga and Mulder (2018) expect light duty transport to be dominated by electric drivetrains by 2050, but only 15% of trucks are expected to be fully electric and not even 10% is expected to be hybrid.

2.1.2: Biofuels, Synthetic Fuels & Hydrogen

For the short and medium term biofuels are seen as the best option for decarbonizing the modalities discussed in this thesis. Currently, all passenger vehicle fuels are already blended with biofuels as the standard gasoline E10 consists of 10% ethanol and the standard diesel B7 consists of 7% FAME (Dutch Government, 2018).

Cluzel (2020) sees a role for liquid fuels up to 2050, with increasing amounts of drop-in by sustainable fuels or replacements by cleaner carbon based fuels. Many of the biofuel production technologies are widely deployed, in early market development or in the demonstration phase (European Technology

and Innovation Platform, 2018). This indicates that the biofuel approach is technologically possible, but the limiting factor for this will be the availability of sustainable biomass. Biofuels are likely to be reserved for decarbonization in the modalities that are hard to electrify and require high energy density fuels. This can be complemented with the production of synthetic or E-fuels. Advanced biofuels and E-fuels are expected to increase production, reaching a total of 20% of European transport in 2030. This is enough to exceed the Renewable Energy Directive (RED) II target for transport of 14% by 2030 (CE Delft, 2020)

When looking more in-depth into synthetic fuels, upscaling of these technologies is already taking place. These developments co-evolve with hydrogen as hydrogen and CO2 are the building blocks for e-fuels. According to Frontier Economics (2018) the production of synthetic fuels will increasingly be produced on larger scales. From 2025 onwards standardization will start taking place to generate economies of scale. Beyond 2040 the technology is expected to be a commodity useful for both synthetic fuels and direct use of hydrogen. They expect that the German hydrogen industry has scaled up its electrolyzer capacity to 25-50 GW by 2030 and to produce 100-350 GW by 2050. The current global stock of electrolyzer capacity is currently only 20 GW. The challenge is not only to increase the electrolyzer capacity, but also the supply of renewable energy. The current installed power capacity in Germany is 218 GW (Smil, 2020), thus this needs to increase by at least 50-150%.

According to The Fuel Cells and Hydrogen Joint Undertaking (FCH), (2019) hydrogen from electrolysis increases from 5% in 2035 to 100% in 2050. Tough, Mulder et al. (2019) sketch a more conservative scenario for the Netherlands. They expect that hydrogen will almost be exclusively produced from natural gas up to 2050. In the most optimistic scenarios, the production of renewable H2 just exceeds the 50% in 2050. So, there are large differences between studies, however it is clear that in the next two decades the majority of hydrogen is produced from fossil sources and it will not reduce the fossil lock-in during this period.

The hydrogen produced can be used either directly or as a building block for synthetic fuels. Currently, there is no infrastructure in place for hydrogen. In the short and medium term it is therefore likely to be used for synthetic fuels. For the long term it is not yet clear which option is will be most favorable for which application.

The roadmaps show clear conclusions for light duty road transport, aviation and international maritime shipping. The first will be electrified and the latter two will keep using liquid fuels in 2050 and beyond. The applications in-between show some potential for electrification, but hydrogen appears to be the more attractive option. However, hydrogen is not yet ready for another 10-20 years and it is questionable whether the hydrogen production will be sustainable by that time. In the electrification road maps the focus is almost exclusively on road transport. The hydrogen road maps apply a wider perspective, but most attention still goes towards road transport. There is some discussion of shipping, trains and aviation, but none of the roadmaps include the agricultural sector.

2.2: Engine Variables

This section provides background information on the characteristics of methanol as a fuel and how it can be used in an ICE. Then, it discusses the variables used for optimization of methanol-diesel PFI dual fuel engines in detail.

Methanol is a low cetane, high octane fuel with a cetane number of 3 and research octane number (RON) of 107-109. This means that it is even more knock resistant than gasoline (RON 90-100) and it cannot be directly in CI engines (Schröder et al., 2020). There are multiple combustions strategies possible, but the focus in this thesis is on dual fuel PFI strategies using methanol as the main fuel and diesel as the pilot fuel. Both the fuel and the combustion strategy affect the emissions.

One of the inherent advantages of methanol is that there are no carbon-to-carbon bonds and it has a high oxygen content. Therefore, combusting methanol is theoretically soot free (Schröder et al., 2020). Next to that, methanol has a high heat of vaporization that cools the intake air and increases the

volumetric efficiency of the engine (Vancoillie et al., 2012). Lastly, methanol is a single molecule fuel that contains no sulfur, so there are no sulfur oxide (SOx) emissions. The downside of methanol is the formation of the toxic formaldehyde in the case of incomplete combustion (Qi et al., 2014).

Even with dual fuel PFI there are multiple combustion strategies. These are in line with the engine research trajectory of low temperature combustion (LTC) strategies. It tries to decrease local in-cylinder temperatures to reduce the NO_x emissions which are formed exponentially above 1800 K (Hoekman & Robbins, 2012). To avoid increasing PM emissions fuel-rich regions should be avoided. This is accomplished in partially premixed LTC strategies by improving fuel-air mixing rates or increasing the time before combustion. For most LTC strategies this comes at the cost of high unburned hydrocarbons (UHC) and carbon monoxide (CO) emissions and formaldehyde in the case of methanol (Krishnan et al., 2016). These strategy combine elements of the conventional CI and SI engines and therefore also the advantages, such as high thermal efficiency of CI and both very low NOx and PM emissions if SI engines. However, it also faces challenges: controlling the ignition timing and burning rate and incomplete combustion (Yao et al., 2006). There are a large number of variables that can be used to optimize methanol-diesel engines. In the literature review the focus is exclusively on variables that are easy to change during a retrofit and are discussed below.

2.2.1: Fuel Injection Timing

The injection timing is a particularly important parameter in dual fuel engines. With PFI injection the only injection timing of interest is the timing of the diesel direct injection. The combustion strategy even depends on how advanced or retarded the start of injection (SOI) is. Advanced SOI before 30 crank angle degrees before top dead center (BTDC) is considered reactivity controlled combustion (RCCI), because both fuels are well mixed the ignition timing is dependent on the reactivity of the mixture (Y. Li et al., 2013). The reactivity of the mixture is controlled by the ratio of low reactivity (methanol) and high reactivity (diesel) fuel. If the timing is retarded the combustion strategy changes to mixing controlled combustion. In this strategy the injection timing is the main determinant for the ignition timing (Li et al., 2013). This can also be generalized to other fuels like gasoline-diesel dual fuel operation (Willems, 2020).

In the case of very advanced SOI, like in RCCI, Tuominen (2016) found that advanced timing resulted in retarded ignition timing. This happens due to a more dispersed spray leading to high mixing and a very lean fuel. Next to that, the ignition delay is also increased due to a lowering in temperature by vaporization of the fuel. A too advanced injection could lead to misfiring or knock if the mixture reactivity is not right. Misfire is more likely to happen at lower loads, while knock is more likely to happen at higher loads.

At mixing controlled injection timing Mansor (2014) describes that advanced SOI in methanol-diesel PFI engines leads to a large portion of the fuel being burned at the end of the compression stroke. This earlier combustion leads to an increased in-cylinder temperature and peak pressure near TDC. This increase in temperature increases the NOx emissions, but generally decreases the HC and CO emissions. If injection is retarded the peak temperature and pressure occur after TDC when the cylinder volume is larger and the ignition delay is shorter. This results in lower NOx emissions due to the lower in-cylinder temperature, but it also lowers thermal efficiency and increases NO and CO emissions. At lower loads, in-cylinder temperatures are lower and NOx emissions are less sensitive to injection timing. At higher loads this trade-off becomes more apparent.

Krishnan et al. (2016) add that advancing the injection timing leads to one stage gaussian heat release profiles, while retarding leads to a diesel like two stage combustion process. The two stage combustion process is caused by the limited time of mixing of methanol with diesel as the end of injection and the start of combustion are close together.

2.2.2: Boost Pressure

Willems (2020) investigated the effect of boost pressure on a gasoline-diesel RCCI engine. An increase in gross indicated efficiency (GIE) was found for increasing boost pressures, while there was a small decrease in combustion efficiency and an increase in CO emissions. The increase in efficiency was almost exclusively due to a decrease in heat losses. Increasing the boost pressure reduces peak global temperatures and this reduces the heat losses. The exhaust losses remained the same, but were expected to decrease, because higher boost pressures shortens the combustion duration which normally reduces the exhaust losses. However, the ignition timing was also advanced with higher boost pressure and it was advanced beyond the optimal value. The ignition timing advances at higher boost pressures, because more mass is trapped in the cylinder which increases both pressure and temperature during compression. Excessive boost pressures resulted in lower global temperatures, decreasing CO oxidation rates and increasing CO emissions and combustion losses. The over-lean conditions increased the combustion losses more than the heat losses decreased. The increase in boost pressure also reduced the NOx emissions. This could be explained by the decrease in peak global temperature according to Krishnan et al. (2016). The findings are in line with Wang et al. (2020) for natural gas-diesel and Di Blasio et al. (2015) for ethanol-diesel dual fuel engines.

For a methanol dual fuel engine Y. Li et al. (2013) found a sharp increase in efficiency which flattens after a threshold. They did not find a significant effect on NOx, while they did found a decrease in CO and UHC with increasing boost pressure. Their explanation is that the UHC and CO emissions mainly formed in the low temperature region near the cylinder wall and around the axis of the cylinder. The high boost pressure leads to compression temperature and oxygen concentration which promotes the oxidation near the walls. So, there are contrasting finding of the effect of the boost pressure on CO and UHC emissions in literature.

2.2.3: Methanol Energy Fraction

The amount of diesel fuel has a strong effect on the combustion and emissions, since it determines whether the engine operates more like a CI or SI engine. For smaller quantities of diesel the engine resembles a SI engine in which there is a relatively large quantity of main fuel. For methanol as a main fuel this means that the compression pressure is reduced due to the cooling effect of the methanol vaporization. It also results in a faster combustion due to a larger amount of premixed charge. If a large quantity of pilot fuel is used it resembles a CI engine.

Tuominen (2016) discusses the effect of different quantities of diesel fuel extensively. If the methanol energy fraction (MEF) is high there is a large ignition delay due to a smaller concentration of a high reactive fuel. Larger quantities of diesel increases the reactivity as there are locally rich mixtures and reduces the ignition delay, but this effect diminishes with larger quantities of diesel. The flame spread limit is also affected by the MEF. Decreasing the MEF allows for flame propagation in leaner mixtures and therefore higher boost pressures. The optimum MEF changes for each operating condition. At low loads a larger quantity of high diesel is required to decrease the risk of partial burn or misfire. The MEF limit is reached when the in-cylinder temperature is just enough for auto-ignition of the mixture. As the load increases the limiting factor is not misfire, but knock.

Larger MEF resulted in a lower PM emission, due to the larger amount of premixed fuel combustion, irrespective of the load. Also, NOx significantly decreased with smaller quantities of pilot fuel. This is due to the reduced rich regions and faster combustion and high temperature zones. Interestingly, the NO_2 share of NOx increased when the MEF increased. This was due to the reaction of NO with HO_2, a free radical from the methanol oxidation process. Unregulated emissions like unburned methanol and formaldehyde increased with larger MEF.

According to Y. Li et al. (2013) the lean methanol-air mixture in the low temperature region near the cylinder wall cannot be completely oxidized with low MEF. However, this region is also problematic with high MEF due to the decreased combustion temperatures resulting in high UHC and CO emissions.

Han et al., (2020) investigated ethanol-diesel dual fuel combustion. Their experiments showed similar results in which UHC and CO emissions increased and PM emission decreased for increasing ethanol fractions. However, they found no consistent effects on NOx emissions. The NOx emissions were found mostly dependent on the combustion phasing, which differed for each load point and ethanol fraction. The efficiency was found to increase for intermediate ethanol fractions and it decreased again at high ethanol fractions. At low loads this is because of incomplete combustion and at high loads it is due to sub-optimal combustion phasing. An important limitation of the ethanol fraction was found to be the maximum pressure rise rate (MPRR), especially at high loads due to knock.

2.2.4: Intake temperature

Y. Li et al. (2013) describe that increasing intake temperature advances the ignition timing, shortens the combustion duration. With increasing MEF the intake temperature may need to increase to maintain the ignition timing with a larger fraction of low reactivity of methanol. Increasing the intake temperature also helps to promote combustion in the low temperature region near the cylinder wall. Increasing the intake temperature increases the mass burning rate during the flame propagation, leading to more complete combustion improving the thermal efficiency and reducing HC and CO emissions (Krishnan et al., 2004). The downside is a higher temperature increasing NOx emissions. Y. Li et al. (2013) found that a minimum intake temperature was needed and further increases drastically increased both NOx emissions and knock.

2.3: Transition Framework

A working technology alone is often not enough to successfully solve problems on a system level. It also requires changes of other aspects of the system and these need to be managed. In the innovation sciences literature there are multiple theories that attempt to manage these changes to make new technologies a success. Two of these are innovation ecosystems theory and transition theory. Innovation ecosystems theory takes an economics or management approach in analyzing the structure and dynamics of technological change in industries. It focusses on aligning stakeholders in cross-sectoral industries. Meanwhile, transition theory takes a sociological approach in managing transition from old to new socio-technical regimes. It attempts to help the technology in the initial phases of upscaling in emerging industries.

Generally, these streams are applied independently for different problems, but Walrave et al. (2018) argue that for path-breaking innovations both theories can complement each other. They found that many ecosystems that tried to introduce path-breaking innovations failed, despite overcoming the technological challenges and achieving alignment of the key actors. They identified the strong social resistance, due to conflicts with the prevailing socio-technical regime, as the key reason for this failure. They argue that next to the internal alignment achieved through an innovation ecosystem approach, attention should be paid to external viability. The socio-technical selection environment favors the locked-in regime and these are difficult to break as actors often have invested substantially in these in the proven solution. Transition theory addresses the change in socio-technical regimes.

In the case of methanol both internal and external viability are crucial for success. The innovation ecosystem will change with the introduction of methanol. There will be new supplier, transport, storage and distribution companies need to add methanol to their portfolio and shippers need to retrofit the engine of their vessels. These changes need to be managed in order for methanol to have any success. However, this does not solve the likely increase in fuel price if methanol is used. Next to that, the supply of methanol itself needs to change from fossil to renewable sources before contributes to the energy transition. This requires a change in the selection environment as it will not be able to compete on the most important selection criteria: price (Hansson et al., 2019).

2.3.1: Innovation Ecosystems Theory

The innovation ecosystem, henceforth ecosystem, is inspired by natural ecosystems where organism affect each other and the environment. Just as in nature, companies do not exist on their own and they do not create value on their own. They interact with, and are interdependent on, other companies. The

value propositions are becoming increasingly complex with more and different actors involved, within and across industries (Adner, 2012). It is therefore important to include the entire ecosystem when analyzing pathbreaking innovations.

The ecosystem is conceptualized in different ways. One of the concepts is defined by Autio and Thomas (2014) as: "a network of interconnected organizations, organized around a focal firm or a platform, and incorporating both production and use side participants, and focusing on the development of new value through innovation". They focus on the structure and dynamics of the ecosystem, investigating the interactions and relationship between actors. Based on the structure it is possible to determine interdependencies, bargaining power and potential for symbioses. Adner (2017) calls this concept "ecosystem-by-affiliation".

Another conceptualization, the one used in this thesis, is ecosystem-as-structure. This concept, for a large part developed by Adner himself, is defined as: "the alignment structure of the multilateral set of partners that need to interact in order for a focal value proposition to materialize" (Adner, 2017).

Therefore, the ecosystem-as-structure is defined by its goal, the common value proposition to the final customers. Walrave et al. (2018) calls this the ecosystem value proposition, or EVP. So, the EVP includes all activities, with their corresponding actors, required to provide the value proposition to the ultimate customers. The challenge in the ecosystem is to align the different actors, meaning that the goals of each of the actors and therefore their behavior are in line with the EVP. Failure of aligning the activities of all the actors is likely to result in failure of the innovation (Adner, 2012). In order to help aligning the ecosystem use can be made of mapping and orchestrating the ecosystem (Adner et al., 2013).

Mapping the ecosystem is done through value blueprints. These are very similar to supply chains and value chains. The main difference is that the latter focusses on the linear sequence of activities, while value blueprints emphasize the importance of complementors that might lie off the direct path to market, but can be critical for success (Adner, 2012). The value blueprints starts with the mapping of all relevant actors and activities with respective position and links. Then, for each element on the blueprint it is assessed how capable and how willing the actor is to undertake the required activity. If one of the elements proves problematic, a viable solution should be found. Naturally, when an innovation is introduced only the elements that change in the blueprint should be assessed. This means that for small incremental innovation most of the ecosystem is latent, while pathbreaking innovations could face challenges in aligning the EVP.

Alignment of the ecosystem is often done by the main proponent of the EVP, the focal actor (Adner, 2017). The focal actor can shape the ecosystem model (EM), the structure of how value is created, delivered and appropriated by the actors in the ecosystem (Walrave et al., 2018). While certain aspects of the ecosystem and EM are simply fixed, there is room for the focal actor to "orchestrate" the EM through entrepreneurship in framing, revising and transforming the ecosystem (Zahra & Nambisan, 2012). There is evidence that it is possible to successfully orchestrate the ecosystem to achieve the EVP, however it proves to be a challenging task (Walrave et al., 2018).

2.3.2: Transition Theory

Many different streams of literature exist within transition theory that try to answer how transitions from old to new socio/technical systems can best be managed. This thesis is limited to the multi-level perspective (MLP) and strategic niche management (SNM).

2.3.2.1: Multi-Level Perspective

MLP provides a framework for analyzing socio-technical transitions. It analyses the dynamics of a system, by dividing it in three analytical levels: the landscape (macro-level), the regimes (meso-level) and niches (micro-level). This is visualized in figure 2.3.

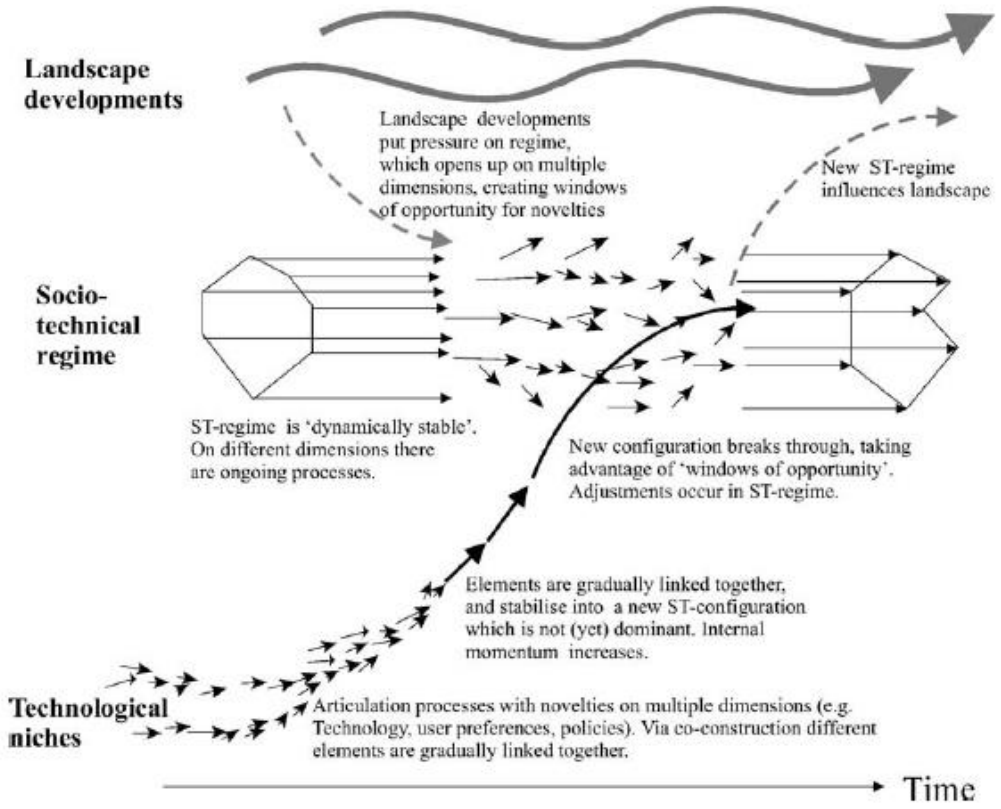

Figure 2. 3: The levels of the multi-level perspective (Geels, 2004).

The regime level represents the dominant technology that is currently embedded in society. The technology is deeply rooted in society and it stabilizes the regime in multiple ways (Geels, 2004). The most visible is the material network. Technologies are obdurate due to the sunk costs in the technologies itself, but also in the complementarity of its components and sub-systems. However, also less visible mechanisms provide stability to the regime. Formal and informal rules (e.g. values, routines, regulations and institutionalized practices) guide perceptions and organizations are embedded in interdependent networks, like industrial networks. These stabilizing mechanisms function as a selection and retention mechanism, promoting incremental and opposing pathbreaking innovation (Geels, 2002). The regime is locked-in and resistant to transitions.

The landscape consists of technology-external factors that are shaped by broad contextual developments, which actors cannot influence in the short run. Van Driel and Schot (2005) distinguished three types of factors: factor that do not change or only slowly, like climate change; long-term changes, such as industrialization or digitalization; rapid external shocks, such as wars or pandemics. The landscape exerts pressure on the regime and potentially destabilizes it, creating opportunities for the technologies in the niche level.

The niche is conceptualized as the "locus where radical variety is generated" (Geels, 2002). Niches are protected spaces where innovations can be incubated away from market and regulation influences. So, they are protected from the selection and retention mechanism of the regime (Schot & Geels, 2008). Once the niche has developed enough it can challenge the regime and potentially take over when the conditions are right.

2.3.2.2: Strategic Niche Management

The MLP is a framework to help analyze the dynamics in socio-technical systems, however it is does not provide any solution for the management of such a change. SNM uses the MLP as a basis in its

framework for the development of socio-technical niches. SNM is defined as: “the creation, development and controlled phase-out of protected spaces for the development and use of promising technologies by means of experimentation, with the aim of (1) learning about the desirability of the new technology and (2) enhancing the further development and the rate of application of the new technology” (Kemp et al., 1998).

Important elements are the shielding against regime selection pressures, so the niche can be nurtured to make it more robust by increasing the performance and expanding the socio-technical network. During this phase it should be determined whether the niche is promising enough to continue developing or not. If the technology is found promising it should be nurtured until it can be empowered. Where nurturing is focused on ‘inward-oriented system building’, empowering is about ‘out-ward oriented’ activities aimed at challenging the niche (Verhees et al., 2012). Smith and Raven (2012) discuss two strategies of empowerment: Fit-and-conform and stretch-and-transform. The first implies that, after shielding is removed, the innovation successfully can compete under mainstream selection pressures. Conversely, stretch and transform implies that innovation champions will promote that shielding is not (fully) removed, but that parts of it become institutionalized: the innovation does not conform to, but instead changes conventional selection criteria.

The key niche nurturing processes in the strategic niche management literatures are: assisting learning processes, articulating expectations, and helping networking processes (Smith & Raven, 2011). These nurturing processes take place while engaging in sociotechnical experimentation, through for example experimental projects such as pilot cases (Raven et al., 2010).

Chapter 3: Methodology

This thesis answers its research question by answering three sub questions. Each of the sub questions have their own methodology which are discussed in this chapter. First, in section 3.1, the approach in determining which applications are suitable for methanol is discussed. Second, in section 3.2, the optimization approach of methanol-diesel PFI engine simulations is discussed. Lastly, in section 3.3, it is explained how the innovation ecosystem is mapped and how the barriers and opportunities are determined.

3.1: Heavy duty applications suitable for methanol

The analysis of the roadmaps in section 2.1 makes clear that electrification will be limited to certain applications in the coming decades and that the other application will make use of either fuel cell technology or the combustion engine. This thesis investigates the state of art of the electric drive train for the agricultural, truck and inland shipping sector. The performance of electrical pilot cases is compared to that of the common alternative, diesel engines. Next to that, calculations are made to determine the amount of work that can be performed by the different drivetrains for different sizes of energy storage. Then, the implications of the changes in energy storage size or potential work are discussed in perspective of its application. To gain knowledge about the typical use of the applications interviews are conducted with the relevant trade associations. This assessment does not include economic feasibility, because the costs of electrification are dropping rapidly. However, the performance of battery storage, often the limiting factor for electrification, is developing rather slowly. Therefore, if electrification of an application is considered unfeasible it will not change quickly, unless the application or the rules of the system change drastically.

3.1.1: Pilot Cases

To obtain information about the pilot and planned pilot cases an online search was conducted. Each of the cases found during the search for analyzed in detail to obtain all relevant publicly available information. The list of pilot cases was considered complete when no new cases could be found anymore. Next to the search for pilot cases, a search for the common diesel alternatives was conducted to establish the benchmark performance. The search for diesel alternatives was limited to the newest models of the most common brands.

3.1.1.1: Road Transport

The search for trucks was limited to medium and heavy duty trucks. The search resulted in 12 electric trucks, 1 hybrid and 18 diesel trucks. The electric and hybrid trucks range from a weight limit of 7.3 t to 40 t. The cases are described in Appendix A.1.

3.1.1.2: Agriculture

For the agriculture sector the electrification is currently limited to tractors, the most versatile agricultural machine, since no pilot cases of specialized machinery like harvester could be found. Therefore, the search for the diesel alternatives was also limited to tractors. However, the engine and fuel requirements for tractors and specialized heavy machinery are similar. So, except for the possibility to optimize for a specific application the conclusions can be generalized.

The search resulted in 2 full electric and 5 hybrid electric pilot cases, of which any specification were published. These are compared to 20 diesel tractors spreading the entire performance range of tractors. An overview of the specification and an in depth description of the most important pilots can be found in Appendix A.2.

3.1.1.3: Inland shipping

The focus of the search for inland shipping pilot cases was on the full range of inland vessels, ranging from ferries to cargo vessels. 5 pilot cases are analyzed, 2 of which are ferries and 3 are containerships. The pilot cases are described in Appendix A.3. Finding information about the diesel alternatives proved difficult. Most ships are produced in very limited numbers and the published

specifications are often limited to size, power and capacity. Therefore, the comparison is not made with specific ships, but with common industry values.

3.1.2: Energy Storage Calculations

The calculations are based on the energy density of the different energy sources. An overview of the gravimetric and volumetric energy densities can be found in table 3.1. The battery energy density is derived of the Tesla Model S, which is often considered as the benchmark (Earl et al., 2018). It is clear that both energy densities of the batteries are significantly lower than those of the fuels. Naturally, with continuous development the energy density can be improved but the often used lithium-ion batteries have a theoretical maximum energy density of 0.45 kWh/kg (Lajunen et al., 2018) and battery energy density developments have been slow compared to for example the chip development which has followed an exponential growth according Moore's Law. As can be seen in figure 3.1, the development of battery energy density has been and is expected to be linear for the next 10 years. Cao, Zhang, & Li (2020) have predicted that the energy density of some batteries could get up to 1.3 kWh/kg and 3 kWh/l, however with the current and predicted development rate it will take decades before this will be a commercial reality.

Table 3. 1: Energy density and specific energy for different energy sources.

Energy source	Energy density kWh/l	Specific energy kWh/kg
Batteries	0.721	0.250
Methanol	4.98	6.31
Diesel	10.0	11.8

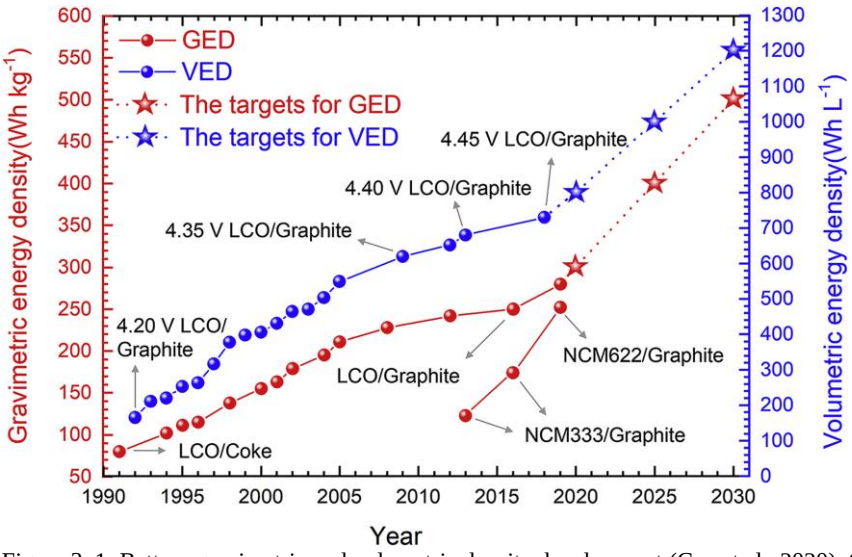

Figure 3. 1: Battery gravimetric and volumetric density development (Cao et al., 2020). GED is the gravimetric energy density and VED is the volumetric energy density. The dots represent actual values and the stars represent expected values.

The analysis is based on a comparison of the size and weight of the energy storage with regard to the effective work stored. So, the differences in drivetrain efficiencies are taken into account. For all modalities the electric drivetrain is considered to have a total efficiency of 85%, including battery discharge losses, and a battery utilization rate of 90% (Earl et al., 2018; MTZ Equipment Ltd., 2019). This means that only 90% of the battery is effectively used, because complete depletion of the battery might cause damage to the battery cells.

3.1.2.1: Road Transport

Different to tractors, the energy consumption of trucks is usually expressed in L/100km. However, these numbers change severely based on the truck load and operating profile. Next to that, it is

difficult to obtain information about the energy consumption of the different models. Therefore, a drivetrain efficiency of 40% is used, which is in line with new diesel trucks (Earl et al., 2018).

3.1.2.2: Agriculture

For diesel tractors the fuel consumption reported in the brochures is given in kg/kWh. To calculate the effective energy consumption 0.25 kg/kWh is used. This is the average reported fuel consumption plus 15% and comes down to an efficiency of 32.4%. The energy consumption penalty of 15% is set, because it is difficult to predict the operating profile of a tractor and the manufacturer is likely to present favorable numbers (Farmers Weekly, 2018).

3.1.2.3: Inland shipping

As it is difficult to obtain ship specification, besides engine power and carrying capacity, the analysis is based on common industry practices. For the drivetrain efficiency a fuel consumption of 200 g/kWh is used, similar to Simić (2014). This corresponds to an efficiency of 40.5%. As LNG inland shipping is becoming a trend, due to its lower CO2 emissions and lower local emissions, it is included in the calculations. For LNG an energy density of 6.25 kWh/L and a specific energy of 13.74 kWh/kg are assumed (Elgas, 2019). The efficiency is assumed similar to that of the diesel engine as Box et al. (2011) found only 0-2% lower efficiencies in LNG shipping vessels.

3.2: Methanol ICE Optimization

To find out the performance of a methanol retrofitted ICE, and the unavailability of an engine test bed at the time of the research, simulations are conducted in CONVERGE. CONVERGE is a commercial CFD code used for multidimensional analyses. It is known for its adaptive mesh refinement (AMR) to efficiently solve complex and moving geometries like in ICE. For the simulations a single cylinder set-up of the Paccar MX-13 is used. The MX-13 is a 6 cylinder heavy duty truck diesel engine with a maximum power of 390 kW. The engine specifications can be found in table 3.2. and are similar to a small-medium sized inland shipping engine (SPB, 2016). In fact the MX-13 is used as engine in inland shipping vessels by NPS Diesel (NPS Diesel, 2020) The engine will be optimized at the average operating point of inland shipping ships. Depending on the kind of vessels this is equal to 25-51% of the installed power (Abma et al., 2018). The decision has been made to set the engine load at 35% of maximum power and run the engine at 1200 rpm. This gives a gross indicated mean effective pressure (IMEP) of about 6 bar. The operating point is close to the highway operating point of heavy duty trucks for which the engine is designed (Nylund & Erkkilä, 2005). This section will first discuss the model set-up in CONVERGE. Then, the experimental design and optimization approach are discussed.

Table 3. 2: Test engine specifications.

Base engine	Paccar MX-13
Stroke	162 mm
Bore	130 mm
Connecting rod length	261.6 mm
Displacement	12.9 l
Compression ratio	18.5:1
Nozzle holes	7
Nozzle diameter	0.195 mm
Spray cone angle	9°

To be able to test the optimization possibilities first the Digital Twin needs to be created (section 3.2.1) after which the specific parameters of the run-cases need to be defined (section 3.2.2). Since the amount of parameters is large the so-called Design-of-Experiments (DoE) technique is applied. This is introduced briefly in 3.2.3. Finally, in 3.2.4, the an example of the optimization approach is given.

3.2.1: CONVERGE Set-up of the Digital Twin

In CONVERGE a single cylinder 3D model of the MX-13 is used for the simulations. The simulations are performed for the closed part of the cylinder, from intake valve closing at 120 BTDC, to exhaust valve opening at 108 crank angle degrees after top dead center (ATDC). This assumes a homogeneous mixture in the cylinder at the start of the simulation. The mixture composition is initialized based on mass fraction consisting of air, 0.233 O2 and 0.767 N2, and depending on the simulation methanol as well. The set-up of a CFD model consists of several parts. One is the description of the mathematical sub-models that are used to describe the complex phenomena like liquid injection, combustion and their interaction with the flow field. Second is how the computational domain is discretized (meshed) to render the continuous equation into a set of discrete equations that can be solved numerically. First the mathematical sub-models are described after which the approach to effectively 'mesh' the computational domain is introduced.

3.2.1.1: Mathematical Sub-models

The model set-up is using the default models and options, similar to Lele, Soni, Narayanaswamy and Krishnasamy (2019). For the spray modelling, the "blob" injection model is used, which initializes the diameter of the droplet to the effective nozzle diameter (Pal et al., 2017). The no-time counter (NTC) collision model is used for the subsequent atomization and collision processes, including the dynamic drop drag model. Spray break-up is modelled using the Kevin-Helmholtz and Rayleigh-Taylor (KH-RT) model, with the "blob" injection model. The Frossling model is used for droplet evaporation with the O'Rourke model for turbulent dispersion.

The combustion process is simulated with the SAGE detailed chemistry solver and the turbulence is modelled using the Reynolds-Averaged Navier Stokes (RANS) approach. Specifically, the re-normalized group (RNG) variant of the two equation k-ε model in combination with the O'Rourke and Amsden wall heat transfer model. As input for the liquid part of the models (i.e. the injection model), diesel2 from the CONVERGE library is used for to describe the properties of diesel. For the gas-phase diesel is treated as N-heptane (C_7H_{16}), a chemical surrogate. This is similar to Li et al. (2019) and common practice in engine simulations. The chemical kinetic mechanism used here is that of Chang et al. (2015). It includes a reduced skeletal n-heptane oxidation mechanism and a detailed methanol chemical kinetic mechanism containing 53 species and 176 reactions. The reason for the use of a simple surrogate is that diesel is a very complex fuel consisting of a mixture of molecules. It is a specific fractional distillate of oil of which the properties conforms to the diesel standard. In Europe this standard is EN590. Often N-heptane, or a simplified mixture of other hydrocarbons is used as a surrogate, because the Cetane number is close to that of diesel (Mansor, 2014).

The reaction mechanism includes NOx reactions which will be used to determine the NOx emissions, as this does not require the assumption of the NO to NO_2 ratio used in the CONVERGE calculations. The NOx is determined through the sum of the NO and NO_2, as these emissions are part of the NOx regulations (Ministry of Infrastructure and Water Management, 2003). For the soot emissions the empirical Hiroyasu model is used, coupled with the Nagle and Strickland-constable model. This empirical model determines the amount of soot based on the soot formation and oxidation rates with acetylene (C_2H_2) as the precursor for soot formation. According to Ibrahim et al. (2017) detailed soot models perform significantly better as empirical models tend to overestimate the soot production. However, the detailed models also increase the simulation time by a factor 3 to 6. Tang et al. (2018) also performed a similar comparison and found that, when using the RANS turbulence model the accuracy of the empirical Hiroyasu model is similar or even better than the detailed soot model. Only when using large eddy simulation (LES) to describe the turbulence the detailed soot model drastically outperforms the empirical model.

3.2.1.2: Meshing

The challenge in meshing is to minimize the number of discretization volumes without compromising the solution to much. CONVERGE has a very flexible approach and allows to have locally finer

discretization (smaller volumes). This local refinement can be set a priori (static) and be combined with an adaptive approach that does this dynamically (AMR).

The base mesh of the simulations is rather coarse with a cell size of 10mm. The local refinement is set to have a so-called 'max embedding level' set at 3. An embedding level means a 'halving' of the parent cell size. Hence, a level of 3 means in this case 10*(1/2)^3, thus a minimum mesh size of 1.25mm. For the spray area a fixed 4 scale embedding is used with a minimum mesh size of 0.625mm. The cell density at the start of simulation is similar to Kokjohn et al. (2011). In figure 3.2 shows an illustration of the static and dynamic mesh refinement procedure.

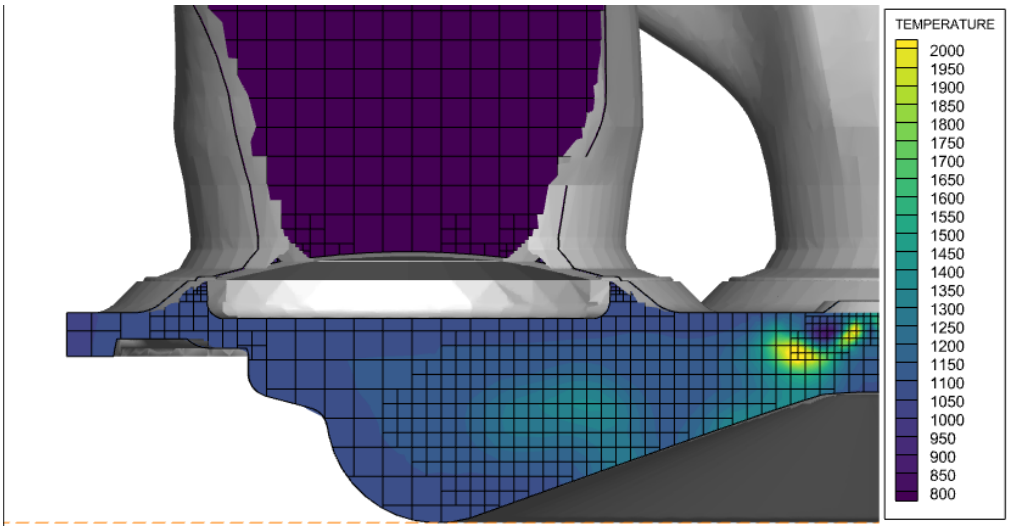

Figure 3. 2: An illustration of the meshing procedure. Indicated are the static refinement mesh with level 3 at the point where fuel is injected and the dynamic adapted mesh where the gradient of the Temperature was large.

To test the demands for the base mesh size a small sensitivity study is performed. Figure 3.3 shows the comparison between pressures traces and heat release rate (HRR) for simulations with a different base mesh-size in a standard diesel benchmark test. The pressure traces are almost identical and the HRR are also relatively closely matched. Similar to Y. Li et al. (2013) the coarse mesh has a slightly advanced and higher peak HRR. Interestingly the finest mesh has a higher peak HRR than the medium sized mesh. Table 3.3 shows the results of the mesh-sizes. The most obvious trend with increasing mesh resolutions is the decrease in GIE. Furthermore, there is a decreasing trend in indicated specific particulate matter (ISPM) and increasing trends in the indicated specific formaldehyde (ISFORM) and indicated specific unburned hydrocarbon (ISUHC) emissions. The other variables are balancing between the meshes. Increasing the grid resolution drastically increases the computing time by a factor 2.5 for the medium grid and a factor 7 for the fine grid. A sector simulation of part of the cylinder would reduce the computation time, but there is no symmetric slice with the spray and valve position. This would mean having to remove the valve from the geometry which is a significant source of ISUCH, indicated specific CO (ISCO) and ISFORM emissions in PFI engines. In Y. Li et al. (2013) the fine grid was not always closer to the experiments than the coarse grid, while most importantly similar trends were observed. It has been decided to run the coarse grid favoring computational time over the potential increase of accuracy, because the trends are most important and not the absolute values.

Table 3. 3: Simulation results for different meshes.

	CAD 10	CAD 50	CAD 90	MPRR	GIE	ISNOX	ISUHC	ISPM	ISCO	ISFORM
Unit	CAD	CAD	CAD	Bar/CAD	[%]	g/kWh	g/kWh	g/kWh	g/kWh	mg/kWh
10 mm	-1.19	3.10	11.14	12.3	47.1 %	14.3	0.014	0.0119	0.32	2.9

7.5 mm	-1.09	3.11	10.32	10.1	46.3 %	15.8	0.018	0.0083	0.41	4.5
5 mm	-0.90	3.12	9.91	10.7	45.4 %	15.7	0.033	0.0059	0.31	8.1

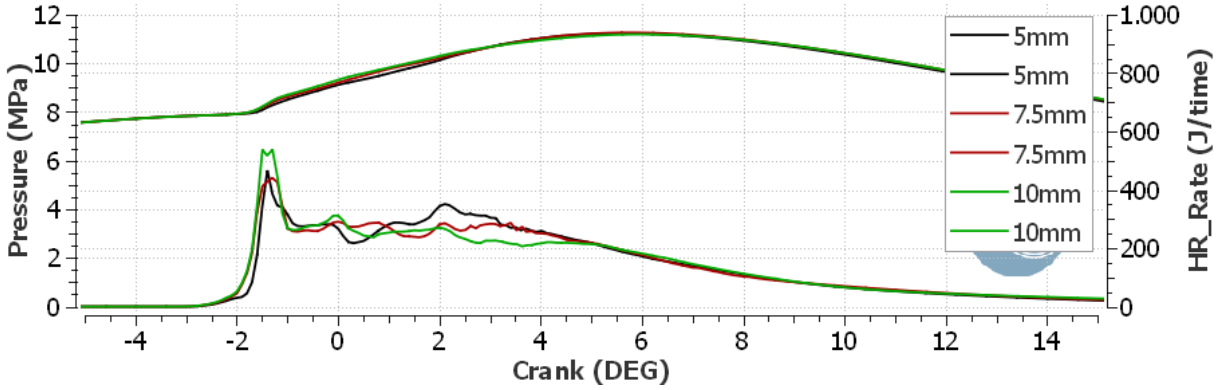

Figure 3. 3: Pressure traces and HRR for different meshes.

3.2.2: Case set-up and Key Performance Indicators (KPI's)

To test the performance of methanol-diesel dual fuel retrofit engines, both the diesel set-up and the dual fuel set-up are optimized. For the diesel optimization this consists of two parameters: the inlet pressure and the injection timing. For the dual fuel set-up two parameters are added: the MEF and in the last optimization cycle the inlet temperature. The injection timing is set directly in the spray model. The inlet pressure is set as the cylinder pressure at the start of the simulation, thus at the inlet valve closure. According to Sawant and Bari (2018) the inlet valve should be closed when the maximum amount of air is trapped, this is the case when the inlet pressure is equal to cylinder pressure. If the closure is retarded, the assumption of equal pressure still holds as air is squeezed out of the cylinder to match pressure. Only in the case of early inlet valve closure and pressure waves in the intake does this assumption not hold. The initial cylinder temperature is set at 400 K, in line with Y. Li et al. (2015) and Li (2019).

The amount of diesel and methanol used is determined by equation 3.1 and 3.2.

$$E_{req} = \frac{(P_{max} * load)}{N_{cylinders} * \frac{\omega}{60}} * \frac{1}{\eta_{assumed}} * 1000 \quad (3.1)$$

Equation 3.1 states the energy required per cycle per cylinder in J. The maximum power of the engine is 390 kW and the load is set at 35%. The MX-13 has 6 cylinders and the engine speed, ω, is set at 1200 RPM. The assumed efficiency of the engine is set at 40%.

$$m_{fuel} = \frac{E_{req} * E_{frac}}{LHV_{fuel}} \quad (3.2)$$

Equation 3.2 determines the mass of the fuel in kg, with E_{req} the required energy and E_{frac} representing the energy fraction of the fuel. The lower heating values (LHV) are of n-heptane and methanol, 44.9 MJ/kg and 22.1 MJ/kg respectively, are specific to the reaction mechanism and are calculated by CONVERGE. The amount of n-heptane is directly set in the Spray model. To keep the injection pressure at (nearly) 1800 bar, the injection duration is adjusted until the injection pressure is as close as possible to 1800 bar, with a maximum error of 0.5%. The amount of methanol is set through the mass fraction in the cylinder at the start of the simulation.

After each simulation the engine performance tool is used to determine the gross work, the pressure peak and CAD 10, 50, 90. The integrated heat release rate (IHRR) and the integrated apparent heat release rate (IAHRR) are extracted as well to provide a more detailed breakdown of the efficiency.

The HRR is the rate in which energy is released during the combustion process and is calculated through formula 3.3.

$$HRR = \frac{dQ_c}{dt} = \frac{\gamma}{\gamma - 1} * p * \frac{dv}{dt} + \frac{1}{\gamma - 1} * V * \frac{dp}{dt} \quad (3.3)$$

The apparent heat release rate (AHRR) is the heat release rate minus the heat losses as seen in formula 3.4.

$$AHRR = \frac{dQ_a}{dt} = \frac{dQ_c}{dt} - \frac{dQ_{HL}}{dt} \quad (3.4)$$

Both the HRR and AHRR are given in CONVERGE as dQ/dt and in integrated form as dQ. In experimental studies The AHRR is calculated from measured pressure data, while the HRR is determined through an empirical heat-loss model.

Equations 3.5 to 3.8 show the calculation of the combustion losses, heat losses and exhaust losses and gross work in percentages.

$$\eta_{combust} = \frac{IHR}{m_{fuel} * LHV_{fuel}} * 100 \quad (3.5)$$

The combustion efficiency is calculated by dividing the IHRR by the total energy in the fuel.

$$Heat\ loss\ [\%] = \frac{IHRR - AIHRR}{m_{fuel} * LHV_{fuel}} * 100 \quad (3.6)$$

The heat losses are calculated through the difference between the integrated heat release and the AIHRR. It is divided by the total energy of the fuel to convert it to percentages.

$$Exhaust\ loss\ [\%] = \frac{AIHRR - Gross\ Work}{m_{fuel} * LHV_{fuel}} * 100 \quad (3.7)$$

The exhaust losses are determined through the difference between AIHR and the gross work. This energy is not lost within the engine, but also not converted into work. It leaves the cylinder through the exhaust.

$$\eta_{gross} = \frac{Gross\ Work}{m_{fuel} * LHV_{fuel}} * 100 \quad (3.8)$$

The gross efficiency, η_{gross}, is the energy that is converted into work and is the performance measure used in the optimization process. It is the gross work as is does not include pumping and mechanical losses due to the fact that the intake and exhaust processes are not modelled in this study (closed cycle simulation).

The emissions outputs are given in kg and are converted to indicated specific emissions through formula 3.9.

$$Indicated\ Specific\ Emission\ \left[\frac{g}{kWh}\right] = \frac{Emission\ [kg]}{Gross\ Work} * 3600 \quad (3.9)$$

3.2.3: Experimental Design

Even though the experimental design concerns a steady state single point optimization, it can become complicated and time consuming. The optimization considers 2 to 4 continuous parameters. In theory one could map the performance with infinitively small accuracy, or at least to the level of the experimental error. However, doing so will increase the experimentation time to infinity. Therefore, use is made of statistical models to use less data while still obtaining high accuracy results. Still, acquiring the data can be a highly time consuming task as the number of tests required grows with Yates ordering (Ö. Andersson, 2012) as shown in formula 3.10.

$$n = x^y \quad (3.10)$$

With n the number of required tests, x the number of levels of variable and y the number of variables. This is an exponential formula and therefore the number of tests increases rapidly if more levels are added, and even more rapidly if more variables are added. This formula represents a full orthogonal design which means that every combination of variables is tested. This helps in the analysis of data as not only the direct effect of changing a variable can be tested, but also potential interaction effects. Luckily, it is possible to have all effects included while only using a part the combinations with a fractional orthogonal design (Ö. Andersson, 2012). Further reduction is also possible, but this comes at the cost of reducing the information that can be extracted from the data.

Table 3.4 shows a 3-factor full factorial design in which all combinations of main effects are run and all effects including the interaction effects can be determined. The interaction effects are obtained by multiplying the respective main effects. In a 3-factor half factorial design like in table 3.5 it contains only half of the runs. When these are grouped together it can be seen that the third and highest order interaction effect does not provide any information as it does not change over the runs. The second order interaction effects are confounded with the main effects and the first order interaction effects are confounded with one other first order interaction effect. For the confounded effects it cannot be determined which of the two effects is responsible for the change in results. This trend can also be used in higher factor designs. Also in those cases the highest interaction effects cannot be measured, the second highest interaction effect is confounded with the main effects and the third highest interaction effects are confounded with each other.

Table 3. 4: Example of a full factorial design.

Run	A	B	C	AB	AC	BC	ABC
1	-1	-1	-1	1	1	1	-1
2	1	-1	-1	-1	-1	1	1
3	-1	1	-1	-1	1	-1	1
4	1	1	-1	1	-1	-1	-1
5	-1	-1	1	1	-1	-1	1
6	1	-1	1	-1	1	-1	-1
7	-1	1	1	-1	-1	1	-1
8	1	1	1	1	1	1	1

Table 3. 5: Example of a fractional factorial design. The grey cell pairs illustrate indistinguishable effects.

Run	A	BCD	B	ACD	C	ABD	D	ABC	AB	CD	AC	BD	BC	AD	ABCD
1	-1	-1	-1	-1	-1	-1	-1	-1	1	1	1	1	1	1	1
2	1	1	-1	-1	-1	-1	1	1	-1	-1	-1	-1	1	1	1
3	-1	-1	1	1	-1	-1	1	1	-1	-1	1	1	-1	-1	1
4	1	1	1	1	-1	-1	-1	-1	1	1	-1	-1	-1	-1	1
5	-1	-1	-1	-1	1	1	1	1	1	1	-1	-1	-1	-1	1
6	1	1	-1	-1	1	1	-1	-1	-1	-1	1	1	-1	-1	1
7	-1	-1	1	1	1	1	-1	-1	-1	-1	-1	-1	1	1	1
8	1	1	1	1	1	1	1	1	1	1	1	1	1	1	1

When using continuous variable it is sometimes efficient to use a central composite design. This is a (fractional) factorial design including axial points, helping to identity non-linearity. However, the disadvantage is that these axial points require additional runs, namely two times the number of variables. The approach is depicted in the figure 3.4 below.

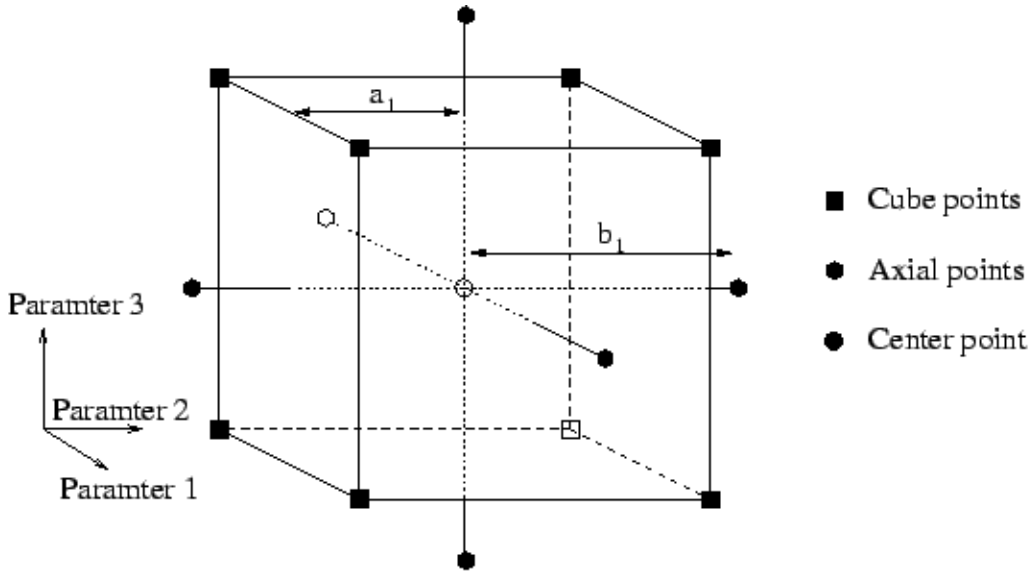

Figure 3. 4: Central composite design (Plasun, 1999)

The use of a central composite design is not considered efficient in this thesis, because only a small number of variables is analyzed. The axial points would be a large share of the total number of runs, while the non-linear behavior will also be captured by doing multiple optimization cycles.

For the optimization of the diesel set-up 2 variables are used and therefore no sensible simplifications are possible, resulting in 5 runs per cycle. The first cycle of the dual fuel will use three variables, which results in 9 runs when including a center run. When a fractional factorial design is used, the first order interaction effect is confounded with the main effects. This could be problematic as first order interaction effects are likely to have a significant effect. When including the inlet temperature, four factors are used. In this case a fractional factorial design is used, since this reduces the total runs from 17 to 9. This confounds 3-factor interaction effects with the main effects and each 2-factor interaction effect with one other 2-factor interaction effect. Since there is already data on each of the effects not related to the intake temperature, this approach only excludes information of the 3-factor interaction effects.

3.2.4: Optimization Approach

The literature about engine optimization can be divided in two streams. The first stream directly uses the simulations results as input for an optimizer. The second uses it as input to a model which in its turn is used for optimization. Generally, the second stream requires less input and it is elaborated in this section.

There are two types of models used: machine learning models or statistical models. The Artificial Neural Networks (ANN) is the model most commonly used among machine learning models. ANNs are found to accurately predict the engine performance if given sufficient data for training and testing (Atkinson & Mott, 2005). One of the biggest downsides of ANNs is that is uses a black box approach. ANNs do not provide a clear function between the input and output, making it difficult to find a relation between the ANN and what is actually modelled. It is also challenging to find the impact and relevance of the input variables (Beck et al., 2018). There are ways to “uncover” the relationships, however these are limited in their success. Generally, ANNS are found to perform the same compared to statistical models (Fang et al., 2015; King, 1999), with some studies finding that ANNs perform better (Tosun et al., 2016).

Another method is to use models derived from statistics. Most statistical methods use the same calculations as regressions. Linear regression uses an independent variable to predict a dependent variable, while using a linear fit. For multiple linear regression the mechanism is similar, but multiple independent variables are used. Interaction effects and higher order terms can be incorporated in linear regressions as long as the independent variable remains linear. In many cases this method can provide a reasonable model, however in very complex cases it can be necessary to resort to nonlinear regression. The latter is expected to have a better fit to the data, but it is more difficult to understand and interpret. Since, the goal is not just to measure performance but also understanding, linear regression is used to model the simulation output.

STATA is used to process the data and to build the regression model. A bidirectional elimination approach is used, with the commonly used threshold of p=0.05. However for the first iterations the significance threshold for the main effects is relaxed, due to the still very small dataset. The regression starts with the main effects, which are likely to be nonlinear. If applicable the nonlinear terms are added to the model. Then, the first order interaction terms are added. They are added one by one using the principle of forward selection (Myers, 1990). If this has been done for each variable the model is extended each time with the most significant interaction until all significant interactions are included. Then, a backward elimination (Myers, 1990) is performed starting with all the interaction effects, including the nonlinear terms if the residuals and scatter plot suggest the effect is nonlinear. The least significant interaction effect is dropped until all effects are significant. When both the forward selection and backward elimination have been performed both models are compared to see whether the final models are equal. If so, it is likely that all significant terms are included and this model is used for optimization. If this is not the case, the model with the highest R-squared is used to continue. The R-squared is used as it describes the goodness of fit between the model and the data. It does so by using equation 3.11.

$$R - squared = \frac{SS_{reg}}{SS_{tot}} = 1 - \frac{SS_{res}}{SS_{tot}} = 1 - \frac{(\sum y_i - \hat{y}_i)^2}{(\sum y_i - \bar{y}_i)^2} \quad (3.11)$$

The total variance is equal to the variance of the dependent variable. This means that the R-squared is the percentage of variance the independent variables in the model can explain. This is calculated by dividing the square of the difference between the predicted value and the actual value and dividing this by the square of the difference between the average and the actual value. This is then subtracted from 1 to give the R-squared.

In order to use multiple linear regression some assumptions should be fulfilled (Osborne & Waters, 2002). First of all, the independent variables should be independent and must not be highly correlated with other independent variables. If this is the case these variables could have conflicting effects. If independent variables are correlated, there is multicollinearity which can be tested using the variance inflation factor or VIF. The VIF is determined through equation 3.12.

$$VIF = \frac{1}{1 - R_2} \quad (3.12)$$

The R-squared in this case is the R-squared of a multiple linear regression in which one of the independent variables is predicted by the other independent variables. A rule of thumb is that none of the variables should have a VIF higher than 3 and the total VIF should be lower than 10 (Acock, 2011). The VIF is only tested for the main effects, as it is likely that the interaction effects are correlated to the main effects. Still, these should be included as the model is improved if interaction effects are causing the multicollinearity (Friedrich, 1982).

The other assumptions have to do with the prediction error. The regression model is should be homoscedastic, which means that the variance is equal along the variables and this is tested with the Breusch-Pagan or Cook-Weisberg Test for Heteroskedasticity. Secondly, the prediction error is assumed to be normally distributed and is tested with the Shapiro–Wilk normality test. When either

one of these assumptions fails a robust regression is used (Verardi & Croux, 2009). The robust regression estimates the variance and covariance of the error without assuming a normal distribution. It only changes the confidence interval and significance of the variables, generally reducing the certainty.

3.2.4.1: Finding the Optimum

There are a many different optimization approaches used in literature and can be divided in local and global solvers. The local solvers often use a gradient based approach in which a starting point is chosen and the solution moves towards the better result. The downside is that often a local optimum is found and that a different starting point could have resulted in a better solution. Global solvers on the other hand are designed in such a way that the best solution is most likely to be found. The most commonly used global optimizer is the genetic algorithm (GA).

The genetic algorithm is inspired by the theory of evolution. As in Darwin's survival of the fittest, an ecosystem consisting of variables with different values is simulated and each time they are scored on the optimization criteria. The best scoring sets of values are used to create the calibration of the next generation and this is done until the solution is sufficiently converged or a certain number of generations has been exceeded. In order to avoid local optima, there are also random changes in the variables. The optimum found is likely to be the global optimum (Costa et al., 2014).

3.2.4.2: Merit Function for Multiple Objective Optimization

The optimization goal is not only to maximize efficiency, but to minimize emissions and remain within the engine constraints as well. Therefore, a multiple objective optimization has to be conducted. A merit function, a function combining multiple functions for different dependent variables into a total score, is used for optimization. A similar approach to Badra et al. (2020) is used in which the criteria have certain thresholds and if it is exceeded the merit function is penalized. Each of the criteria has their own weight: 100 for the efficiency, 10 for the maximum pressure (P_{max}), 5 for the MPRR and 1 for each the emissions. In this thesis the weight for efficiency is reduced to 50 to put more emphasis on the emissions. The weight for the MPRR is increased to 10 to prevent practically infeasible optima.

Table 3.3 gives an overview of the weights and thresholds used. For the emission threshold a 10% margin below the Stage V emission standards for engines in inland waterway vessels is used (DieselNet, n.d.). Currently, formaldehyde emissions are not regulated in the EU. However methanol might give rise to higher formaldehyde emissions (Verhelst et al., 2019). Therefore, the California standard is used. The standards is 10mg/km, which has to be converted to mg/kWh (K. Zhao, 2019). When using 1.23 kWh/km for heavy duty trucks (Earl et al., 2018), this comes down to 12.3 mg/kWh.

To keep operating point within the mechanical limits of the engine the P_{max} is set at 220 bar and the MPRR is set at 15 bar/deg, similar to the HD engine used in Probst et al. (2019). Exceeding the MPRR is not necessarily problematic for the engine as CI engine are built for auto-ignition. However, a high MPRR could lead to severe engine noise.

Equation 3.11 gives the merit function, which is built out of the individual optimization formulas in the form of equation 3.12 and 3.13.

$$Merit = 100 * g\left(\eta^*_{gross}\right) - 10 * f(P^*_{max}) - 10 * f(MPRR^*) - f(sNO^*_x) - f(sPM^*) - f(sCO^*) - f(sUHC^*) - f(sCH_2O^*) \quad (3.11)$$

With:

$$g(parameter^*) = \frac{Parameter - Threshold}{Threshold} \quad (3.13)$$

$$f(parameter^*) = \begin{cases} \frac{Parameter - Threshold}{Threshold}, & if\ Parameter > Threshold \\ 0, & if\ Parameter \leq 0 \end{cases} \quad (3.14)$$

The final step is the creation of response surfaces and contour plots to investigate the influence of the different variables and to determine the ranges for the next round of optimization. This process continues until high enough confidence is achieved about the optimum outcome.

Table 3. 6: Overview parameters with their respective weight and threshold.

Parameter	Weight	Threshold
Gross Efficiency	50	40%
Maximum Pressure	10	220 bar
MPRR	10	15 bar/deg
$ISNO_x$	1	1.62 g/kWh
ISPM	1	0.0135 g/kWh
ISCO	1	3.15 g/kWh
ISUHC	1	0.17 g/kWh
$ISCH_2O$	1	12.3 g/kWh

3.2.5 Example of the Procedure

The first step of the procedure is the experimental design. For the first cycle diesel benchmark optimization a full factorial design is used with a center point run. It is a two factor design, therefore it has 5 runs. For the first cycle an inlet pressure range of 1.5 to 2.5 bar is used and a SOI of -15 to -5 ATDC. Table 3.7 shows an overview of the first round design. The inlet pressure is given in MPa, because the pressure in CONVERGE is given MPa.

Table 3. 7: Experimental design first optimization cycle diesel benchmark.

Run	PINLET [MPa]	SOI [ATDC]
1	0.2	-10
2	0.25	-5
3	0.25	-15
4	0.15	-5
5	0.15	-15

The runs of Table 3.7 are performed in CONVERGE and the results are then processed in Stata. The first step is to look the scatter plots of the dependent variable with all the independent variables to see whether there is a clear visual relation between the variables. From figure 3.5 and 3.6 it can be derived that the change in SOI has a bigger effect on the GIE than the change in inlet pressure. Next to that, the inlet pressure in figure 3.5 appears to have a rather linear effect on GIE, while there seems to be some indication of a non-linear effect for the SOI in figure 3.6.

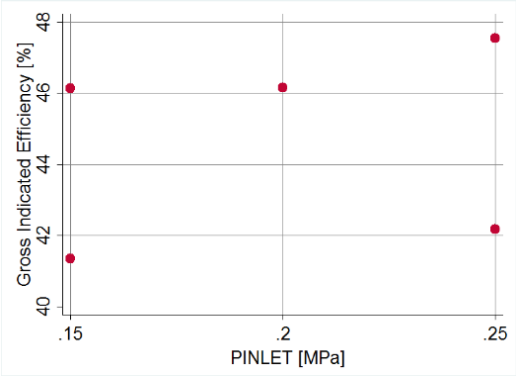

Figure 3. 5: GIE and PINLET scatter plot.

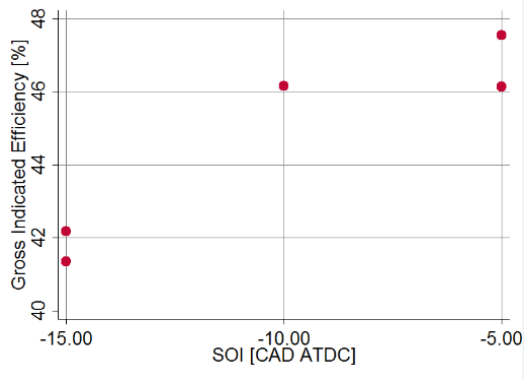

Figure 3. 6: GIE SOI scatter plot.

Then, a regression analyses is performed as explained in section 3.2.4. The bidirectional elimination approach is used, thus the regression model is build by both adding effects from the most basic model and eliminating effects from a model including the potential non-linear and interaction effects. This results in the regression model in table 3.8.

Table 3. 8: Regression model GIE first cycle diesel benchmark optimization.

GIE	Coef.	St.Err.	t-value	p-value	[95% Conf	Interval]	Sig
PINLET	.113	.029	3.88	.161	-.257	.482	
SOI	-.01	.003	-3.74	.166	-.043	.023	
SOI2	-.001	0	-5.72	.11	-.002	.001	
Constant	.416	.012	33.69	.019	.259	.572	**
R-squared		0.997	Number of obs			5.000	
F-test		118.011	Prob > F			0.068	

**** p<.01, ** p<.05, * p<.1*

This regression model consist of a linear term of the inlet pressure and SOI and a quadratic term of the SOI, indicated by SOI2. If there was a significant interaction effects this would have been indicated by PINLET#SOI. The predicted GIE can be obtained by multiplying the values of the independent variables by their coefficient. None of the effects, except for the constant, is significant at the commonly used p-value of 0.05. That means that there is a larger than 5% chance that the results could have occurred by random chance. However, in the first optimization cycles it is difficult to achieve significant results, because there are very few observations. Therefore, the 0.05 p-value is less strictly enforced. If a quadratic term or second order term changes the significance of the main effects, a nested regression is performed to see whether the addition of that term significantly improves the model.

Overall, the regression model in table 3.8 explains the variance in the GIE extremely well with an R-squared of 0.997, explaining 99.7% of the variance of the GIE. Still, the overall model is not significant as Prob > F is only 0.068. This is not considered problematic for the first cycle as it only contains 5 observations. In the third optimization cycle a very similar regression model is obtained as seen in table 3.9, but this time all variables are significant with p<0.001.

Table 3. 9: Third cycle diesel benchmark optimization.

GIE	Coef.	St.Err.	t-value	p-value	[95% Conf	Interval]	Sig
PINLET	.146	.005	27.84	0	.134	.158	***
SOI	-.002	0	-10.46	0	-.002	-.001	***
SOI2	0.0003	0	-6.67	0	0	0	***
Constant	.437	.001	396.96	0	.434	.439	***
R-squared		0.991	Number of obs			12.000	
F-test		306.949	Prob > F			0.000	

**** p<.01, ** p<.05, * p<.1*

Lastly, the regression models are tested for the assumptions behind the regression analysis. With the IM-test the regression model is tested for heteroskedasticity and normality. The homoscedasticity is assessed by testing the residuals for normality and the independence is tested with the VIF. If one of the tests fails a robust regression analysis is performed.

When the regression models for all independent variable from table 3.6 are determined, they are exported to Matlab. There they are used as input for the merit function, which is then optimized through the GA. The results of the GA are used as a direction for the next optimization cycles. In Matlab response surfaces are made from the regression models to visually show the effects found in the regression analyses.

3.3: Operationalization of the Transition Framework

The approach in answering the third sub question: "What are the opportunities and barriers for different stakeholders in the sustainable methanol ecosystem and how can these be exploited or overcome?" is inspired by the framework of Walrave et al. (2018). They suggest combining ecosystem theory with MLP and SNM for pathbreaking innovations. This would ensure that not only internal alignment is achieved, but also external viability. In this thesis the framework of Walrave et al. is operationalized through the perspective of the inland shipping industry instead of a single actor.

The first step is mapping the value blueprint of diesel. The diesel value blueprint is obtained by analyzing reports and articles discussing the diesel and LNG network in the shipping sector. A separate analysis was conducted for the fuel supply chain of oil, gas and methanol as this plays a major role in the value blueprint. Then, this blueprint is adapted to represent the value blueprint of methanol. The adaptations are based on work by the Green Maritime Methanol consortium and personal conversations with a consultant renewable chemicals & fuels at the Port of Rotterdam. The mapping of the blueprints is limited to the most important activities of the EVP. These consist of the oil and gas production routes, with a discussion of the alternative, more sustainable, production routes. The mapping of the actors in the ecosystem is limited to actor groups with examples of certain actors within that group. The global differences between the diesel and methanol EM and EVP are discussed before the methanol value blueprint is assessed. In the assessment attention is paid to both the barriers and opportunities of methanol compared to diesel, LNG and hydrogen.

The barriers and opportunities are qualitatively and where possible quantitatively assessed. For all activities of the EVP a literature search is conducted to find the barriers and opportunities. This literature search is enriched by unstructured interviews to increase the understanding of the activities. Among the interviews are the CBRB, the branch association for inland shipping, and the Methanol Institute, the branch association for methanol producers. To help understand the retrofitting process and the impact on ship operations interviews were held with Menno Mertz, engine researcher, and Prof. Sebastian Verhelst, engine researcher and coordinator of Fast Water.

The quantification is limited to the emissions and the commercial aspects of the different fuels. The scope of the emissions is limited to the fuel, which is investigated on a Well-to-Wake (WTW) basis of the fuel, with separate attention for the Well-to-Tank (WTT) and Tank-to-Wake (TTW). Where possible a single comprehensive report is used to ensure consistency in the methodology. If this is not available a collection of sources is used to gain a comprehensive image of the costs or emissions.

The next step is an in-depth analysis of the dynamics within the ecosystem, using the MLP. A recap will be given of the landscape forces pressuring the regimes, but more interestingly the dynamics between the niches and regimes are discussed. The scope of the MLP is not limited to the fuels discussed in the assessment of the barriers and opportunities. This analysis shows how the different emerging and current technologies align and interact.

When the barriers and opportunities and the ecosystem dynamics are clear, the situation is analyzed through the lenses of ecosystem theory, MLP and SNM. The application of the three theories provides lessons on how the transition to methanol as a fuel should be could be managed.

3.4 Methodology Recap

This chapter discussed the methodology used to answer the three sub questions. Section 3.1 showed the approach used in determining for which HD applications methanol provides a solution. This is determined by analyzing for which applications electrification is not feasible option, through analyses based on the state-of-art of the current electric pilot cases and calculations of the energy storage calculations. The latter calculates the weight and size of the energy storage required for the currently required operating profile. This is calculated for electrification, diesel, methanol and for inland shipping natural gas as well. Then, in 3.2 the approach used to determine the potential of a retrofitted methanol-diesel PFI engine compared to its diesel operation is discussed. It is explained how CFD

simulations are performed on a digital twin in CONVERGE and how it is optimized through cycles of DoE and GA algorithm optimization. Lastly, section 3.3. addressed how the value blueprint of diesel and methanol are established based on report and interviews and how this is used to determine the challenges and opportunities for methanol compared to the most common alternatives. Finally, it is discussed how innovation ecosystem theory, MLP and SNM are used to draw lesson how methanol as a fuel could be managed. In the next chapter SQ1 will be answered through the approach discussed in section 3.1.

Chapter 4: Electrification frontier

This chapter provides answers for which applications methanol may provide an option by determining for which applications electrification is not feasible option. The approach discussed in section 3.1 is followed for applications in road transport, agricultural machinery and inland shipping.

4.1: Road Transport

As already seen in the electrification roadmaps of Chapter 2, road transport is one of the most discussed modalities. Most roadmaps indicate that passenger cars will be electrified quite rapidly taking over the market completely before 2050, while also the short distance cargo could follow soon. However, for long haul heavy duty trucks ICEs were expected to remain dominant. VMS Insight (2019) came to a similar conclusion for the Dutch market.

When comparing the electric trucks with the current diesel trucks in figure 4.1, it can be seen that the engine power is on par for similar classifications of trucks. Electric trucks even have a higher peak power. Next to that, electric trucks only have a Gross Combined Weight Rating (GCWR) of 36-40 ton. Diesel trucks often have GCWRs of 50 ton, equal to the maximum weight in the Netherlands (International transport forum, 2011). Some have an even higher GCWR and can be used for special purposes.

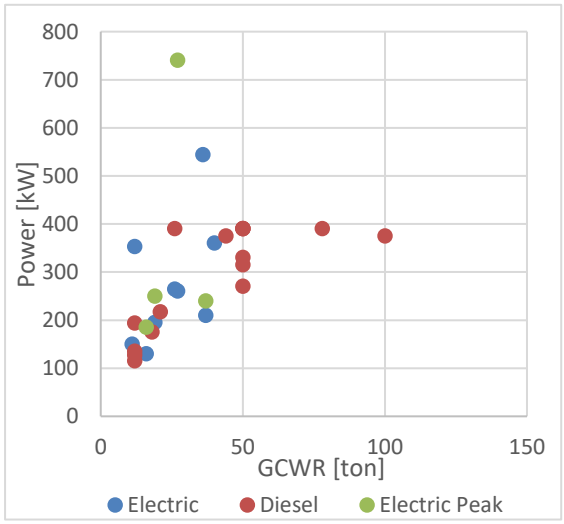

Figure 4. 1: Comparison of electric and diesel trucks in the power to GCWR ratio.

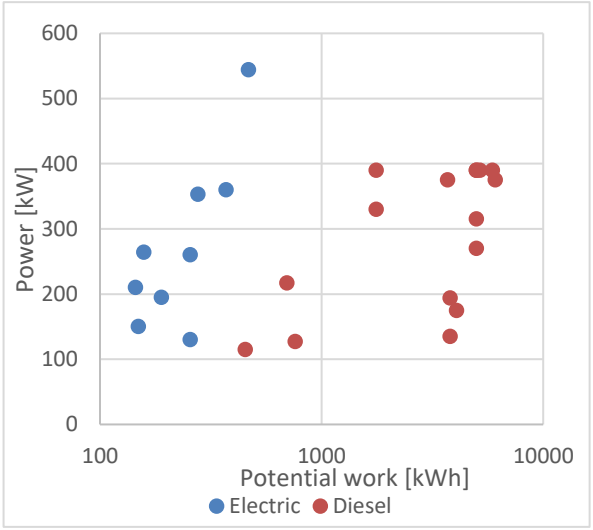

Figure 4. 2: The ratio of power to potential work stored for electric and diesel trucks.

If the power and the potential work of the energy storage are compared in figure 4.2, it can be concluded that the potential work is a lot higher for diesel trucks. The electric trucks are approaching the capacity of medium duty (MD) urban trucks. This means that the range of diesel trucks, under the same conditions, is significantly larger. This allows diesel trucks to be more flexible in its operations and refueling strategy.

Many of these pilots are focused on short distance and urban transport and have a maximum range of 200 km with some of the later projects aiming for 400 km. This is not enough for long haul transport as they often have to travel up to 800 km a day ("Big Rigs Begin to Trade Diesel for Electric Motors - The New York Times," n.d). For electric trucks to replace long haul trucks they need to be capable of transporting 50 ton over a distance of 1000-1400 km. Elon Musk is claiming that his Tesla Semi will have a range of 800 km, with an expected 1MWh battery. Originally, expected for 2019 Musk claims that it is ready for production in 2021 (Etherington, 2021).

The problem with the low energy density is that the battery takes up a lot of space and weight that will come at the cost of cargo that can be transported. In most EU countries the maximum weight for trucks is 40 or 44 ton with some exceptions like Sweden that allows up to 60 ton. On the Dutch roads a maximum of 50 ton is allowed (International transport forum, 2011). That means that every ton of additional weight comes at the cost of a ton of cargo that can be transported.

However, the electrification of trucks does not necessarily make it heavier as the electric drivetrain has a typical weight of around 400-500 kg, while the typical drivetrain of a truck weighs in the order of 1.5-2 ton (Mareev, Becker, & Sauer, 2018; US Office of Energy Efficiency & Renewable Energy, 2010). So, without considering the batteries an electric truck has a weight advantage compared to the diesel truck. However, the batteries make them heavy as can be seen in figure 4.3. If the driving range 36 ton truck is increased it clearly comes at the cost of cargo until at one point more batteries are transported than cargo. For city trucks this does not really pose a major problem as they do not require a large range, but for long haul trucks it certainly can become a problem.

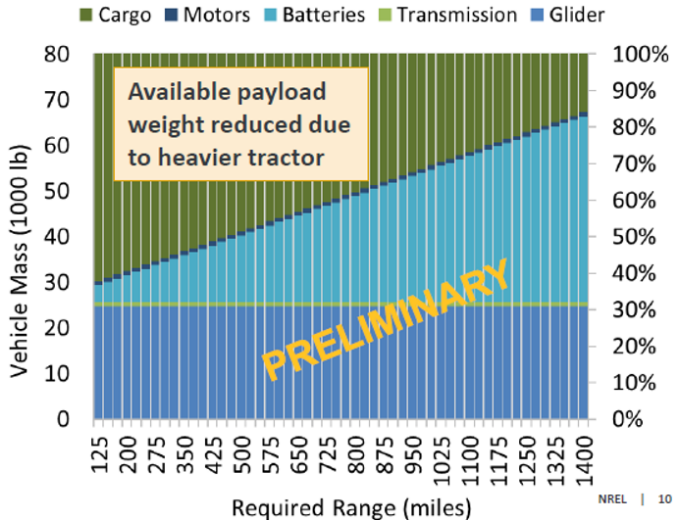

Figure 4. 3: Driving range and weight distribution of a battery electric truck (Hunter & Penev, 2019).

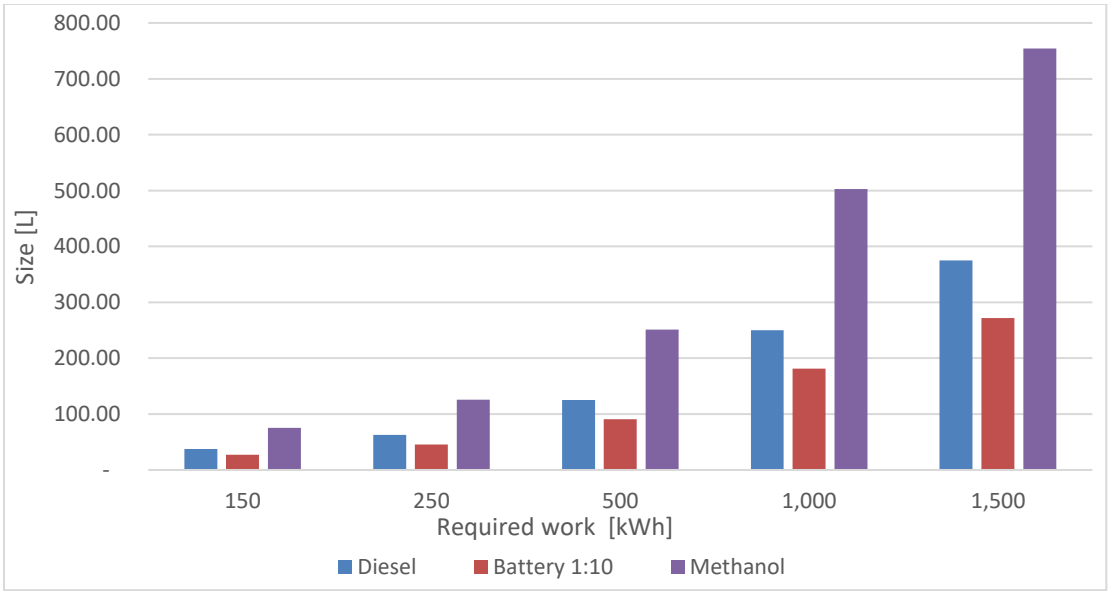

Figure 4. 4: Storage size comparison for trucks. The battery size has a scale of 1:10.

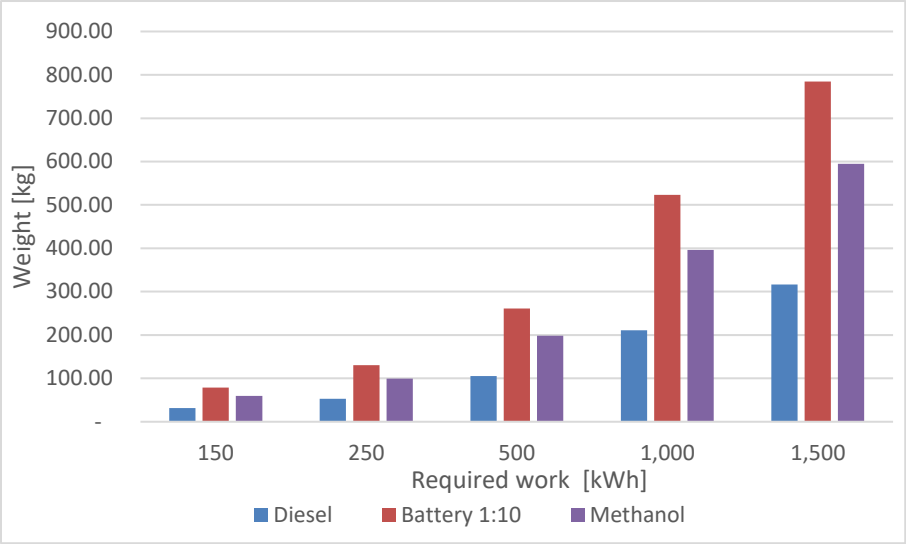

Figure 4. 5: Storage weight comparison for trucks. The battery weight has a scale of 1:10.

Figures 4.4 and 4.5 show the effective work, so the work delivered to the wheels, up to 1500 kWh. When looking at a DAF 12 ton city truck with the tank of 127 L it could deliver just over 500 kWh of work. If this is electrified this would require a 907 L battery, 780 L more than the diesel alternative. However, due to the smaller size of the electric drivetrain and the possibility to use multiple smaller batteries, this increase in size cannot be considered a major problem for this application (Mareev et al., 2018). The weight of the battery could provide an even bigger challenge as the battery would increase the weight by just over 2.5 ton. For HD truck the drivetrain weight savings can be up to 1.5. Since the MD truck only has a third of the engine power, the savings will be smaller as well. If the drivetrain change would save 750 kg, the electric truck would still weigh 1.75 t more. This is a very significant reduction of the cargo capacity and can be considered infeasible. However, there is potential to reduce the battery capacity. Firstly, the electric truck can regenerate some energy under braking (W. Zhang et al., 2019). Secondly, the efficiency curve of electric engines is relatively flat compared to diesel engines, gaining advantage in transient operation (Hjelkrem et al., 2020). Lastly, the required work of a truck can be reduced through optimization of the battery capacity to the application. Due to the high energy density of diesel it is attractive to slightly oversize the tank for the required application as it does not pose a big trade-off in space and weight. The electric trucks in this segment carry about 30-50% less energy. This means that they have the same weight with a significantly reduced action radius. The reported action radius of these trucks is 100-300 km and are likely to require daily charging.

When looking at HD trucks, the problem drastically increases if a one-to-one substitute is required. These trucks have 200-600 L tanks, which translates into a range of 1-3 MWh of potential work and a battery of 5-15 t. For long haul HD trucks 1000-1500 L tanks are used, which translates in a potential work of at least 4 MWh and a battery of at least 21 t and 7 m^3. It is clear that all heavy duty trucks require right sizing of the battery for daily operations.

For the pilot cases 350 to 550 kWh batteries are used for 40 ton trucks and have a reported action radius of 200-400 km, which would be sufficient for urban applications. This would limit the weight increase to an acceptable 0 to 1 t. Right sizing the battery for every application is therefore crucial for electric trucks. However, when considering long haul trucks carrying a full 40-50 ton over 800 km a day, the minimum requirements are more challenging. Until Tesla's ambitious plan for chargers over 1 MW is realized (Lambert, 2020), the distance should be driven on a single load. Earl et al. (2018) state that a new aerodynamic truck has a road load 0.98 of kWh/km during highway cruising. Thus, in an optimal situation this would require only 784 kWh of work. A realistic bare minimum would be about 1 MWh of work. When subtracting a drive train weight advantage of 1.5 t, this results in a weight increase of 3.5 t. which can be considered reasonable. However, this would be the absolute minimum

performance required of long haul HD trucks. As the actual energy use of the truck would be 1176 kWh it needs at a rate of 84 kW to fully recharge during required 14 hours off for truck drivers. This requires an extremely well-developed charging infrastructure throughout the EU as every truck needs a charger at its immediate disposal at every stop. This charging network is greatly exceeding the expectations of the next decade (Mathieu, 2020). Alternative, the battery capacity could be increased, but this would greatly decrease the loading capacity of the truck.

Electrification of trucks will without a doubt change the operating profile of all trucks. Due to the high energy density of diesel there was only a limited trade-off between extra range and extra weight. If right-sizing takes place for daily operation and the infrastructure is appropriate for overnight charging both MD and HD urban trucking could reasonably be electrified, provided that the infrastructure is available. If all traffic is electrified this requires a significant upgrade of the electricity grid and production capacity (PBL, 2018). Until great advances are made in the energy density of batteries the long haul trucks are not likely to be electrified. Nonetheless, there is still the option to use hybrid trucks. Electric engines are relatively light and it only requires a small battery. The size of the engine could be reduced to just above the nominal required power to save weight. A small electric engine could be used to provide the peak power required during acceleration or when climbing a hill and to profit from regenerative braking.

4.2: Agricultural Machinery

The agricultural mechanization is one of the sectors that is difficult to electrify due to the relatively high power required by the machinery for sustained periods of time. When comparing the electric, hybrid and diesel tractors it can be seen in figure 4.6 that there is a relatively linear relationship between the power of the tractor and the maximum allowed weight. The lower left electric tractor is the Vario E100 and has a peak power of 150 kW exceeding the diesel tractors in that segment. The second electric tractor is the Concept SESAM of which it is not known whether the 300 kW is peak or nominal power. It is assumed to be peak power as it exceeds its diesel variants in the same weight class. Overall, the tractors have a similar power to weight ratio.

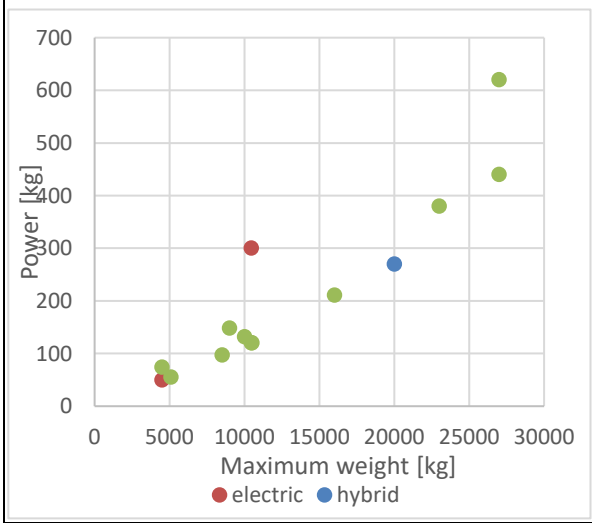

Figure 4. 6: Power versus maximum weight of electric, hybrid and diesel tractors.

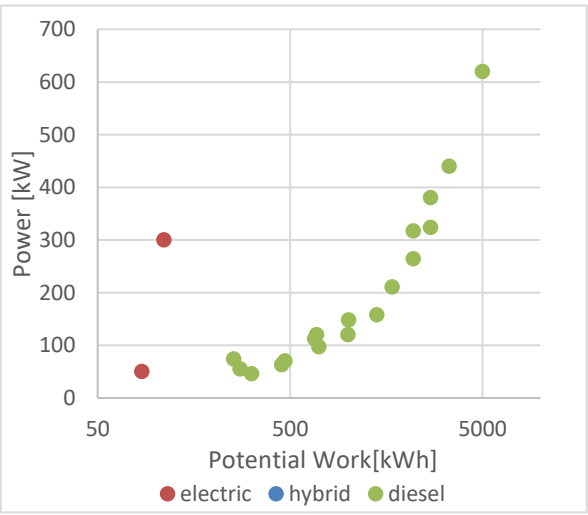

Figure 4. 7: Power versus potential work of electric, hybrid and diesel tractors.

When comparing power and maximum weight, the electric and hybrid tractors are on par or even have an advantage due to the peak power of electric engines. However, this changes when looking at the potential work that they can perform in figure 4.7. The electric tractors have a far lower capacity to perform work than the diesel tractors. The Vario E100 is still relatively close to the diesel tractors in the same category, but still there is a factor 3 difference. The Concept SESAM is far off compared to similar diesel tractors. With a maximum reported operating time of 4 to 5 hours for electric tractors,

the amount of work that could be done on a day is significantly smaller than that of a similar diesel tractor.

When considering the electrification of a tractors with similar performance to diesel tractors, the biggest challenge is the battery capacity. This can be seen in the comparison between electric and diesel tractors, the main difference is in the potential work stored as seen in figure 4.7. Batteries are big and heavy and every kg of extra weight would make the tractor tire sink deeper in the ground increasing the rolling resistance and thus the energy use. However, equally important is maximum weight since a tractor that is too heavy could exert too much pressure on the ground damaging to the soil characteristics (Du et al., 2018). To prevent this bigger tires are necessary which on its own increases the rolling resistance.

Therefore, it is important to calculate the impact of changing the ICE drivetrain to an electric drivetrain. Figure 4.8 displays the size of the storage for relatively small tractors. The smallest tank in the series of diesel tractors investigated is 76 L, corresponding to roughly 250 kWh. When comparing this to the size of a battery it would require 453 L. So, even for a small tractor it can be challenging to integrate the battery in the tractor design. A bigger challenge is the weight as displayed in figure 4.9. The equivalent of 250 kWh in diesel weighs only 62.5 kg, while the battery weighs 1307 kg, almost 1250 kg more. However, the energy storage is not the only piece of the puzzle as the drivetrain also needs to be replaced and this is an advantage of the electric tractor. The John Deere 5065E 2017 edition, used in the example of Du et al. (2018), has a drivetrain and tank that weighs 581 kg and takes up 532.5 L. The electric replacement only weighs 317 kg and takes up just 137.5 L. This indicates that the battery size of smaller tractors is not a big issue, since the electric drivetrain saves almost as much space as the battery requires. However, in terms of weight it only reduces the extra weight from about 1250 kg to just over 1000 kg. With the truck weighing 3300 kg and a maximum weight of 5100 kg, this reduces the vertical load of the tractor by 50%. One of the important aspects to look at is the actual required work for the tractors applications and to see if a smaller battery will suffice for the application in mind. This is done with the Fendt E100 Vario, as it has an energy storage capacity of only 30% of its diesel variants. This allows an operating time of 5 hours and it only increases the weight by 142 kg compared to the diesel alternative.

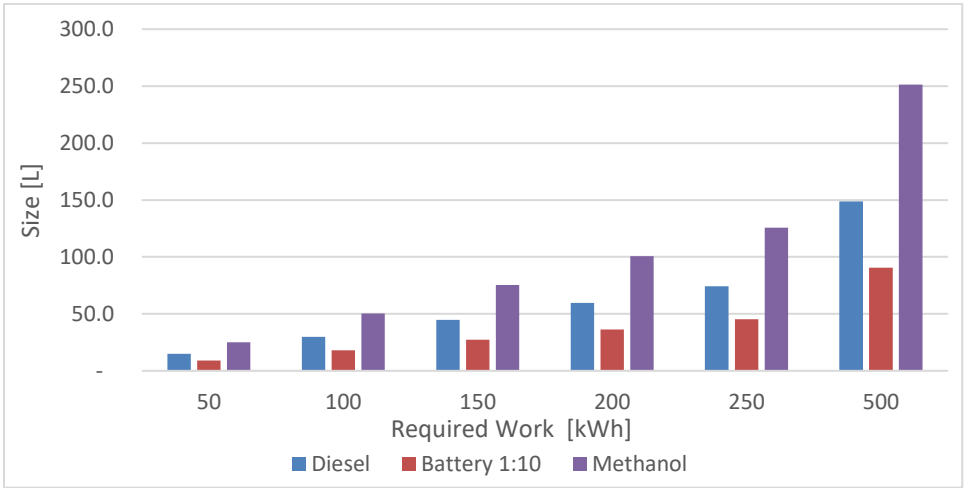

Figure 4. 8: Energy storage size for the potential work that can be performed.

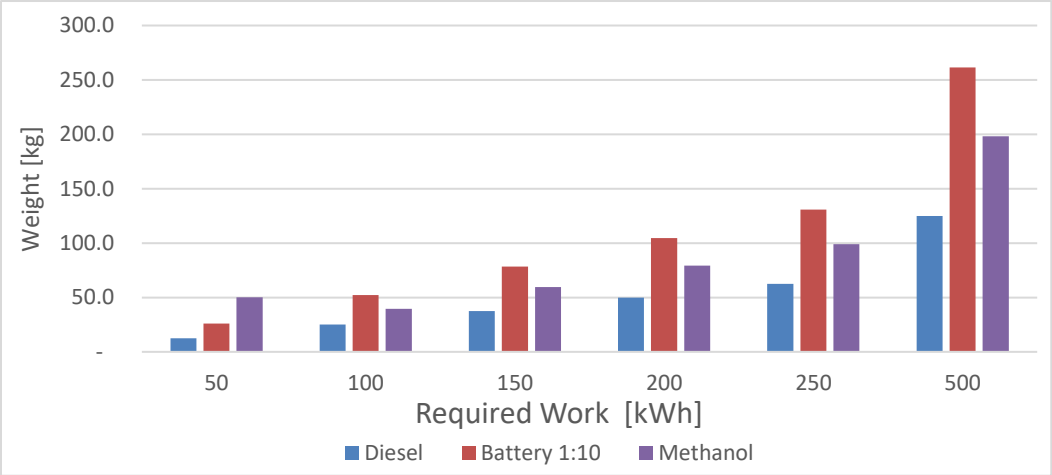

Figure 4. 9: Energy storage weight for the potential work that can be performed.

The example of the E100 Vario is just a relatively small tractor. There are tractors with tank sizes 15 times larger like the John Deere 9260R with a tank of 1490 L. Naturally, the engine weight savings are larger, but this is in no proportion against the weight gains of the battery. The 620 kW engine of the 9620R weighs 1,365 kg, 4 times the 5065E engine. If every part of the drive would be 4 times as heavy, the total drivetrain weight would be 2400 kg. The equivalent energy is equal to 5000 kWh and this would correspond to a 26 ton battery and it taking up 9 m^3 as seen in figure 4.8. In this case the drivetrain savings are negligible compared to the extra weight of the battery. If the same storage capacity factor is used as for the Fendt E100 Vario, this still comes down to a weight increase of about 7.5 ton after correcting for the lighter drivetrain.

With the current technology and the battery developments expected in the next decade tractors will be difficult to electrify. It is currently possible to electrify smaller tractors with a nominal power up to 50 kW with some limitations in its operating capabilities compared to diesel tractors of the same size. Electrifying larger tractors can be considered impractical. Nonetheless, hybridization is an option for larger tractors as the battery capacity can be limited and the additional weight of electric drivetrain can be compensated to some extend by the decrease in engine size as the ICE only has to be fulfil the nominal demand. For tractors, hybrids could be a way to increase efficiency as the efficiency curve is rather flat and the ICE can perform at its maximum efficiency point. However, for single purpose applications, like harvesters, it might decrease the efficiency or unnecessarily increase weight, since the engine can be optimized at a very specific operating point.
Electrification agricultural machinery is not possible if the operating time of diesel tractors is used. However, if the operating times can be reduced like what has been done with the pilot cases, electrification of smaller tractors is possible. Due to the limited battery capacity (100-130 kWh), it is also possible to charge them during a break if an ultra-fast charger is available, making full day operation possible. However, for larger tractors the weight increase is too severe even with a 30% reduction in energy storage. Next to that, the battery cannot be recharged during unless MW chargers would be available. With the diesel tractor the energy capacity is roughly the rated engine power for 10 hours, thus a reduction beyond 30% will result in insufficient energy as farmers use their equipment for up to 10 hours a day during some periods each season. The only way to electrify these applications is to autonomize the machines and to use multiple smaller autonomous machines to do the work. Even though electrification is not possible there is enough overcapacity to use fuels like methanol with an energy density of 50% compared to diesel.

4.3: Inland Shipping

In the electrification roadmaps shipping is considered to be one of the most difficult to electrify modalities and only aviation is considered more challenging. However, there are opportunities for electrification in inland shipping. When comparing the electric ships it is quite remarkable to see the

difference in estimated range with their respective battery capacity. The Yara Birkeland can carry 120 TEU, has a battery capacity of 7 MWh and a range of 120 km. The Port-liner EC110 will have a similar battery capacity, but with a load of 280 TEU and an expected range of 230 km. Naturally, the range is dependent on the cruise speed, current and elevation. It is stated that the Port-liner is built for low current rivers of the Netherlands and Belgium and the Yara Birkeland is built for short sea shipping as well, which may explain some of the difference.

In figures 4.10 and 4.11 the respective size and weight of the energy storage with their potential work stored are visualized for typical inland shipping vessels. Inland LNG vessels typically have tanks of 40 to 160 m^3 (LNG Masterplan Consortium, 2015), while a typical 110m diesel vessel has a tank of 57m^3 (Zomer et al., 2020). Electrification with the same operating profile, 112.5-450 MWh, would require a battery of 588-2353 t and 204-816 m^3. With inland shipping vessels having a typical DWT of around 3000 t, the batteries would take up a significant share carrying capacity of the vessels. In terms of size this is equal to 6-25 containers. When looking at the operating profile of a fully loaded diesel vessel, it can sail a roundtrip Rotterdam to Basel almost 3 times, while a push barge requires 32 m^3 of diesel for its roundtrip Antwerp-Basel (Zomer et al., 2020). Thus, it can be concluded that most vessels have an oversized tank, indicating that similar storage size can be used for lower density fuels like methanol. However, the energy density of batteries is not in the order of a factor 2 smaller like methanol, but a factor 14 in size and 51 in weight.

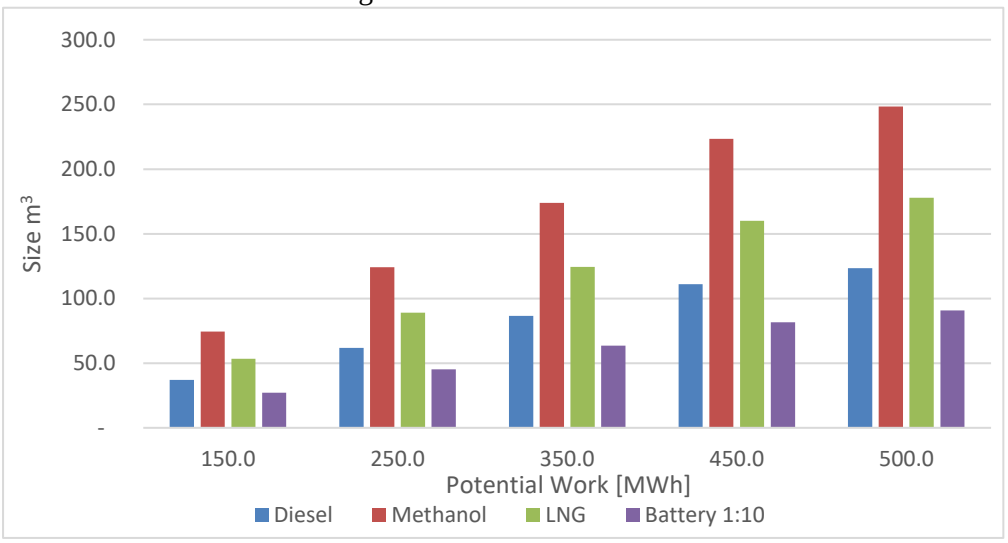

Figure 4. 10: Energy storage size for the potential work that can be performed.

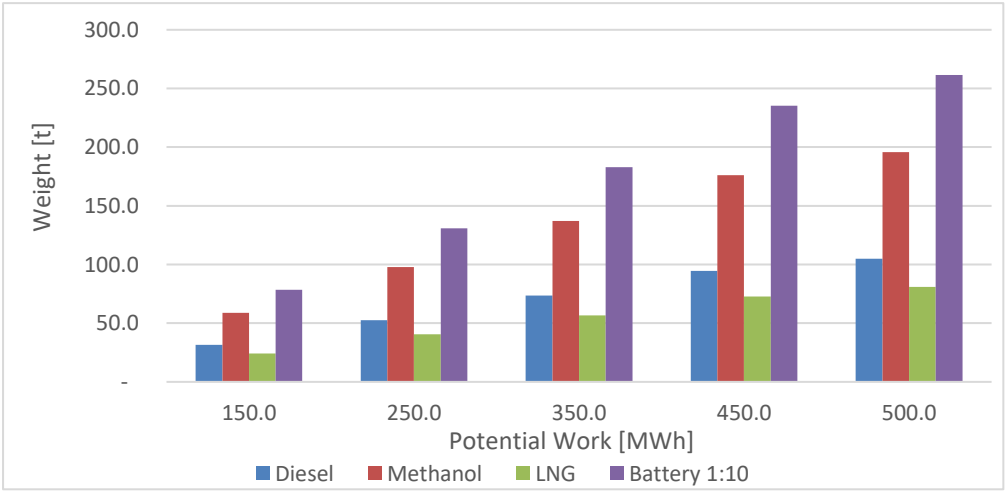

Figure 4. 11: Energy storage weight for the potential work that can be performed.

If the diesel example is used with a similar storage size, it would still increase the weight by 116 t. More importantly, it would require the ship to stop 3 times to swap the batteries on a roundtrip Rotterdam-Basel, instead of up to 3 roundtrips for diesel. Fast charging is not an option, because it would take a staggering 72 MW charger to recharge in 30 minutes. So, while it is technically possible with battery swapping it can be considered impractical and it is questionable whether this meets the performance requirements set by shippers.

The major advantage of the electric cargo ships versus other modalities is that there is often space on a ship to place the containers with batteries instead of having to integrate them as part of the vessel. This makes it possible to swap the batteries at a port instead of having to wait until the batteries are charged. The MEC consortium is building its business model around this. By providing "Pay-per Use" battery containers the capital investment of electrifying a ship is reduced. The twenty feet containers weigh 20-22 t and have a gross energy capacity of 2 MWh and a net energy capacity of 1.6 MWh (Kruyt, 2019). This is considerably less than the Tesla battery used for the calculation in this thesis, which would only weigh 8 t and take up 2.8 m^3, which are high-end batteries and do not take into account the cooling and structure of the set-up. Another major challenge is getting the appropriate charging infrastructure in place (Duurzaam Bedrijfsleven, 2018; Schootstra, 2018). Ports are already investing a lot in increasing the power supply of the ports and other locations along the routes. It is challenging as ships often have a power of more than 1 MW and can operate 24 hours a day (Roldán, n.d.). It is expected that this will first be operationalized for certain shipping corridors.

It is clear that for the foreseeable future electrification in inland shipping has to be limited to short distance point-to-point shipping. Current pilots focus on distances below the 200 km and on fixed routes as the infrastructure has to in place. For distances beyond the 200 km the batteries become too large and heavy or operating profiles have to be adjusted. For theses distances hybrid ships might be a better solution. This allows for sailing electrically in emission zones and for short range purposes, but it can use a higher density fuel for the long range. Besides, a hybrid configuration can decrease the size of the ICE motor as they are often oversized to allow the ship to be used for multiple purposes on different rivers (Panteia, 2019). Next to that, it can optimize the efficiency of the ship as the efficiency curve per load point is rather flat for electric engines compared to ICE engines (Panteia, 2019). There are already more than 40 diesel-electric or hybrid ships. An example is the Sendo Liner a 164 TEU 110m ship which can sail up to 3 hours on batteries with its 564 kWh battery (EFIP, 2019). 95% of the time it can sail on just one of its 425 kW generators, which powers the battery or the 2 electromotors of 350 kW each (Sendo Shipping, n.d.).

4.4 Recap

For all three modalities the conclusions are similar: if there is no significant change in operating profile or extreme changes in infrastructure, electrification will be limited to short range solutions. In all of the applications there is an overcapacity in energy storage of diesel, because there is a very small trade-off between storage size and weight and the operating range. Therefore, there is room for fuel with lower energy density fuels like methanol without changing the operating. However, right sizing for electrification does not provide a solution for long distance HD trucking, larger agricultural machinery and inland shipping other than short distance point-to-point shipping. For these application methanol may provide a solution. In the next chapter it is explored how a methanol-diesel PFI dual retrofit engine performs compared to its original diesel operation.

Chapter 5: Simulation Results

This chapter discusses the results of the optimization. First the results of the diesel benchmark optimization are discussed. Then, the diesel-methanol dual fuel set-up optimization is analyzed and finally the results are compared. The results that are not discussed here can be found in Appendix B.

5.1: Diesel Benchmark

For the diesel benchmark optimization 3 optimization cycles have been run with a result check after the last optimization cycle to assess the accuracy of the predicted results. The first DoE cycle is executed with the inlet pressure ranging from 1.5 to 2.5 bar and SOI ranging from -15 to -5 ATDC. This resulted in a clear very clear optimization direction towards a retarded SOI. For the second DoE cycle the same pressure range was used and the SOI was changed to a SOI of -6 to -2 ATDC. Again the optimum SOI was at the edge optimization interval at a SOI of -2 ATDC. Therefore, for the third run the SOI was changed again to 0 to 2 ATDC. For the analysis all runs with a SOI between -5 and 2 ATDC are included. In all simulations UHC, CO and formaldehyde emissions were well within the norms and are therefore not discussed. Figure 5.1 shows the most important trade-off in the optimization. It shows the GIE ISNOx trade-off in which higher efficiencies come at the cost of higher NOx emissions. Figure 5.2 shows the well-known soot-NOx trade-off in diesel engines. As the injection pressure is high there is only a small amount of ISPM in all simulations. The ISPM balances around the stage V soot norm of 0.015 g/kWh and the trade-off is hardly visible.

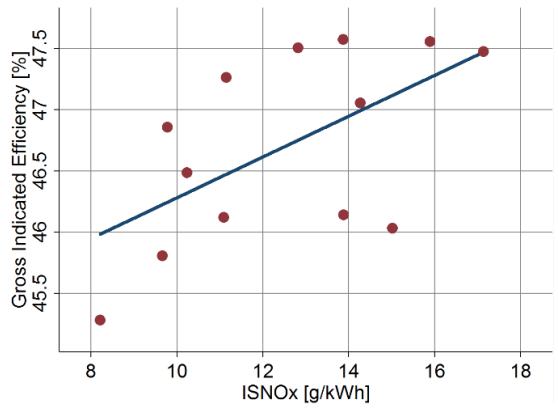

Figure 5. 1: GIE ISNOX trade-off, the blue line is a linear fit.

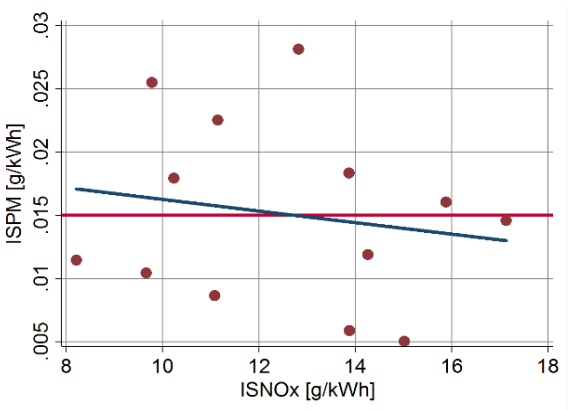

Figure 5. 2: ISPM and ISNOx trade-off. The red line indicates the stage V norm. The blue line is a linear fit.

The response surfaces obtained from the regression analyses in Appendix C show the effect of the SOI and inlet pressure for all dependent variables. For the GIE presented in figure 5.3, the inlet pressure is the most important parameter obtaining higher efficiencies with higher inlet pressures.

Figure 5.4 shows a comparison of the Sankey diagram of run 251 and 252. Both runs have the same SOI, so the effect of the inlet pressure is isolated. It shows a slight decreases in heat losses and a larger decrease in exhaust losses. The decrease in exhaust losses can be explained by a higher ratio of specific heats (γ) (Khajepour et al., 2014). If γ is increased a larger part of the released energy is turned into pressure which can be extracted during the expansion stroke. Increasing the inlet pressure decreases the peak mean temperature, but it only has a small effect on heat losses. This may be due to an increase in the density leading to a larger heat transfer coefficient as seen in figure 5.5.

The SOI shows maximum GIE around -3 ATDC, but is significantly less important. Advancement of the SOI reduces the GIE, because a larger amount of fuel burns before TDC building up pressure against the upward movement of the piston increasing exhaust losses (Teoh et al., 2015). Next to that, it increases the peak mean temperature as more energy is released before to TDC resulting in larger

heat losses. Retarding SOI on the other hand would reduce the heat losses, but increase the exhaust losses as the energy released is not effectively converted into work. If a larger amount of fuel burns during the expansion when the volume is rapidly expanding, less effective pressure is produced and more energy is loss through the exhaust (Teoh et al., 2015). All these effects can seen in figure 5.6.

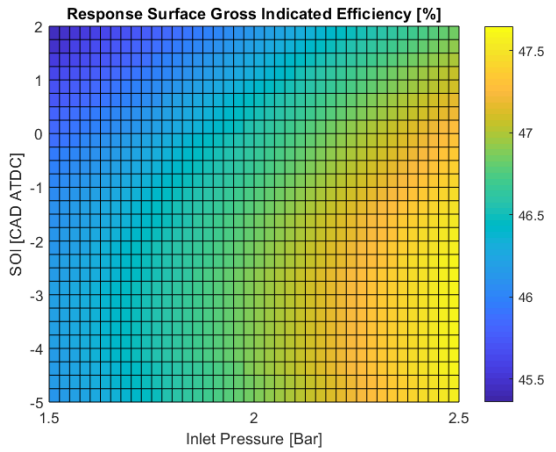

Figure 5. 3: GIE response surface of Pinlet and SOI.

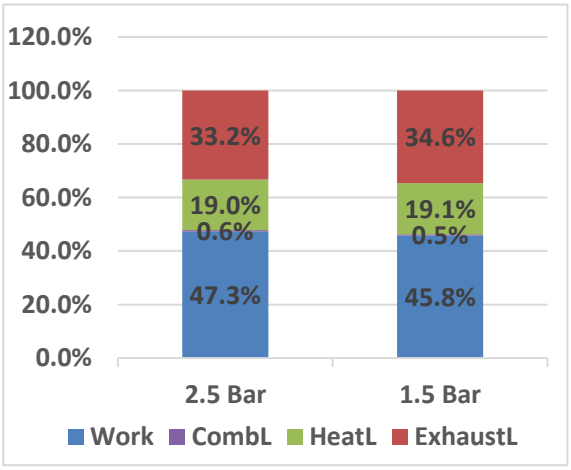

Figure 5. 4: Sankey diagram run 251 & 252, SOI 0 ATDC.

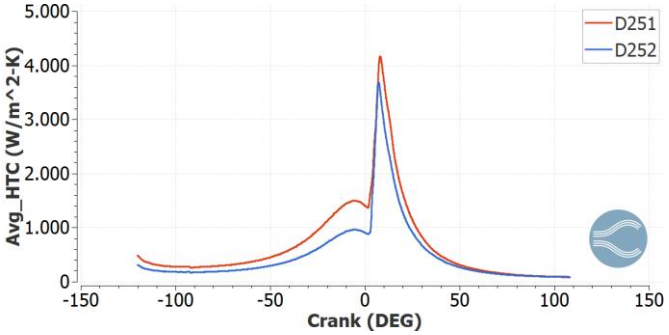

Figure 5. 5: Piston surface average heat transfer coefficient for run 251 and 252.

For the NOx emissions the SOI is vastly more important than the inlet pressure as seen in figure 5.7. Retarding the SOI reduces the NOx emissions. This explanation is rather intuitive as the energy is released in a larger volume reducing peak temperatures, which is the main determinant of NOx production (J. Li et al., 2014).

Increasing the inlet pressure slightly increases NOx. This is rather counter intuitive, because a higher inlet pressure reduces the peak temperature due to the larger mass in the cylinder that needs to be heated. However, the NOx formation rate is also dependent on the O_2 concentration. Larger boost pressures reduce the equivalence ratio and increase the partial pressure of the oxygen. It seems that the partial pressure of the oxygen has a greater effect than the reduction in peak temperature. This is also seen in HD-engine experiments by Colban et al. (2007).

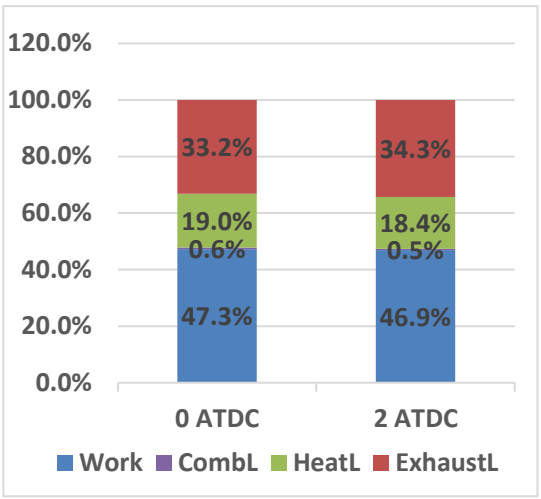

Figure 5. 6: Sankey diagram run 251 & 254, P 2.5 bar.

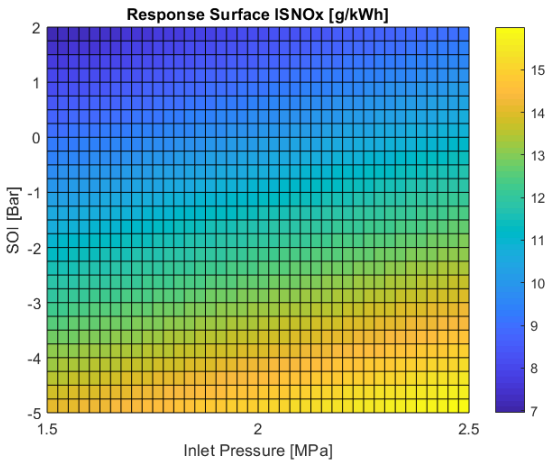

Figure 5. 7: ISNOx response surface of P and SOI.

Figure 5.8 shows the response surface of the ISPM and the relations are very clear. Retarding SOI and increasing the inlet pressure both decrease the peak temperature which results in lower PM oxidation and higher PM emissions.

The GA optimization within the used parameter intervals gives an optimum with an P of 1.754 bar and a SOI of 2 ATDC. It predicts a GIE of 45.73%, an ISNOx of 8.43 g/kWh and an ISPM of 0.0135 g/kWh. When checking the results using these optimal settings in a simulation it resulted in a GIE of 45.84%, a ISNOx of 9.29 g/kWh and a ISPM of 0.0153 g/kWh. With this set-up it is unlikely to reach the Stage V norms without major sacrifices in GIE or the introduction of an aftertreatment system. If aftertreatment is used the engine optimization can be focused on the efficiency. If the merit function is changed to focus solely on the GIE, the optimum was found at a inlet pressure of 2.5 bar and a SOI of -3.59. The predicted performance is 47.65% with a ISNOx of 14.63 g/kWh and a ISPM of 0.0179 g/kWh. The simulation shows a GIE of 47.76%, a ISNOx of 14.29 g/kWh and a ISPM of 0.178. Table 5.1 provides an overview of the results and it is clear that regression model predicts the simulation results fairly well.

From the results it can be concluded that the benchmark diesel set-up cannot be optimized to reach stage V emission norms as the ISNOx emission norm of 1.8 g/kWh cannot be reached. The results show ISPM levels close to the norm, while all other emission level are well below the limits. Depending on the priority in the ISNOx-GIE trade-off the GIE ranges from 45.8 to 47.8% and the ISNOx from 9.3 to 14.3 g/kWh.

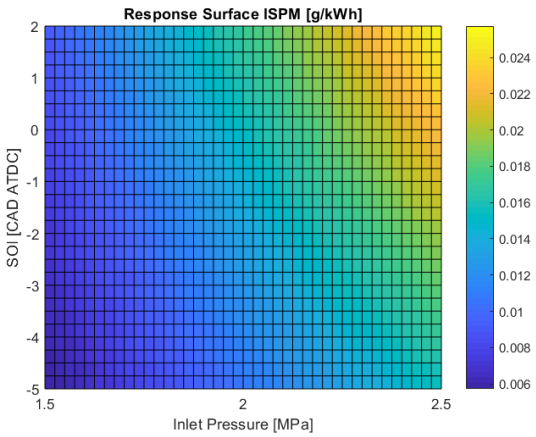

Figure 5. 8: ISNOx response surface of Pin and SOI with MEF=50%.

Table 5. 1: Overview GA optimization results, regression and simulation.

Run	Pin	SOI	MPRR	GIE	ISNOX	ISUHC	ISPM	ISCO	ISFORM
	Bar	CAD ATDC	Bar/CAD	%	g/kWh	g/kWh	g/kWh	g/kWh	mg/kWh
GA	1.754	2.00	10.8	45.73%	8.4	0.020	0.0135	0.482	3.97
SIM	1.754	2.00	10.0	45.84%	9.3	0.021	0.0153	0.586	5.14
GA GIE	2.50	-3.59	12.2	47.65%	14.6	0.020	0.0179	0.282	3.08
SIM GIE	2.50	-3.59	12.3	47.58%	14.3	0.022	0.0178	0.287	2.40
Stage V norm					1.8	0.19	0.015	3.5	12.8*

* Norm used in the State of California (Zhao, 2019)

5.2: Methanol-Diesel Dual Fuel

The methanol-diesel optimization started with a rather broad parameter range. The inlet pressure remained similar with a range of 1.5 to 2.5 bar, the SOI was varied between -5 and -25 ATDC and the MEF varied between 25 and 75%. These ranges were similar to ones applied by Li et al. (2013), with the early injection being in the RCCI category and the late timing in the mixing controlled combustion category.

In the diesel combustion the diesel is injection relatively close to TDC and it is ignited by the elevated temperature of the air in the cylinder caused by the compression stroke. In methanol-diesel PFI engines the methanol is brought into the cylinder through the air intake. In the mixing controlled compression combustion the diesel is injected close to TDC and the methanol is ignited through a propagating flame from the diesel ignition. In the RCCI the diesel is injected earlier and is allowed to mix with the methanol. This mixture is then auto-ignited. Controlling the combustion phasing is one of the main challenges of dual fuel PFI engines and this also becomes clear in the first optimization cycle.

Figure 5.9 shows that all but one simulation breached the MPRR limit of 15 bar/CAD. This was due to the early ignition timing and the short combustion duration caused by the autoignition of the methanol charge. Controlling the combustion appears to be the greatest challenge and mixing controlled combustion is easier to control than RCCI. Therefore, the second-round optimization is focused on mixing controlled combustion with late SOI (-5 to -2 ATDC), high inlet pressure (2.0 to 2.8 bar) and medium levels of MEF (30 to 60%).

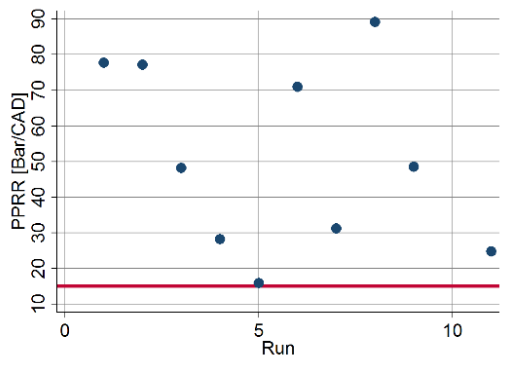

Figure 5. 9: MPRR optimization cycle 1.

The second round optimization showed results with more feasible MPRR and the characteristics of dual fuel LTC engines become visible. Run 207 for example shows a high efficiency of 49.59% with a

relatively low ISNOx of 9.0 g/kWh, just 0.0022 g/kWh ISPM and a reasonable MPRR of 16.8 bar/CAD. However, the main downside also becomes clear with a ISUHC emission of 0.892 g/kWh, ISCO emission of 15 g/kWh and ISFORM emission of 168.8 mg/kWh. These greatly exceed the stage V norm. The GA optimization of all runs with a SOI later than -10 ATDC indicates that a low inlet pressure, late injection and high MEF give optimum results. As seen in table 5.2 it predicts a GIE of 49%, ISNOx of 6.89 g/kWh and negligible ISPM. Also, the ISUHC and ISCO emissions remain within the norm with values of 0.17 and g/kWh, respectively. The ISFORM emissions of 46 mg/kWh are still beyond the limit, but more importantly the expected MPRR is 29.3 bar/CAD despite the factor 10 penalty for exceeding the norm. The test simulation shows that the prediction has a reasonable accuracy for the ISNOx, ISUHC, ISPM and MPRR. The GIE in the simulation is higher than expected at 50.76%, while the ISCO and SFORM are lower than expected at 1 g/kWh ISCO and 29.3 mg/kWh, respectively. If a higher weight is set for the MPRR the solution changes towards higher inlet pressures having a particularly strong effect on the CO emissions exceeding the stage V norm by more than a factor 10.

Table 5. 2: Results second optimization cycle.

Run	Pin	SOI	MEF	Tin	MPRR	GIE	ISNOX	ISUHC	ISPM	ISCO	ISFORM
	Bar	CAD ATDC	%	K	Bar/CAD	%	g/kWh	g/kWh	g/kWh	g/kWh	mg/kWh
201	2.00	-5	30%	400	18.3	48.64 %	15.3	0.851	0.0043	22.8	146.9
202	2.80	-5	30%	400	17.2	46.81 %	14.8	1.081	0.0102	37.0	216.1
203	2.00	-2	30%	400	23.9	46.99 %	13.5	1.038	0.0066	26.0	166.8
204	2.80	-2	30%	400	15.3	46.60 %	12.2	1.320	0.0138	40.0	254.2
205	2.00	-5	60%	400	40.6	49.10 %	11.3	0.645	0.0008	13.5	141.5
206	2.80	-5	60%	400	34.2	46.42 %	11.1	1.098	0.0032	61.4	222.5
207	2.00	-2	60%	400	16.8	49.59 %	9.0	0.892	0.0022	15.0	168.8
208	2.80	-2	60%	400	15.3	46.65 %	9.4	1.137	0.0052	66.0	209.2
209	2.40	-3.5	45%	400	19.6	46.98 %	12.1	1.149	0.0060	44.4	190.3
GA	1.63	0.20	75%	400	29.3	49.06 %	6.9	0.171	0.0008	3.1	46.7
SIM	1.63	0.20	75%	400	28.7	50.76 %	6.7	0.145	0.0003	1.0	29.3
Stage V norm							1.8	0.19	0.015	3.5	12.8*

* Norm used in the State of California (Zhao, 2019)

When taking a closer look, all of the second round runs have knock. The methanol combustion starts by auto-ignition instead of the propagation flame front of the diesel injection. The increase in inlet pressure used to counter the severe MPRR increases the compression temperature and therefore the knock tendency. One of the solutions to reduce knock is to reduce the inlet temperature (Y. Li et al., 2013; Wang et al., 2017). Therefore, in the third run the inlet temperature is added as an optimization parameter. The inlet temperature range is set at 365 to 400 K. The SOI is slightly retarded to -4 to -1 ATDC to delay the ignition timing and reduce the MPRR and ISNOx. The inlet pressure is set back to 1.6 to 2.2 bar as the SOI and the inlet temperature should be able to control the MPRR. Increasing the

inlet pressure would only increase ISUHC, ISCO and ISFORM emissions. The MEF is maintained at 30-60%.

In the third optimization cycle used a fraction factorial design keeping the number of runs per cycle at 9. Of the third optimization cycle only run 8 showed clear signs of knock in the CFD images. In figure 5.10 shows run 308 with auto-ignition and run 302 with a propagating flame front. Both runs have a SOI of -1 ATDC, wile the left image is obtained at 2 and the right image at -2 CAD ATDC. Figure 5.11 confirms a HRR before SOI in run 308, resulting in an earlier and higher peak cylinder pressure than 302 which cannot be explained through the higher inlet pressure alone.

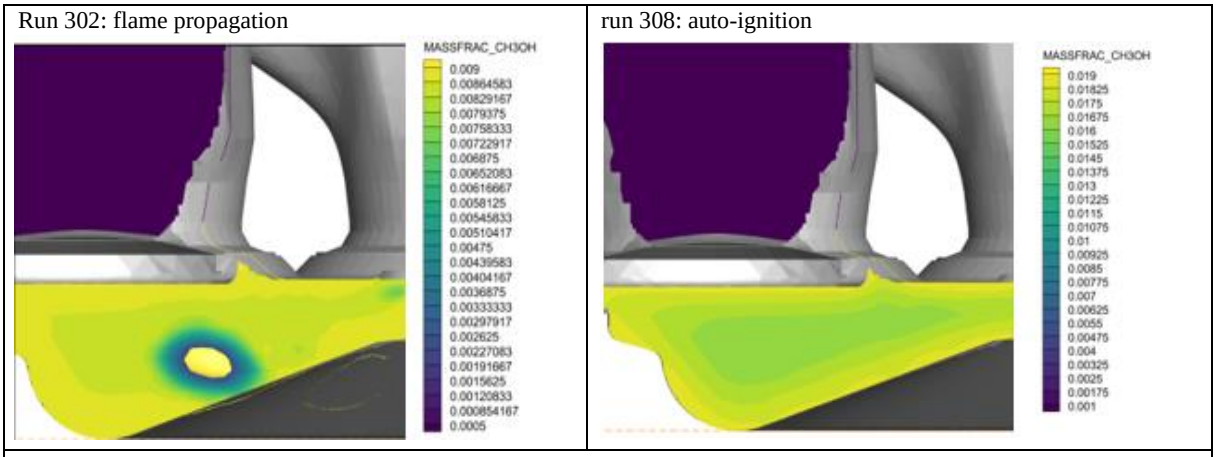

Figure 5. 10: Illustration of flame propagation versus an auto-ignition (knocking) simulation.

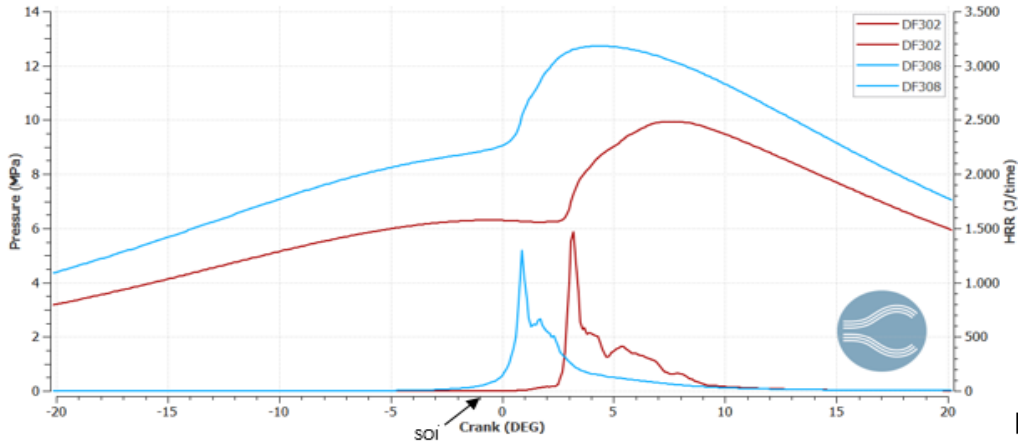

Figure 5. 11: Pressure and HRR plot run 502 and 508, the arrow indicates the SOI.

When analyzing all runs with a SOI later than -10 ATDC the results show a clear difference in the trade-offs in comparison to the diesel only simulation. Figure 5.12 shows that the GIE NOx trade-off is gone and actually reversed the trend showing lower ISNOx emissions with higher GIE. With the exception of a few runs in which the PM emissions approach the stage V norm, most runs show PM emissions well below it. The most important trade-off for the dual fuel are related to the MPRR. As seen in figure 5.13 and 5.14 both the GIE and ISCO emissions show conflicting trends with the MPRR. This indicates that the MPRR is the limiting factor.

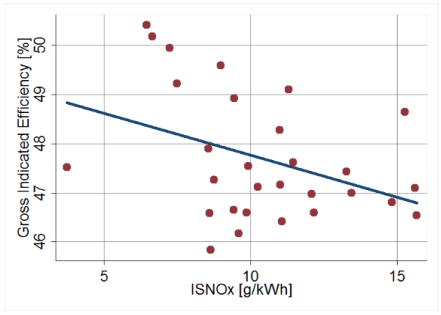

Figure 5. 12: GIE-NOx trade-off.

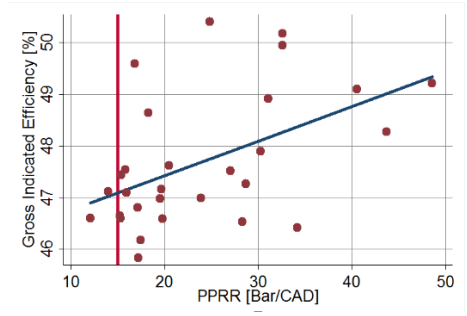

Figure 5. 13: GIE-MPRR trade-off.

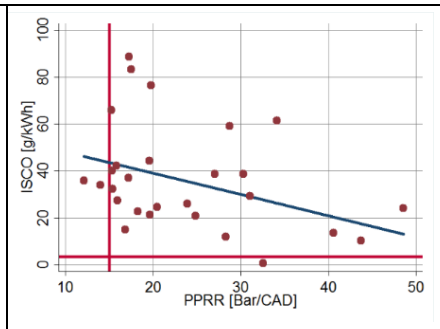

Figure 5. 14:ISCO-MPRR trade-off.

The blue lines represent linear fits and the red lines represent the emissions norms or engine limitations

5.2.1: GIE

The GIE is most significantly affected by the inlet pressure as seen in table 5.3. In contrast to the diesel only results, the regression shows a negative correlation between the inlet pressure and the GIE. Although the effect of the inlet pressure similar to the diesel only results show a decrease in both heat- and exhaust losses the GIE still decreases. This is solely due to a strong increase in combustion losses when the intake pressure increases.

The SOI appears to have an insignificant effect on the GIE. This can be partially explained by the relatively small interval of the SOI and the many runs with knock that are included in the data. The latter decouples the ignition timing from the SOI. Only in the third DoE run, the SOI becomes equally important to the other variables, though the relation is the same. The mechanism is similar to the diesel only benchmark with the addition of increased combustion efficiency for advanced injection timing due to the higher combustion temperatures closer to TDC.

Table 5. 3: GIE regression of optimization cycle 3.

GIE	Coef.	St.Err.	t-value	p-value	[95% Conf	Interval]	Sig
PINLET	-.1536	.037	-4.13	0	-.231	-.077	***
SOI	-.00055	.001	-0.59	.562	-.002	.001	
MEF	-.428	.215	-1.99	.059	-.873	.017	*
TINTAKE	-0.0002	0	-0.64	.528	-.001	0	
TINTAKE#MEF	.0011	.001	2.16	.042	0	.002	**
Constant	.570	.124	4.59	0	.313	.827	***

R-squared	0.695	Number of obs	29.000
F-test	10.499	Prob > F	0.000

*** p<.01, ** p<.05, * p<.1*

The effect of the MEF and inlet temperature are analyzed through the surface plot in figure 5.15 because the interaction effect is significant. The efficiency increases with higher inlet temperatures and the effect is more pronounced at higher MEF. Higher inlet temperatures increase the heat losses through two effects. Firstly, it raises the overall temperature. Secondly, the increase in initial temperature advances ignition timing and shortens the combustion duration, which increases the peak mean temperature. As discussed previously the advancement ignition timing and the shortening of the combustion duration also decreases the exhaust losses. The interaction effect increases the GIE more at higher MEFs because the higher inlet temperature decreases the combustion losses and these are almost exclusively from the homogeneously distributed methanol.

On its own the increase of MEF also increases the GIE. Due to the pre-mixed methanol there is a quick combustion decreasing the heat losses. While the quick heat release and advanced combustion phasing would be expected to decrease exhaust losses it is actually increased slightly in most

simulations. Kokjohn et al. (2011) found something similar with their RCCI engine. It could be that the reduced heat losses are partly lost in the exhaust losses. The MEF does not have a significant effect on the combustion.

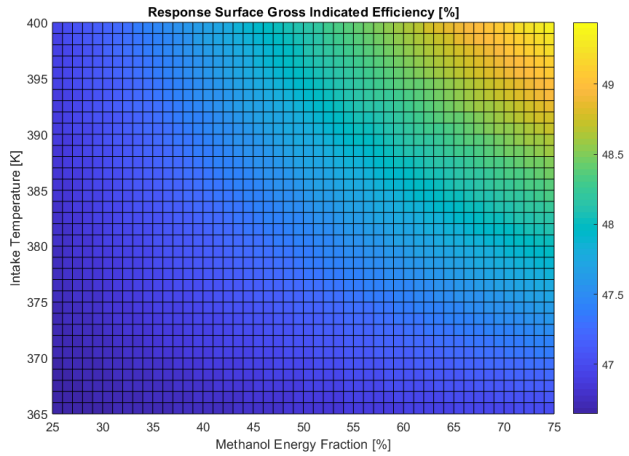

Figure 5. 15: Surface plot GIE with Pintake 2 bar and SOI 0 ATDC.

5.2.2: MPRR

One of the biggest challenges of methanol fumigated engines is to keep the MPRR at acceptable levels. Table 5.4 shows that the inlet pressure has the greatest impact on the MPRR. While a higher boost pressure increases the temperature during compression and advances the ignition timing it actually decreases the MPRR. This happens because a higher inlet pressure decreases the equivalence ratio and the combustion duration is increased with leaner mixtures (Polat, Yücesu, Uyumaz, Kannan, & Shahbakhti, 2020). A leaner mixture increases the combustion duration, because it lowers the reaction rate. This reduces the reaction rate in the case of autoignition, but it also results in a lower laminar flame velocity. Formula 5.1 shows the equation for the pressure rise rate (PRR).

$$PRR = \frac{\gamma-1}{\gamma} * \frac{1}{V} * HRR - \frac{1}{\gamma} * \frac{p}{V} * \frac{dV}{dt} \quad (5.1)$$

This clearly shows that a longer combustion duration, thus a lower HRR, leads to lower PRRs. Retarding the SOI delays the heat release to a moment with a larger volume while it is expanding. Formula 5.1 shows that the first term with the HRR is divided by the volume, thus a the HRR in a larger volume results in a lower PRR. Next to that, the second term is positive in the case of an expansion of the cylinder resulting in a small decrease of the PRR. All these effects result in a lower MPRR.

Table 5. 4: MPRR regression of optimization cycle 3.

MPRR	Coef.	St.Err.	t-value	p-value	[95% Conf	Interval]	Sig
PINLET	-104.608	29.456	-3.55	.002	-165.402	-43.815	***
SOI	-2.088	.709	-2.95	.007	-3.551	-.625	***
MEF	34.001	6.61	5.14	0.01	20.359	47.643	***
TINLET	.212	.082	2.57	.017	.042	.382	**
Constant	-58.914	30.82	-1.91	.068	-122.524	4.696	*

R-squared	0.641	Number of obs	29.000
F-test	10.697	Prob > F	0.000

*** $p<.01$, ** $p<.05$, * $p<.1$

Increasing the MEF and inlet temperature both lead to higher MPRRs. Higher MEFs increase the amount of premixed fuel, which leads to shorter combustion duration as seen in figure 5.16. Increasing MEF also increases the knock tendency. The figure shows that 60% MEF auto-ignites (knocks) as the second peak in the HRR is the injection of the diesel. In the case of knock the ignition timing is also

advanced. The inlet temperature has a rather straightforward effect, as it affects the bulk temperature. Lower inlet temperatures would decrease the reactivity and reaction rate and therefore retard ignition timing, increase combustion duration and reduce MPRR. It also reduces the knock tendency.

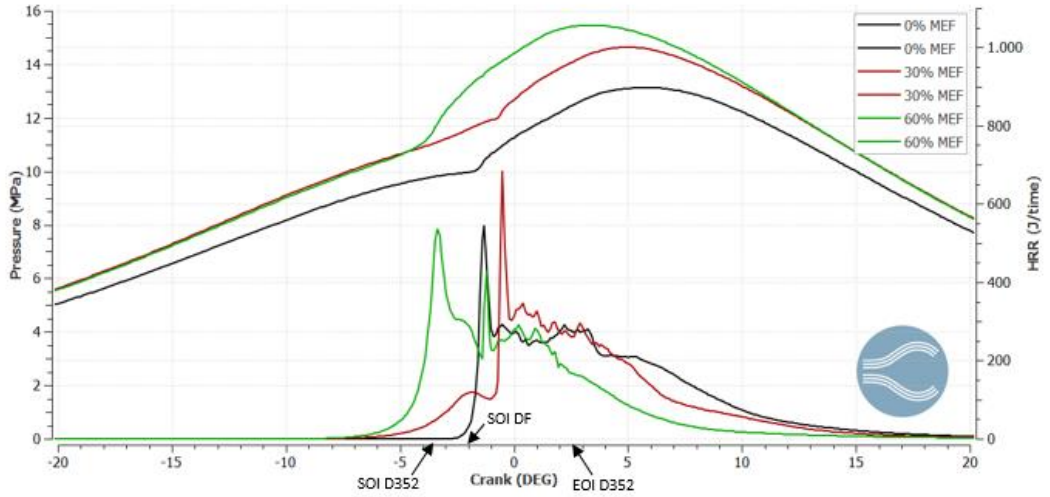

Figure 5. 16: Pressure and Heat release rate run D352, DF204 and DF208.

5.2.3: ISNOx

In the case of NOx emissions table 5.5 shows that the inlet pressure does not appear to play significant role. The reduction in maximum bulk gas temperature and the higher partial oxygen pressure for increased inlet pressures seem to match up with the first effect being slightly dominant. The other effects play a larger role in the determining NOx. A very straightforward effect is the inlet temperature. Higher intake temperatures increase the overall temperature, advances the ignition timing and shortens the combustion duration. All effects lead to higher peak mean temperatures, thus NOx emissions.

Table 5. 5: ISNOx regression optimization cycle 3.

ISNOX	Coef.	St.Err.	t-value	p-value	[95% Conf	Interval]	Sig
PINTAKE	-1.601	4.012	-0.40	.694	-9.901	6.699	
SOI	-1.02	.173	-5.91	0.001	-1.378	-.663	***
MEF	-9.44	1.188	-7.94	0.001	-11.899	-6.981	***
Tin	.056	.015	3.89	.001	.026	.086	***
SOI#MEF	1.015	.396	2.56	.017	.196	1.834	**
Constant	-7.929	5.327	-1.49	.15	-18.948	3.09	

R-squared	0.938	Number of obs	29.000
F-test	108.358	Prob > F	0.000

*** p<.01, ** p<.05, * p<.1*

The main effect of the SOI is the same as for the diesel benchmark simulations in which retarding SOI decreases the NOx emissions. The MEF main effect is also negatively correlated to the NOx emissions. This is because larger fractions of premixed fuel lead to shorter combustion durations and therefore a shorter residence time at the very high local peak temperatures. The interaction effect of the SOI and MEF can be seen in figure 5.17. This shows that the SOI is more effective for lower MEF. The interaction shows that SOI is less important at higher MEFs because increasingly less diesel will be injected and it is absent at MEF equal to 1. Run 107, mimicking, an RCCI engine shows a NOx emission of only 0.6 g/kWh. This is because the diesel is not immediately ignited and has more time to

mix with the methanol-air mixture. The results in a more premixed mixture mimicking homogeneous compression ignition at a lean condition, hence a low local and mean peak temperature.

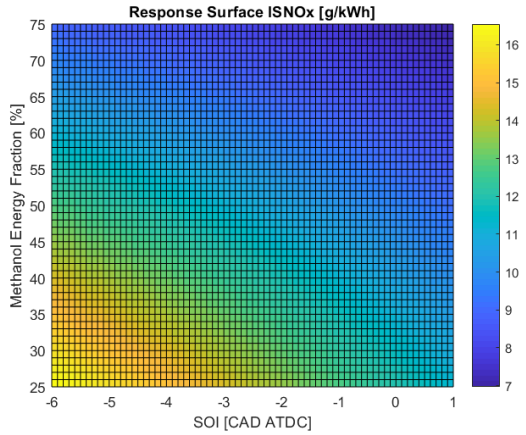

Figure 5. 17: Surface plot ISNOx with Pinlet 2 bar and SOI 0 ATDC.

5.2.4: ISUHC, ISCO, ISFORM & ISPM

The ISUHC ISCO, ISFORM and ISPM emissions are grouped together because all four emissions are products of incomplete combustion. Tables 5.6, 5.7, 5.8 and 5.9 show the regression results for the ISUHC ISCO, ISFORM and ISPM emissions. The inlet pressure is an important parameter for all of them, since higher inlet pressures reduce the peak mean temperatures and it therefore reduces the oxidation of these intermediate species. The inlet temperature appears to be the greatest influencer, except for the ISPM emissions. It raises the compression temperature, advances the ignition timing and reduces the combustion duration. All three effects increase the peak mean temperature and reduce incomplete combustion. The same holds true for the ISPM emissions, but the effect is less important as the soot is only formed during the combustion of the rich diesel spray. The inlet temperature has a large effect on the mean temperature and a only minor effect on the local temperature of the rich diesel spray where the PM is formed.

Table 5. 6: Regression ISUHC optimization cycle 3.

ISUHC	Coef.	St.Err.	t-value	p-value	[95% Conf	Interval]	Sig
PINLET	7.326	1.565	4.68	0	4.081	10.57	***
SOI	3.962	2.759	1.44	.165	-1.76	9.684	
MEF	28.901	20.753	1.39	.178	-14.138	71.94	
TINTAKE	-.063	.047	-1.36	.188	-.16	.033	
TINTAKE#MEF	-.074	.052	-1.42	.17	-.183	.034	
SOI#TINTAKE	-.01	.007	-1.42	.171	-.024	.005	
Constant	24.867	18.22	1.36	.186	-12.918	62.652	
R-squared		0.893	Number of obs			29.000	
F-test		36.798	Prob > F			0.000	

**** p<.01, ** p<.05, * p<.1*

Table 5. 7: Regression ISCO optimization cycle 3.

ISCO	Coef.	St.Err.	t-value	p-value	[95% Conf	Interval]	Sig
PINLET	372.091	57.884	6.43	0	252.35	491.832	***
SOI	.491	1.329	0.37	.715	-2.259	3.241	
MEF	307.127	103.83	2.96	.007	92.338	521.916	***
MEF2	-300.286	104.512	-2.87	.009	-516.486	-84.086	***
TINTAKE	-.857	.16	-5.35	0	-1.188	-.525	***
Constant	221.382	67.502	3.28	.003	81.745	361.02	***
R-squared		0.790	Number of obs			29.000	

F-test	17.338	Prob > F	0.000

*** p<.01, ** p<.05, * p<.1*

Table 5. 8: Regression ISFORM optimization cycle 3.

SFORM	Coef.	St.Err.	t-value	p-value	[95% Conf	Interval]	Sig
PINLET	1254.648	670.709	1.87	.074	-129.626	2638.922	*
SOI	8.718	18.74	0.47	.646	-29.961	47.396	
MEF	-108.062	199.473	-0.54	.593	-519.754	303.63	
Tin	-11.654	3.539	-3.29	.003	-18.958	-4.35	***
Constant	4586.671	1385.08	3.31	.003	1728.007	7445.334	***

R-squared	0.577	Number of obs	29.000
F-test	4.003	Prob > F	0.013

*** p<.01, ** p<.05, * p<.1*

Table 5. 9: Regression ISPM optimization cycle 3.

ISPM	Coef.	St.Err.	t-value	p-value	[95% Conf	Interval]	Sig
PINLET	.121	.01	11.72	0	.1	.143	***
SOI	4.5e-4	0	4.78	0	0	.001	***
MEF	.014	.004	3.53	.002	.006	.023	***
TINTAKE	-1.05e-5	0	-0.72	.479	0	0	
PINLET#MEF	-.141	.019	-7.35	0	-.18	-.101	***
Constant	-.01	.005	-2.16	.042	-.019	0	**

R-squared	0.958	Number of obs	29.000
F-test	104.227	Prob > F	0.000

*** p<.01, ** p<.05, * p<.1*

For SOI on the other hand the roles are turned. It is very important for the ISPM emissions and plays a less significant role for the ISUHC and especially for the ISCO and ISFORM emissions. Still the mechanisms are similar. Figure 5.18 shows that retarding the SOI reduces the peak mean temperature, especially at lower intake temperatures. So, retarding SOI increases these emissions. The SOI is especially important for the ISPM emissions, because the SOI determines the ignition delay and the time for mixing with the methanol-air mixture.

In the UHC regression there is an interaction effect between SOI and the inlet temperature, as seen in table 5.6 and figure 5.19. It shows that at higher inlet temperatures the effect of the SOI diminishes. This is likely because at high inlet temperatures there is a decoupling between SOI and the start of ignition due to knock. Figure 5.20 shows the CAD10, the CAD in which 10% of the total heat is released, and it is clear that for high inlet temperatures and relatively late SOI the ignition timing is knock ignited and independent on the SOI .

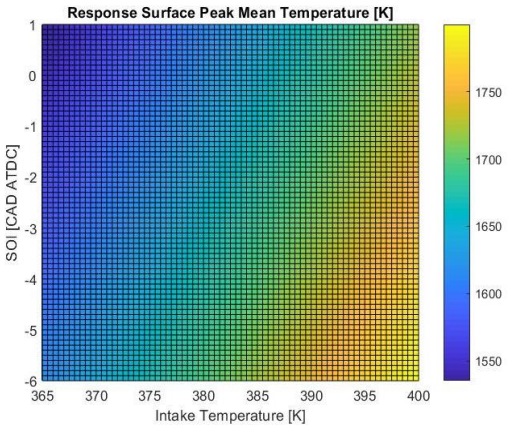

Figure 5. 18: Peak mean T Response surface with Pinlet=2 bar and MEF=50%.

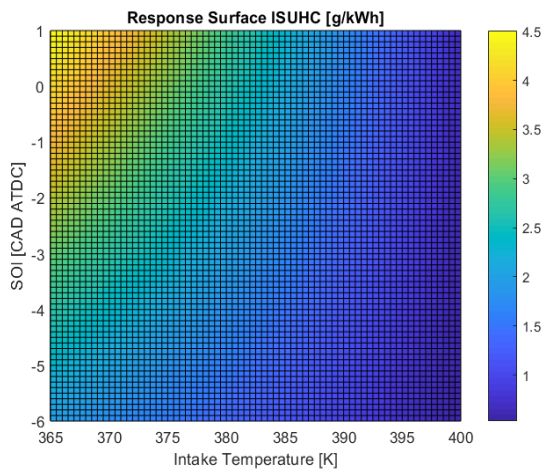

Figure 5. 19: ISUHC response surface with Pinlet=2 bar and MEF=50%.

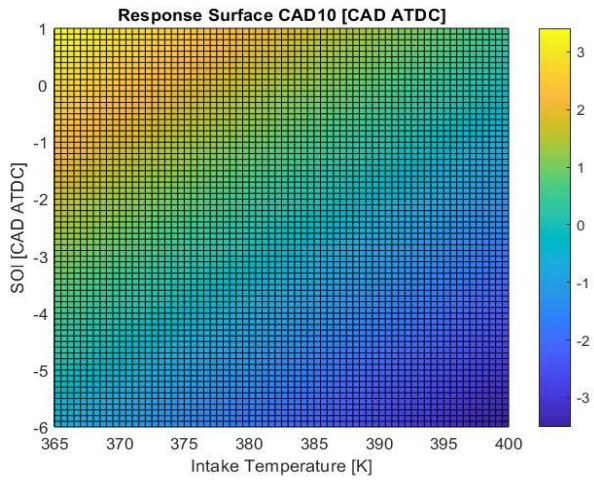

Figure 5. 20: CAD10 response surface with Pinlet=2 bar and MEF=50%.

The MEF has a slightly more complicated effect on these emissions. The regression in table 5.8 for the formaldehyde emissions shows a straightforward relationship with increasing ISFORM emissions with increasing MEF. The second order term for MEF was close to significance (p=0.0783), but did not significantly improve the model. In the CO emission regression in table 5.7 it did improve the model. The formaldehyde and CO emissions increase with MEF and after 50% it starts to decrease again. The ISCO and ISFORM emissions are formed by the pre-mixed methanol and not by the DI diesel. If the fraction of pre-mixed methanol is increased the peak temperature is decreased and at low MEFs it increases the incomplete combustion. If the MEF is further increased the premixed methanol becomes richer and the premixed methanol reactive. This in its turn decreases the incomplete combustion and explains the second order term. For the UHC emissions an interaction effect between MEF and the intake temperature has been found. In figure 5.21 it can be seen that UHC emissions increase with MEF at lower inlet temperatures. At higher inlet temperatures it appears to be the opposite and there is a slight decrease in UHC emissions at higher MEF. It is likely that this is also due to the higher reactivity, but then due to the higher inlet temperature instead of the premixed equivalence ratio.

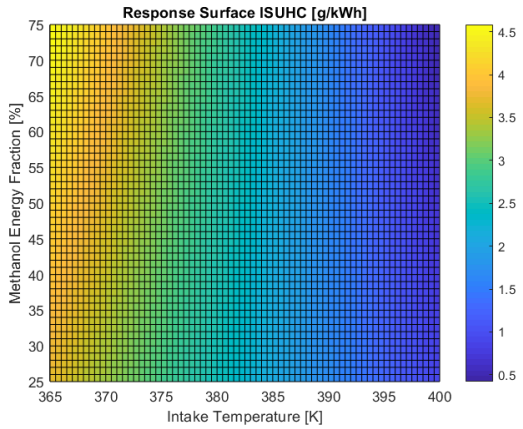

Figure 5. 21: ISUHC response surface with P=2 bar and SOI=0 ATDC.

The relation between ISPM and MEF is also more complicated as there is an interaction effect with the inlet pressure as seen in table 5.9 and figure 5.22. The figure shows that higher MEF decreases the ISPM emissions. This is simply because there is less DI diesel to cause the soot. The interaction effect clearly visualizes this, because at low MEF the inlet pressure plays an important role while at high MEF the role the effect of the inlet pressure becomes negligible

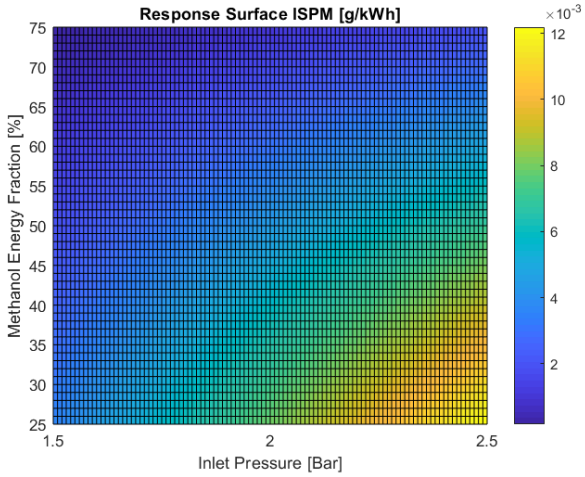

Figure 5. 22: ISPM response surface with SOI=0 ATDC and Tin=400 K.

As already mentioned earlier, a maximum emission has been set for the UHC and formaldehyde emissions at 5 g/kWh and 1000 mg/kWh. Both emissions showed exponential trends in the case of more severe incomplete combustion. When looking at the CFD images in figure 5.23. it can been seen that the emissions are formed near the wall and around the valves. The flame is quenched near the relatively cold wall and cylinder head leading to incomplete combustion. In the case of more severe CO emissions the flame quenches further away from the wall and piston head and it even stars to quench around the piston head. In the case of knocking combustion it is not necessarily the flame that quenches, but it simply fails to combust completely.

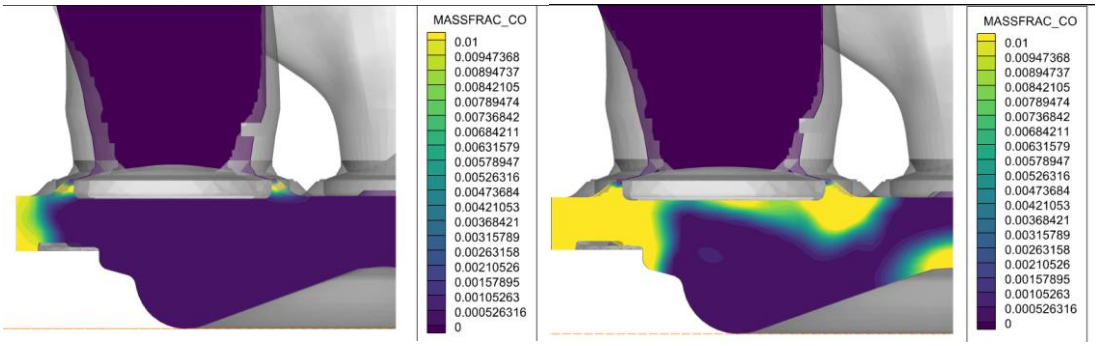

Figure 5. 23: The CO sources of Run 306 (left) and run 302 (right).

5.3: Diesel Benchmark and Dual Fuel Optima

When running the final GA optimization the optimum is similar to the second optimization run: low inlet pressure, late SOI, high MEF and high temperature. The solution has a MPRR of 30 and is therefore not a feasible option. If the MPRR penalty is increased to 30 in the merit function the solution is similar except for the MEF which is reduced to low values. Table 5.10 states the result of the final optimization and the test simulation with this optimized set of parameters. The prediction is fairly accurate with a GIE of 46.38 % compared to the predicted 47.27%. The MPRR show similar accuracy and both the ISNOx and the ISPM match closely. However, the ISUHC, ISFORM and especially the ISCO emissions are a bit further off. Generally, the diesel benchmark regression models are more accurate than the diesel-methanol dual fuel regression models. This is partly due to the larger

number of parameters used, but the dual fuel is also a far more complex concept that is more difficult to capture in a statistical model. Especially with relatively few data points for the number of parameters.

Table 5. 10: Overview GA optimization results, regression and simulation for diesel benchmark and the dual fuel.

Run	Pin	SOI	MEF	Tin	MPRR	GIE	ISNOX	ISUHC	ISPM	ISCO	ISFORM
	Bar	CAD ATDC	%	K	Bar/CAD	%	g/kWh	g/kWh	g/kWh	g/kWh	mg/kWh
D GA	1.754	2.00	0%	400	13.7	45.73%	8.4	0.020	0.0135	0. 48	4.0
D SIM	1.754	2.00	0%	400	10.0	45.84%	9.3	0.021	0.0153	0.59	5.1
D GA GIE Only	2.50	-3.59	0%	400	12.2	47.65%	14.6	0.020	0.0179	0.28	3.1
D SIM GIE Only	2.50	-3.59	0%	400	12.3	47.58%	14.3	0.022	0.0178	0.29	2.4
DF GA	1.63	0.2	75%	400	29.3	49.06%	6.9	0.171	0.0008	3.1	46.7
DF SIM	1.63	0.2	75%	400	28.7	50.76%	6.7	0.145	0.0003	1.0	29.3
DF GA Low MPRR	1.77	1.00	25%	400	13.7	47.27%	11.2	0.693	0.0064	8.6	129.0
DF SIM Low MPRR	1.77	1.00	25%	400	15.1	46.38%	11.0	1.113	0.0087	21.3	181.1
Stage V norm							1.8	0.190	0.0150	3.5	12.8*

* Norm used in the State of California (Zhao, 2019)

When comparing the results of the methanol-diesel dual fuel to the diesel benchmark in table 5.10 the results differ greatly depending on the optimization approach. The optimal dual fuel run with a too high MPRR provides the by far the highest efficiency, the lowest ISNOx and ISPM while the all other emissions except for ISFORM are within the norms. It increases the GIE by 11%, reduces the ISNOx by 28% and almost eliminates ISPM emissions. When upholding the MPRR limit the results are less positive. Then, the GIE only increases by 1.2%, the ISNOx increase by 19% and the ISPM decreases by 43%, while the ISUHC, ISCO and ISFORM all breach the emissions limits at an MEF of 25%. If it is assumed that emissions are treated by an aftertreatment system, the diesel benchmark has a 3% higher GIE.

5.4: Simulation Result Consequences

From the results it can be derived that retrofitting can increase the efficiency, but that aftertreatment is still needed for all configuration tested in the analysis, because the ISNOx emissions exceed the norm in all cases. If methanol-diesel dual fuel is used a PM filter would not be needed anymore, but it would require a diesel oxidation catalyst for the ISFORM and in many cases also the ISCO and ISUHC emissions. Because of the lean operation a three-way catalyst is not an option and both a Selective Catalytic Reduction (SCR) system for the NOx and a diesel oxidation catalyst will be required. Thus, retrofitting diesel engines to methanol fumigated engines seems to be no alternative for installing aftertreatment systems to comply with the Stage V norm as it only swaps a PM filter for a diesel oxidation catalyst. Besides the emissions norm the amount of methanol that can be used is fairly limited to MEF levels around 30%, before the MPRR limit is breached. This means that only a small part of the diesel can be substituted.

Other retrofit solutions may be able to achieve the emissions limits. As discussed in the introduction dual direct injection is a retrofit used in the larger low speed engines. The direct injection of methanol would allow to increase the MEF without the high MPRR CO and UHC emissions. Principally, it uses the original diesel principle of injection all fuels close to TDC only using a diesel pilot to create the ignition temperature for the DI of methanol. This does require custom made cylinder heads and two high pressure injection system and space is minimal. Next to that, the direct injection of methanol does not provide a solution for the NOx emissions as it is less premixed than PFI injection. Alternatively, RCCI engines could pose a solution as the emissions are even lower. The first optimization cycle

included RCCI runs and showed emissions that were below Stage V with very high efficiencies. The problem is the high MPRR and control in dynamic running condition is extremely challenging. Nonetheless, progress with this concept is being made and ArenaRed succeeded in retrofitting a Caterpillar 3512 diesel engine to a RCCI engine fulfilling the Stage V norms (Deen et al., 2020). They achieved this with natural gas and diesel combination, but a methanol-diesel combination is in development.

From an engine performance point of view there is some efficiency gain possible with a methanol fumigation retrofit, but the retrofit cannot be used as a substitute for aftertreatment systems. Methanol appears to provide more advantages in more complex retrofit solutions or new engines. In the next chapters methanol as a fuel will be examined from a broader perspective, comparing methanol to diesel, LNG and hydrogen along the entire value blueprint.

Chapter 6: Innovation Ecosystem, Barriers & Opportunities

To answer the third sub question the inland shipping innovation ecosystem is mapped. The innovation ecosystem of shipping is inspired by Wang & Notteboom (2014) and can be explained by three different streams leading to the shipowner and their customers as seen in figure 6.1. The first is the fuel supply the ship. The second are the engine manufacturer and shipyard that supply the drivetrain and third are the governing bodies. The fossil value blueprint is discussed first in section 6.1. It starts by sketching the current situation of the petroleum supply chain after which the other value parts of the value blueprint are discussed. Then, the changes in the value blueprint for a switch to methanol are discussed in section 6.2. Finally, in section 6.3, the barriers and opportunities of methanol compared to the most relevant alternative inland shipping fuels are discussed.

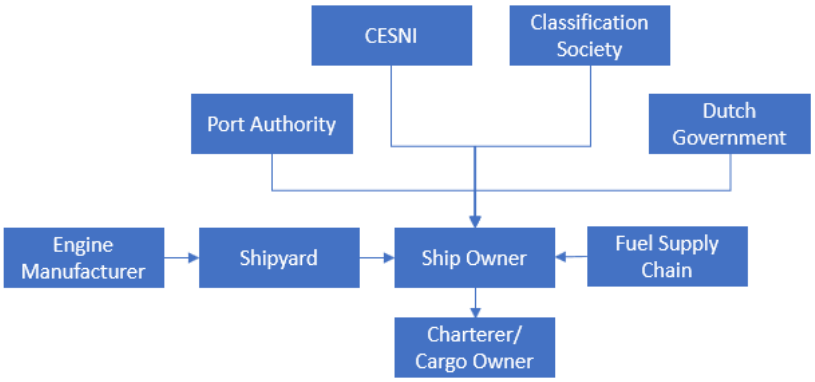

Figure 6. 1: Overview inland shipping innovation ecosystem.

6.1: Fossil Value Blueprint

The current fossil fuel value proposition can be divided in three different segments: upstream, midstream and downstream. Of the three segment the upstream sector is by far the largest with a total revenue of 3.3 trillion USD corresponding to 3.8% of the global GDP in 2019 (IBISWorld, n.d.) and it accounts for roughly 75% of the value created in the oil in gas industry. The midstream activity of transport (~5%) and the downstream activities of refining (~15%) and distribution (~5%) determine the rest of the value (Kemper, 2010; Sutton, 2011).

The upstream segment includes all activities concerned with the production of oil and gas. Ranging from identification, exploration and testing of potential oil and gas reserves to the design construction and exploitation. The time scale associated with initial exploration up to the commercial operation is 5-7 years, however challenging or new remote sites with major infrastructure requirements can take even longer (Extractives Hub, n.d.). Álvarez et al. (2018) have a similar timeframe, but they state that it can stretch up to 20 years in a worst case. When commercial operation has started, the production phase of the project can last from 10 to 50 years or even beyond.

The sector is covered for a large part by national oil companies as the top 15 producing companies are all national oil companies (NOC), after that come the international oil companies (IOC) like ExxonMobil, Shell and BP (Extractives Hub, n.d.). NOCs are oil and gas companies fully or majority owned by a national government. According to the World Bank, NOCs accounted for 75% global oil production and controlled 90% of proven oil reserves in 2010 (Tordo et al., 2011). Then, there are the smaller specialized exploration and production companies like ConocoPhillips and specialized companies providing highly skilled auxiliary services like Schlumberger, Boskalis and Transocean. Typically a project involves a combination of IOCs, NOCs and multiple service contractors. The IOC or NOC is responsible for the funding and the overall project results bearing the risk of the project, while the service contractors implement the majority of work (World Bank Group, 2019).

The upstream segment is also the most risky, technologically advanced and the most complex part of the value chain. It is also the part with the highest rewards (Amor & Ghorbel, 2018). The exploration

and development phase requires enormous investments that often exceed 1 billion USD (Álvarez et al., 2018). There is a significant risk that the investment will not yield any returns since the well could be smaller than expected or a smaller share could be recovered (Álvarez et al., 2018). If returns are made payback periods are long due to the large investment (World Bank Group, 2019). Because of its risk profile these projects are normally equity funded by joint ventures between multiple oil companies. Therefore, the risks and capital requirements are shared between companies. Due to the high risks involved, the margins on the oil are high and the reward for successful project is large.

After the production phase, the midstream activities come into play. Midstream companies gather, store, market and transport the oil and gas products. Often these companies are also involved in the distribution of the petroleum products in the downstream activities of the value chain (API, 2019). Companies involved in the midstream segment are storage terminal operators. This includes IOCs, but also independent operators that do not own the product and act as custodians like Vopak, CLH Group and Oiltanking GmbH (Álvarez et al., 2018).

For long range transport of oil tankers and pipelines are used. Medium range transport is done by barges or rail transport and transport trucks for short range. Gas is purified and in some cases liquified before it is transported by pipelines or tankers (Extractives Hub, n.d.). In the petrochemical plant or refinery oil and gas are used to produce petroleum products like kerosine, gasoline and diesel and chemicals like methanol.

The value of the refined products depend on the overall supply and are highly volatile. Typically, refineries have some flexibility to optimize their product mix, but this is fairly limited due to the stock of the refineries and the complexity of the processes (Álvarez et al., 2018). Typically, mid- and downstream markets are characterized by high volumes and low margins. Even though the midstream infrastructure and the downstream refineries require high capital investments, these projects are less prone to risk than upstream projects. Typically, these projects are only started if the supply is secured and the market is well defined with the potential to spread the supply over multiple sources and to supply different markets to spread the risk. In contrast to upstream activities, which are equity financed, mid- and downstream projects can attract debt due to the limited risk profile, reducing the direct financing costs. Together these factors lead to low risk projects compared to upstream project, but also lower returns on investment (World Bank Group, 2019). Álvarez et al. (2018) indicate that the margin on complex refining and chemistry products, like methanol yielded a significantly larger margin than simple refined petroleum products.

The next downstream step is distribution to the wholesale or retail market. In the case of inland shipping the fuel is sold to a bunkering operator which sells it to the ships that use it as a fuel. Bunkering for inland ships is done in three different ways: truck-to-ship, ship-to-ship, shore-to-ship (Zomer et al., 2020). With shore-to-ship bunkering a ship is bunkered directly from a storage tank, this makes it suitable for ships that need a high frequency and limited demand bunkering, also the ships have to be flexible enough to maneuver inside the port and have a restricted draft size. This make it very suitable for smaller vessels like tugs or inland shipping. Truck-to-ship bunkering connects a truck carrying the fuel with the vessel and is a common option for low volume bunkering in smaller ports that lack the shore to ship infrastructure. Ship-to-ship bunkering brings the fuel from one ship to another and it the most common method used for seagoing vessels due to the flexibility in location and the large bunker capacity of the bunker vessel.

The second consists of the actors in direct contact with the shipowner. The shipowner is responsible for the ship and its business case. The owner either charters the ships to a third party or uses it itself. Either way the shipowner provides a service, either directly or through a charterer, to the final client that needs transport. Each of them having their own demands and preferences. Then, there are the shipyards that sell and maintain the ship. They are also collaborating with engine suppliers like Pon Power, Wärtsilä, Rolls- Royce and GE Jenbacher that are involved in the development and manufacturing of the gas-fueled propulsion systems of the ships (Box et al., 2011). The engine is developed through knowledge developed by the R&D department and academia. The ship has to

adhere to a the technical standards established by classification societies like Lloyd's Register and DNV. They classify ships and validate that their design and calculations are in accordance with the published standards.

Then, the third stream consists of the different authorities. The first is the port authority that guard the maritime safety, security and environmental issues, but also play a more proactive role as facilitators to realize port strategies to gain a competitive advantage (Wang & Notteboom, 2014). At a more general level there are the Dutch Government, CCNR (Central Commission for Navigation on the Rhine), the CESNI (the European Committee for drawing up standards in the field of inland navigation). The Dutch government is responsible for the Dutch waterways and infrastructure, next to that they set the technical norms for the vessels operating in the Netherlands (Government of the Netherlands, n.d.). The Dutch government can set national regulation, though a large part of the regulation has to be set at an international level. The CCNR is the European authority for Rhine navigation and the CESNI is the department that issues international regulation, security and environmental performance at the European level (CESNI, n.d.). Besides the regulation of the waterways which is part of the Ministry of Infrastructure and Water Management, inland shipping is part of the energy policy. Achievement of the climate goals is the responsibility of the Ministry of Economic Affairs and Climate Policy.

6.2: Methanol Supply Chain

The current methanol value chain is very similar to the upstream gas and the downstream oil value chain, since the majority of the current methanol is produced from natural gas (Alvarado, 2017). The gas is transported to a petrochemical refinery to produce methanol. In the petrochemical plant the natural gas is reformed to syngas, a mixture of carbon monoxide, hydrogen and carbon dioxide, which is reacted and distilled into methanol. After this step the value chain is similar to the downstream diesel value chain. The upstream and midstream segment of the methanol value chain is very mature since it is one of the oldest and most widely used chemical in the world (Methanol Institute, n.d.).

The biggest difference in the value chain is the potential to make methanol from many different feedstocks, which can be divided in fossil, biomass and synthetic sources as seen in figure 6.2. The fossil feedstock is currently responsible for 99% of the methanol production of which 59% comes from natural gas, 30% from coal and 9% from coke-oven gas, a byproduct from steel production. The share of coal has risen over the last two decades due to an increase of the methanol production in China, but has stabilized over the last 5 years. (Alvarado, 2017). The coal is gasified to produce syngas (Harney, 1975), while the coke-oven gas is converted in syngas by adding additional carbon to the gas (Yi et al., 2016). In the case fossil feedstocks remain dominant, the major actors in the value chain are not expected to change as the value remains within the oil and gas industry.

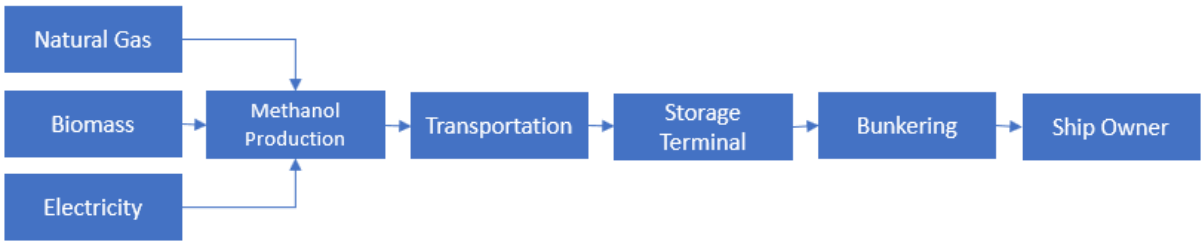

Figure 6. 2: Methanol fuel supply chain.

The biomass feedstock consists of wet biomass, woody biomass, aquatic biomass and municipal solid waste. The wet biomass can consist of organic waste, manure and sewage sludge, second generation biofuel feedstocks. The wet biomass is fermented to biogas and reformed to syngas (Zomer et al., 2020). The other biomass feedstocks are all gasified directly into syngas. The woody biomass can be any lignocellulosic material ranging from wood to grasses or even black liquor, a byproduct from the paper and pulp industry (European Biofuels Technology Platform, 2016). Woody biomass is a second generation biofuel feedstock as it does not compete as a source of food, however it can still be

unsustainable if it is not used as a waste product, but as a dedicated source, like dedicated felling of forestry wood. The aquatic biomass consists of photosynthetic algae and photosynthetic cyanobacteria and are considered third generation biomass. The municipal solid waste (MSW) consists of non-recyclable and non-compostable waste. The sorted MSW is shredded and then fed into a gasifier to produce syngas (ETIP Bioenergy, n.d.). All feedstocks except the synthetic are used to produce syngas that is reacted to methanol. This part of the supply chain still has to developed, as there are only a few biomethanol plants worldwide (Zomer et al., 2020). The technology is relatively mature and the current producers have the skills and knowledge to use biomass to produce biomethanol. However, a new network for the feedstock supply has to be developed. This can be a difficult task as the supply of biomass consist of many different streams of biomass and a decentralized supply (Eisenbach et al., 2011).

The synthetic feedstock uses electricity and an electrolyzer to produce hydrogen and CO_2 obtained through direct air capture or carbon capture of exhaust gasses it is reacted to methanol. The hydrogen is used for hydrogenation of the CO_2 to produce methanol (Borisut & Nuchitprasittichai, 2019). Just as the biomass feedstocks a different network may be required, as it requires a large amount of renewable electricity and carbon. The different feedstocks may seem different processes, but they are not mutually exclusive. All of the production methods use syngas as an intermediate product. Only the ratio between hydrogen and CO_2 differs. It may even be desirable to use a hybrid process as biomass gasification results in syngas with excess CO_2. This excess can be used as a source for the CO_2 hydrogenation to produce methanol more efficiently (Gebart, n.d.).

The methanol market had a size of 31.8 billion USD in 2018 (Grand View Research, 2019) and it is partially fragmented with a wide range of smaller and larger companies in the market. The largest 8 companies accounting for 41.6% of the market (Mordor Intelligence, 2019). The largest companies are Methanex, a Canadian company focusing on methanol only, SABIC, a company from Saudi Arabia producing multiple commodity products and Proman AG, a Swiss company producing gas derivatives. Other large producers in the EU are: Equinor, BASF and OCI. Currently, just 1 percent of the methanol is produced from sustainable sources (Alvarado, 2017). The renewable methanol is currently produced almost exclusively by niche actors like BioMCN, a subsidiary of OCI in the Netherlands, that uses biogas as a feedstock (Duurzaam Bedrijfsleven, 2017) or Carbon Recycling International in Iceland and Germany that produce e-methanol (Doyle, 2020). Despite the low percentage of renewable methanol the number and size of renewable methanol projects in development is increasing and financing of the projects are increasingly done by the bigger methanol producers (Štefančič, n.d.).

After the methanol production, the downstream value chain of methanol is very similar to that of diesel as it is transported to a terminal, after which it is bunkered to a ship and used as a fuel. As methanol is a liquid it is not expected that there will be radical changes in the mid- or downstream value chain.

The largest changes are in the upstream value chain. In the short term the feedstock will change from oil to gas, however these changes are still within the same industry with a majority of the actor in the ecosystem remaining the same. When shifting towards biomethanol or e-methanol from renewable electricity the upstream value chain is completely substituted. The companies active in this field are almost completely different since the feedstock is no longer supplied by the oil and gas industry, but by the agriculture, food, waste industry or energy industry. This change can be considered threatening since the upstream segment of the oil and gas sector accounts for 75% of the value of the industry.

6.3: Barriers & Opportunities

In this section the risks and opportunities of methanol are compared to diesel, LNG and hydrogen. Diesel and LNG are seen as the most viable options for the short and medium run, while hydrogen expected to have potential in the long run.

6.3.1: Safety

The safety hazard of fuels can be divided in flammability, toxicity and environmental impact. Methanol has both risks and opportunities in these categories. The biggest risk is the flammability of a methanol leakage. Methanol is a low flashpoint fuel, with a flashpoint of 11 °C. Since methanol vapor is heavier than air a flammable vapor can develop in lower parts of the ship if a leak occurs (Methanol Institute, 2013). Methanol is a colorless and odorless liquid and has a flame that is barely visible in sunlight and produces no smoke. Therefore, a leak or even fire is difficult to detect. To mitigate these risks, lower elevations of the ships need to be ventilated and a methanol vapor detection system needs to be installed. New firefighting equipment needs to be installed as well. To reduce the risk of a leakage double walled fuel lines are required in rooms that are human accessible or have machinery in them (Harmsen et al., 2020). These measures are similar to other low flashpoint fuels, like LNG and hydrogen. Still, methanol is considered easier to handle those alternatives (MAN Diesel & Turbo, 2014).

The second criteria is the toxicity. Working with methanol requires eye, skin and respiratory protective equipment as methanol is considered toxic (Harmsen et al., 2020). However, diesel and gasoline are toxic as well (Bromberg & Cheng, 2010). With regard to the mortality, methanol is similarly or less toxic than gasoline or diesel. The problem with methanol is the low vapor pressure and the non-lethal negative health effects. Methanol evaporates rather quickly at room temperature and it can cause blindness and other neurological effects when a relatively small amount is ingested. However, it is not carcinogenic like gasoline and diesel. LNG brings along the risk of frostbit in case of a leakage due to the low temperatures .In closed spaces it vapor also works as an oxygen displacement like CO (PGW, 2015). All fuels have their own health risks, however extra care should be taken with methanol in closed spaces due to the low temperature vaporization and its morbidity.

In contrast to diesel, the environmental impact of methanol spills is considered minimal. Methanol is completely soluble in water and it is diluted in a matter of minutes. Methanol is less or even non-toxic to marine life and it is consumed by a variety of marine and terrestrial microbes cleaning up the spill. The effects would only be temporary and reversible (American Methanol Institute & Malcolm Pirnie Inc., 1999). LNG spills also have a limited long term effect on the local environment, but due to its high carbon equivalent it would release a large impact on global warming and it would create a large risk for fire until all fuel is vaporized (Liquefied Gas Carrier, n.d.).

With regard to safety there are risks and opportunities. It is possible to overcome the risks with regard to flammability and toxicity through relatively simple safety measures. While there is relatively little experience with methanol as a marine fuel, there is ample experience with handling it as a good. The IMO has already published interim safety guidelines for methanol as a fuel for marine shipping (ICIS, 2020) and the CESNI has initiated a workgroup investigating this for inland shipping (CESNI, 2020). These are expected to be ready in 2023. Until then, the design has to be approved on a case by case basis. This has to be accompanied by an engineering and risk analysis and is usually supported by a classification society (GMM consortium partners, 2021).

6.3.2: GHG Emissions

When comparing different fuels with respect to sustainability it is important to assess the fuels over the entire chain. This includes both the emissions during the production and transport of the fuel, the well-to-tank (WTT) emissions, and the emission when combusting the fuel, the tank-to-wake (TTW) emissions. Both GHG and pollutant emissions are assessed on a well-to-wake (WTW) base.

The GHG emissions are investigated for different production pathways. The average fossil, biobased and electricity pathways are compared on a WTW combustion of 1 MJ final fuel (LHV). There is no consensus yet of the influence of alternative fuels on the efficiency over different load points (Horvath et al., 2018). TNO (2020) found that the efficiencies of ICE was mainly dependent on engine size and considered an average efficiency of 42% for inland shipping vessels. The highest efficiencies considered were hydrogen fuel cell vessels as the fuel cell efficiency is 50%, but the losses of the electric drivetrain of about 8% are higher than the mechanical drivetrain reducing the effective efficiency 45%. The optimization in this thesis showed a small increase in efficiency for methanol dual fuel compared to diesel. The difference in efficiency only has a minor effect on the WTW emissions in comparison to the carbon footprint of the fuel itself.

6.3.2.1: Fossil Pathways

When looking at the carbon footprint the fossil based production pathways in figure 6.3 it can be seen that the distribution of emissions between fuels is different. Diesel and LNG have rather low emissions during the production, transportation and distribution. Methanol and hydrogen are significantly more carbon intensive in the WTT processes, due to the high emissions in the transformation from primary energy to final fuel. This is especially true for hydrogen as no carbon is stored in the fuel itself and this is only partly compensated by the absence of TTW carbon emissions. The transformation and total emissions are far worse for the coal based pathways than the natural gas pathways. Overall, LNG is the least carbon intensive fuel from fossil sources, decreasing emissions 21% compared to diesel. Fossil methanol increases emissions by 18% even if natural gas is used as a source. Hydrogen is the most carbon intensive fuel, unless c is used. There has been a lot of public resistance against CCS due to the newness of the technology and the fear of leakages. But, the technology is maturing and with provisions of the right information the public may become more receptive (Tcvetkov et al., 2019).

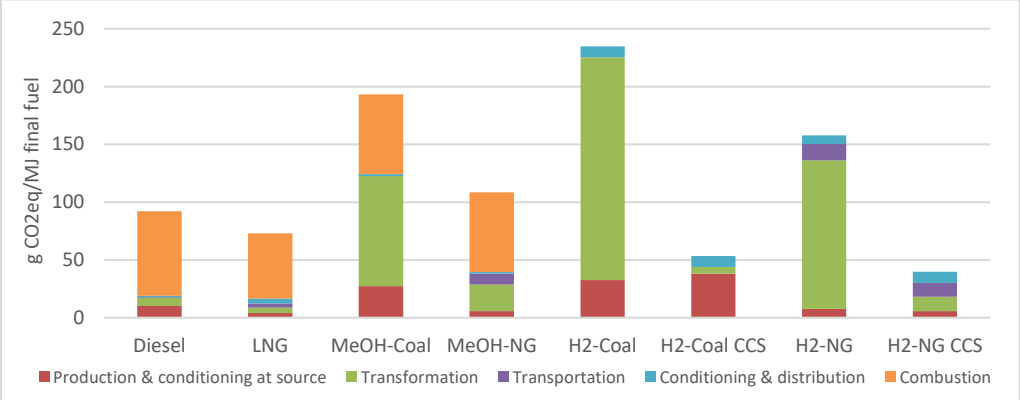

Figure 6. 3: GHG emissions from fossil production pathways derived from Prussi et al. (2020).

6.3.2.2: Biomass Pathways

In the analysis of the biomass pathways two kinds of pathways are excluded: wet manure and the BECCS concept. The pathways with wet manure as primary energy source are not included, because wet manure has high negative GHG emissions ranging from -93 to -140 g $CO_{2\text{-eq}}$/MJ. This due to the natural methane emissions if it is not treated. Methane has a global warming potential (GWP) of 25 (CBS, n.d.-a), so this waste stream should always be processed and it could be used to make all of the considered fuels. The BECCS concept stands for Bioenergy with CO2 Capture and Storage (BECCS). It captures the excess CO_2 in the production processes leading to negative emissions of about -100 g $CO_{2\text{-eq}}$/MJ. This technology is still in development and could be used for all the fuels discussed.

When looking at the remaining pathways in figure 6.4 it is clear that biofuels have a lower GHG footprint than fossil fuels. This is mainly due to the absence of emissions during the combustion, because the CO_2 that is released during combustion was absorbed by the trees and plants used to produce the fuel. Now the main driver for the emissions is the cultivation of the biomass followed by the transformation into biofuels. Methanol is the exception as the production has a fairly low carbon

intensity and the transformation is carbon neutral. The process from wood to methanol requires a lot of energy, but this is all from the wood itself. A large share of the emissions is due to the transportation as the wood is assumed to be transported by truck over 500 km or more. The other pathway for methanol uses black liquor, a byproduct from the pulp industry, and emits only 6.2 g $CO_{2\text{-eq}}$/MJ in total. Conditioning and distribution is only a minor part for the biodiesels and biomethanol. For LNG and hydrogen this is a larger share as LNG and hydrogen need to be cooled to -162 °C and -259 °C. Alternatively, hydrogen is compressed to 500-880 bar. When using biomass as a source, methanol is the least carbon intensive fuel. Bio-LNG is second best with 86% more GHG emissions compared to methanol.

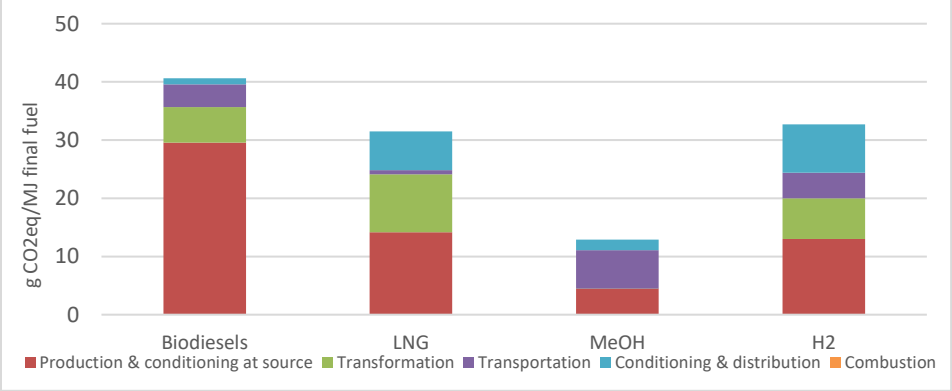

Figure 6. 4: GHG emissions from fossil production pathways derived from Prussi et al. (2020). Biodiesel includes all types, like FAME, HVO and FT diesel.

6.3.2.3: Electrofuels from renewable electricity

The last production method is the usage of electricity to produce hydrogen through electrolysis. Prussi et al. (2020) assume renewable energy to be unlimited. Therefore, the resulting GHG emissions from the production and combustion are zero. They only consider the conditioning and distribution emissions. As discussed in the previous section, diesel and methanol have the lowest carbon intensity of the distribution with 0.8 and 1.8 g $CO_{2\text{-eq}}$/MJ, respectively. Diesel has a higher energy density, so the carbon intensity is less than that of methanol. LNG and hydrogen require much more with 6.7 and 8.3 g $CO_{2\text{-eq}}$/MJ, respectively. However, renewable electricity is not expected to become unlimited in the coming decades. It is important to use electricity as efficient as possible.

In table 6.1 the efficiency conversing electricity to fuel is stated. The hydrogen still needs to be compressed or liquefied. Compression reduces the efficiency by 5-15% (Sdanghi et al., 2020) and compression reduces the efficiency by 12-15% (Elgowainy et al., 2017). The efficiency of LNG also needs to be correct for liquefaction, this reduces the efficiency by 0.7-7.3% (Zhang et al., 2020). The large difference in liquefaction efficiency is highly dependent on the scale at which it is performed. Also, all fuels except hydrogen require a CO2 feed. This could either be a point source from industrial processes or a power plant, or from direct air capture. Point source carbon capture requires 0.72 MJ/kg CO2 (Wang & Song, 2020) and direct air capture requires (DAC) 9.09 MJ/kg CO2 (House et al., 2011).

Table 6. 1: Electrofuel conversion efficiency (Tremel, 2018).

Fuel	Conversion Efficiency	Final Efficiency point source	Final Efficiency DAC
E-Diesel	45.3%	44.2%	34.8%
E-LNG	48.7%	40.7-47.1%	34.2-38.5%
E-Methanol	51.6%	50.3%	39.0%
E-Hydrogen	67.0%	52.0-62.0%	52.0-62.0%

Hydrogen is the most efficient option in the production of the electro fuels, followed by methanol. If a point source is used for the carbon feed methanol follows relatively closely, but with DAC the

difference drastically increases. Therefore, it is unlikely that E-fuels other than hydrogen will be used if not even carbon point sources are available. When evaluating methanol on its carbon footprint it only makes sense to use biomethanol or e-methanol from renewable energy. However, in these cases it can be argued that biomethanol is the best solution until renewable electricity is unlimited available.

6.3.3: Criteria Pollutant Emissions

Criteria pollutant emissions are also emitted across the entire chain. There is a large range in the reported values across literature and there are no recent comprehensive reports available for the WTT emissions of criteria pollutants. Therefore, it is difficult to come to a well-funded conclusion. Table 6.2 shows the WTT emissions of criteria pollutants for different pathways and the stage V norm for TTW emissions for comparison.

Table 6. 2: WTT and TTW Criteria Pollutant Emissions based on top 10% best performing companies in Brinkman et al. (2005)[1], (Otten & Afman, 2015)[2], (DieselNet, n.d.)[3].

WTT			
	CO g/kWh	NOx g/kWh	PM g/kWh
Diesel[1]	0.029	0.117	0.015
LNG[1]	0.036	0.180	0.018
NG-MeOH[1]	0.071	0.258	0.040
NG-H2 [1]	0.089	0.388	0.115
Electro H2 CA-Mix[1]	0.161	0.597	0.291
Dutch electricity NG[2]	-	0.4	0.005
Dutch electricity Coal[2]	-	1.8	0.07
Dutch electricity biomass[2]	-	0.4	0.03
TTW			
Stage V Inland ships[3]	3.5	1.8	0.015

The WTT emissions are similar for each fuel and are mostly dependent on the feedstock used. Compared to the TTW emission norm the WTT emissions are low, except for the PM emissions. However, only less than 10% of the PM emissions are in urban areas where they are most harmful (Brinkman et al., 2005). While, the exact numbers differ between reports the trends are similar. Generally, switching from fossil sources to biomass would reduce the local emissions (E4tech, 2019; Spoof-Tuomi & Niemi, 2020; TIAX LLC, 2007). E-fuels show mixed results. If it is produced from renewables it would reduce almost all WTT emissions (E4tech, 2019). However, using non-renewable electricity would lead to an increase of local emissions beyond the TTW emissions. This is in agreement with the emission numbers of the Dutch electricity grid.

The criteria pollutant emissions do not help or hinder methanol on a WTT basis as it is similar to the other fuels. While all inland shipping vessels have to adhere to the Stage V norm from 2025 onwards, it differs for each fuel whether this is possible with or without after treatment system and what kind of after treatment is required. It depends on the type of engine whether the limit is reached. Fuel cell engines are the exception as they do not emit any pollutant emissions.

6.3.4: Transport, Storage & Distribution

One of the great advantages of methanol, being a liquid at atmospheric conditions, is that the current infrastructure can be used to a large extend. Methanol is already transported by truck, train and ship around the world. Pipelines may also be used as minor impurities are acceptable for fuel applications (American Methanol Institute, n.d.). However, this method is only effective for very large volumes as pipelines need to be cleaned before it can be used for methanol. Next to that, methanol is corrosive and pipeline operators are hesitant to use existing pipelines before more research is conducted (Bromberg & Cheng, 2010).

The storage of methanol can be done in stainless steel, carbon steel, or methanol-compatible fiberglass tanks. Conversion of existing petroleum tanks is relatively easy as it only requires thorough cleaning and in some cases replacement of the liner (Bechtold et al., 2007). Storage of methanol in terminals is similar to those of other biofuels and vegetable oils and is done in smaller tank sizes than oil products. LNG has to be stored in specifically designed cryogenic tanks and cooled to -160 °C (Vopak, n.d.). Currently, methanol is available in more than 100 ports, exceeding the number of ports that have LNG available (Greenport, 2020b, 2020a). Hydrogen is currently not available in ports. Plans are made for hydrogen infrastructure and storage, but these are not yet developed.

The bunkering of methanol can be done in the same manner as diesel. At first it is most likely to be done through truck-to-ship bunkering. This low volume bunkering methods allows for flexible demand and can be done in ports without methanol storage. The downside of this approach is that the costs are relatively high with €14/ton (Zomer et al., 2020). Once the demand increases shore-to-ship and ship-to-ship bunkering will be the most likely options. Shore-to-ship bunkering is the cheapest options at €6/ton, but this requires high demand as it requires infrastructure investment at the port. Methanol can be used with the current infrastructure, but it requires cleaning before switching fuels (Zomer et al., 2020). Ship-to-ship bunkering is generally the most used method of bunkering. As seen in table 6.3, the costs are similar to truck-to-ship bunkering for inland ships due to the relatively low bunkering quantities. In comparison to diesel, the bunkering costs of methanol are slightly higher. Due to the lower energy density of methanol more fuel needs to be bunkered. This reduces the costs per ton, but increases the bunkering costs. The bunkering costs of LNG are in its turn higher than those of methanol as the investment and operational costs of LNG bunkering ships are higher. Next to that, LNG has a similar volumetric energy density to methanol and requires a similar volume. Hydrogen bunkering is far more expensive, but this is mainly due to the low bunker quantity used in the calculation. Hydrogen has the lowest volumetric energy density and requires 2 times more space than LNG. Therefore, for the near future storage capacity of the first vessels is going to be limited. If similar quantities are used the costs are likely similar to LNG. Though, the distribution costs are likely to increase. This is only a minor part of the fuel costs, typically less than 10%.

Table 6. 3: Distribution costs for inland shipping (TNO, 2020)

		Diesel	LNG	Methanol	H2 700 bar
Typical bunker quantity	ton	25	20	40	3
	GJ	1138	1000	908	363
Daily bunker deliveries	#/day	4	4	4	4
Bunker ship costs	€/day	2200	3000	2200	3000
Distribution costs	€/ton	22	38	14	250
	€/GJ	0.48	0.75	0.61	2.07

Besides the costs there are some other considerations. As with all considered alternative fuels the volumetric energy density is significantly lower compared to diesel. Even though it is not likely to change the operating profile of the vessels, it can change the bunkering strategy. There is less flexibility in bunkering, so it is more difficult to take advantage of price differences over time and between ports.

More importantly, the classification of methanol as a dangerous good requires additional safety measures during bunkering. These measures consists of a berthing distance of 50 meters to other vessels, 100 meters from installations and 300 meters from living areas need to be taken into account. This also affects other quayside activities like cargo and passenger handling. For LNG and petroleum products this is 10, and 100 meter (Verenigde Naties & Economische Commissie, 2015). It is possible to get exemptions from the harbor master if the procedure is considered safe. These rules only apply during bunkering and if its used as cargo, since an exemption is made for fuels.

6.3.5: Fuel Costs

The most important determinant of the total cost of ownership (TCO) is the cost of the fuel. In figure 6.5 the price ranges of the considered fuels from different sources are visualized. Currently, the fossil fuels are still significantly cheaper than the renewable fuels and this is not expected to change on the short term. The price of fossil methanol and hydrogen are within the range of fossil diesel. Fossil LNG is clearly the cheapest fuel. When looking at the biofuels the range of fuel prices drastically increases, due to the large variety in feedstocks and production routes. Biomethanol is not the fuel with the lowest price, but it has the smallest price range and it is close to the lowest bottom price of bio-LNG. Biohydrogen also has a small range and is relatively cheap. However, hydrogen needs to offset the higher distribution costs discussed in section 6.3.4 to be competitive. Of the E-fuels the production of hydrogen is the cheapest, since it has the highest efficiency, as discussed in section 6.3.2, and it does not require a carbon source. The price of the E-fuels is dependent on the electricity price and the CO_2-price. This is why the range of the other fuels is larger than that of hydrogen. The production of E-methanol is slightly more expensive than E-LNG and slightly cheaper than E-diesel. The lowest production costs of hydrogen are competitive with fossil fuels. However, in this scenario the electricity price is set at only 0.02 €/kWh (TNO, 2020). In the last 2 decades the Dutch electricity price ranged from 0.06 to 0.011 €/kWh (Statista, n.d.). Production at lower electricity prices is only possible when there is over-production by renewable energy sources. Therefore, realistic current prices for large scale production would be in the upper half pf the price range.

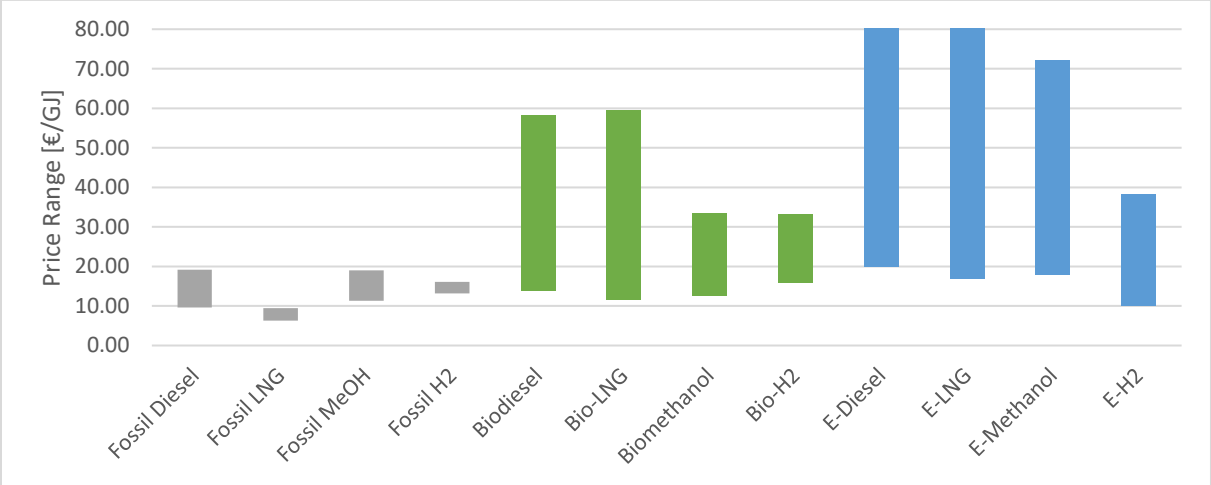

Figure 6. 5: Average price/production cost range found in literature derived from Appendix F.

In order to stimulate the adoption of renewable fuels the Dutch government implemented HBE certificates (Renewable fuel unit). One HBE is rewarded for every GJ of renewable fuel and in the current scheme advanced biofuels are double counted (NEa, n.d.). Biomethanol is an advanced biofuel and for biodiesel and bio-LNG it is dependent on the feedstock used. The price of a HBE has been 10-12 €/GJ (Platform duurzame biobrandstoffen, (2021). This would reduce the price of biomethanol by 20-24 €/GJ, making it a price competitive option. One of the opportunities is that fuel price are volatile. So, shipowners and clients are used to changing fuel prices. If prices would increase due to a higher required share of renewables in the fuel mix this would not be new for the industry.

6.3.6: Drivetrain Costs

Both methanol and LNG can be used in existing engine once retrofitted. Table 6.5 provides an overview of price ranges for retrofitting the engine, new drivetrains and the fuel storage tanks. The costs of retrofits are derived from existing cases of retrofitted engines. These cases are based on relatively large engines, which normally reduce the costs per kW. However, a methanol fumigation retrofit is cheaper than a direct dual fuel retrofit. Next to that, experience and standardization is expected to reduce the retrofit costs. The total capital expenditure (CAPEX) of methanol retrofitting in ships are expected to be similar to adding aftertreatment to the existent diesel engine (CE Delft, 2011; Ellis & Tanneberger, 2015). A large share of these costs are the installment costs. The costs will be

lower at around 100 €/kW if the engine is retrofitted and after treatment is installed. Both options are cheap in comparison to LNG retrofits which are 2-3 times as expensive, due to the complex storage of the cryogen fuels. When implementing methanol in a new drivetrain the costs are only slightly higher than diesel engines. There is a larger difference in the fuel storage, because a larger storage is required due to the lower energy density of methanol. The costs for LNG and hydrogen are a lot higher. Both LNG and hydrogen need cryogenic tanks to cool the fuel -162 °C and -259 °C, respectively. Hydrogen is still considerably more expensive than LNG, because it requires a 3 times larger storage with more stringent requirements to the tanks. Hydrogen is likely to use fuel cells, due to the higher efficiency and the absence of exhaust emissions. The downside is that fuel cell technology is more expensive than ICE technology.

Table 6. 4: Vessel CAPEX ranges for alternative fuel engines derived from Appendix G.

	Retrofit Total [€/kW]	New Drivetrain [€/kW]	Fuel Storage [€/GJ]
Diesel	127-242	538-636	23-27
Methanol	250-390	554-700	39-45
LNG	553-1000	781-1062	85-100
H2 FC	-	1692-2000	231-1180

6.3.7: Business Case

There is a large variety of inland shipping vessels and operating profiles, but generally the total cost of ownership of inland shipping vessels consist for the majority of fuel costs (Korberg et al., 2021; TNO, 2020). Because the fuel costs of methanol are higher than those of fossil diesel and LNG, there is no positive business case without subsidies (GMM consortium partners, 2021; Maritiem Kennis Centrum et al., 2018). However, with the current HBE prices and the double counting of advanced biofuels like methanol the business case for biomethanol becomes feasible (Maritiem Kennis Centrum et al., 2018). Compared to the other biofuels methanol is the cheapest fuel. It is likely that methanol has the best business case among the biofuels, as it also has the lowest conversion or new drivetrain costs close to those of diesel. Bergsma, Hart, Pruyn, & Verbeek (2020) found for a variety of short shipping vessels that methanol has the best business case among biofuels. Its only close competitor was the biodiesel HVO, but it only has a limited availability due to its very specific feedstock.

The business case for E-fuels is more difficult than for biofuels, as the production costs are considerably higher. Even the HBE subsidy is not enough to close the fuel price gap, except in the case of hydrogen. However, the CAPEX of hydrogen are considerably higher. In the case that electro fuels are required due to a lack of biomass for the production of biofuels it is not clear which fuel is the best option. According to Horvath et al. (2018) hydrogen fuel cells would have the best business case, while Korberg et al. (2021) indicate that methanol ICE are better. It all depends on the assumptions in the fuel costs. Horvath et al. use an electricity price of 44 €/MWh. Korberg et al. use an electricity price of 33 €/MWh and includes the infrastructure costs which accounts for 23% of the total hydrogen costs. Potentially, there is also a difference in the carbon capture costs which are not report in Horvath et al.

6.3.8: Availability & Scalability

The inland shipping sector is a relatively small market consuming 1.1 billion kg diesel, or 48 PJ, in 2019 (CBS, n.d.-c). This is roughly 10% of the total engine fuel consumption (CBS, n.d.-c) and 1.6% of the total energy consumption in the Netherlands (CBS, 2020).

6.3.8.1: Fossil Based

A change to another fossil derived fuel in the inland shipping sector will not cause major availability issues. Natural gas is currently responsible for about half of the total energy consumption, so the feedstock it plenty available. The global methanol production is operating at 65% capacity. Therefore, it is possible to meet a short term increase in demand. However, a quick global shift in towards methanol as a fuel could be problematic. It is estimated that in 2018 the Dutch production of methanol was 10.5 PJ and the apparent consumption 17.7 PJ. This means that a large increase in production is

necessary to supply a large scale transition towards methanol. This is exactly what the industry has planned. Production in 2019 in the Netherlands is estimated to ramp up to 21 PJ and the expectations are that the methanol industry is going to double the capacity in the next 5 years (Zomer et al., 2020). The total amount of hydrogen that is currently generated in industry is estimated at 180 PJ, of which 105 PJ is produced from natural gas. Similar to methanol the hydrogen production capacity is only expected to grow (Weeda & Segers, 2020).

6.3.8.2: Biomass Based

When considering the biomass based production pathways the availability is not only limited by the production capacity, but by the availability of the feedstock as well. There is a declining trend in the expected potential of biomass in research in the past 10-15 years. Research in 2008 estimated a potential of about 1000 PJ/y, while research in 2018 estimated 100 PJ/y (Natuur & Milieu, 2018). Natuur & Milieu (2018) estimate an unused potential of 70-85 PJ/y on top of the 120 PJ/y currently in use for energy purposes. The unused potential includes 15-30 PJ of imported biomass. It is clear that there is uncertainty about the national availability of sustainable biomass. This is even more so for the international supply. The Ministry of Economic Affairs (2015) estimated the total international supply of biomass to the Netherlands between 115 and 773 PJ in 2030. Thus, the potential biomass ranges from just enough cover the inland shipping sector to more than enough to cover the total engine fuel demand.

The majority of the currently used biomass is based on oils and fats, while the unused potential exist mainly of wood based biomass followed by sewage sludge (Natuur & Milieu, 2018). The oils and fats are used to produce cheap biodiesels like FAME and HVO and the wood based biomass and sewage sludge is suitable for the production of biomethanol.

If a hybrid biomass-electrolysis approach is used for the production of methanol, a 119% conversion rate of woody biomass to methanol on a LHV basis could be reached (Clausen et al., 2010). It also has a high energy efficiency of 71%. This can be increased to 90% if the low temperature heat is used for district heating. The global production of biomethanol is limited to less than 1% of the methanol production capacity, but it is increasing. There is one biomethanol plant in the Netherlands with a production capacity of 1.2 PJ/y. This is 11% of the Dutch methanol production capacity and 7% of the Dutch methanol consumption. A similar size biomethanol plant is currently under construction (Zomer et al., 2020).

The efficiency of Bio-LNG is similar to biomethanol with an energy efficiency of 72% from biomass to biomethane (Giglioet et al., 2021) and 57-70% after liquefaction to bio-LNG (Zhang et al., 2020). The Dutch biomethane production in 2020 is estimated at 26.85 PJ/y (World Biogas Association, 2017). This is 2% of the Dutch gas consumption.

Hydrogen from biomass can be produced with an efficiency of 69% (Binder et al., 2018), which reduces to 56% after liquefaction or 62% after compression (Elgowainy et al., 2017). Though there is some hydrogen from biomass projects, the majority of sustainable hydrogen projects are focused on electrolysis (De Laat, 2020).

6.3.8.4: Electricity Based

With regards to the electrofuel pathways, the supply is mainly limited by the electrolyzer capacity and the renewable electricity production. Both are expected to rapidly increase in the coming decades. The electricity supply will most likely be the biggest constraint as the current renewable electricity production is only 25% of the total supply (CBS, 2021). In 2030 this is expected to increase to 75% (Planbureau voor de Leefomgeving, 2020). In the calculations they take an electricity consumption 434 PJ of which only 20 PJ is dedicated to transport. This means that a lot of electricity still has to be reserved for electrification of transport. Therefore, it is unlikely that there will enough spare renewable electricity for large scale electrofuel production in the coming decade. Electrofuels could potentially be used for grid balancing. Due to the unpredictability of renewables like solar and wind energy, the

chance of excess electricity increases. As overloading the grid must be prevented this can lead to low and even negative energy prices. One of the solutions for grid balancing would be to use electrofuels for grid balancing (Malins, 2017).

As methanol and hydrogen are a single molecule fuels, there are no differences in the fuels for different production pathways. Bio-LNG and E-LNG have small differences compared to fossil LNG. Bio-LNG and E-LNG are almost pure methane, while fossil LNG also has higher hydrocarbons (Daag, 2013). In the case of diesel there are larger differences between the production pathways and cannot simply be freely mixed (Lappas & Heracleous, 2011)

6.4: Overview Barriers & Opportunities

This chapter shows that there are opportunities for biomethanol compared to diesel, LNG and hydrogen. The value map is shown in figure 6.6 and 6.7. When considering the fossil methanol there only a few barriers. The fuel can be supplied by a mature industry. Since gas is used as a main feedstock oil and gas companies will not likely resist. Many NOCs and IOCs even have methanol in their product portfolio. Transport, storage and distribution can also facilitate methanol without or with only small investments. Almost all main ports already have a methanol terminal, so only the bunkering infrastructure needs small adjustments. A minor short term barrier could be the scale as switching between fuels requires extensive cleaning. However, truck-to-ship bunkering is a cost-effective small-scale option that requires minimum dedication. There are also opportunities for the transport, storage and distribution companies. They could even profit from the switch to methanol as they would handle larger volumes compared to diesel.

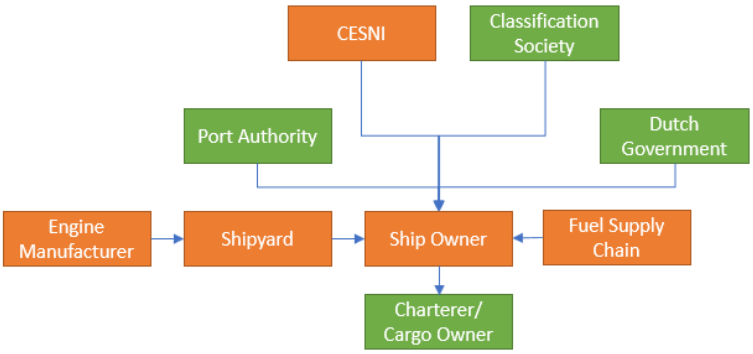

Figure 6. 6: Methanol value blueprint with risks.

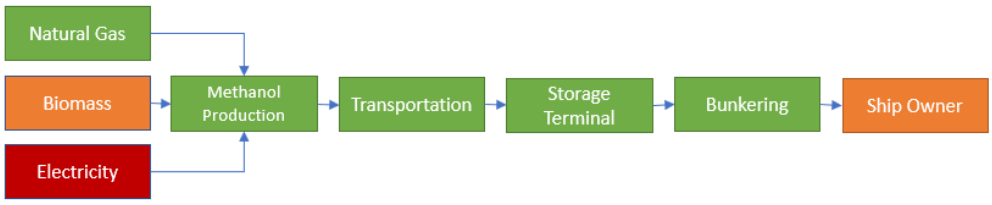

Figure 6. 7: Methanol supply chain with risks.

Other barriers are the case-by-case approval for methanol vessels, but this problem is expected to be solved as the CESNI workgroup is expected to include methanol in its regulations. The only supplier barrier is for the engine manufacturers and shipyards. They are able to fulfill their part in the EVP, but it is questionable if they are willing to do so. The barrier for engine suppliers is the certainty of the demand as they still need to invest in the development of a methanol engine line and the inland shipping sector is a rather small and diverse market. The same holds for shipyards as they can operate within their core competences, but they need to have a certain demand to cost-effectively retrofit the engines.

By far the biggest barrier is with the user group: the shipowners. This is mainly due to the higher fuel costs which is the most important selection criteria for shippers (Hansson et al., 2020). Next to that, they have a smaller operating range, higher investment costs and a higher carbon footprint compared to fossil diesel. There is almost no incentive to adapt fossil methanol in inland shipping vessels. The opportunities are only apparent for biomethanol, because it has the lowest carbon footprint and the lowest fuel costs of the renewable fuels. With the HBE-subsidy biomethanol may even be price competitive with fossil diesel. Though, the establishment of a sustainable methanol supply chain may be a great challenge.

Biomethanol needs to be scaled up rather drastically to provide a sustainable alternative for inland shipping. The technology is mature enough, but the production costs of biomethanol are higher than grey methanol (IRENA & Methanol Institute, 2021). Moreover, 75% of the value is created in the upstream sector which will be substituted in the case of sustainable methanol. This may lead to resistance by the oil and gas sector. At the moment there is a Catch-22 situation. On one hand there is no incentive for the industry to produce biomethanol without specific demand for it. On the other hand engine producers and shippers are hesitant to invest in methanol engines as long as there is limited to no supply of biomethanol. The origin of this problem does not solely lie within the methanol EM. It is an issue faced by the entire fuel industry and will be explored in the next chapter together with strategies to solve this problem.

E-methanol is only a viable solution if there is redundant renewable electricity and this will not be the case any time soon. The only short and medium term scenario in which it is a viable solution is if it is deployed as a grid balancing solution. This will only allow for small scale production of e-methanol and the production of hydrogen may be the more profitable option.

Chapter 7: Ecosystem, Dynamics & Management

Chapter 6 shows that there a few barriers that actor are not capable of overcoming in the next few years. The major issue is the interdependence of stakeholders and the uncertainty about the solution which make actor unwilling to invest. It is an issue faced by the entire fuel and transport industry and this will be explored in this chapter and potential resolution strategies are discussed. The issues is analyzed deeper with the MLP framework. It provides insight into the reining uncertainty problem by analyzing the industry dynamics.

7.1: Multi-Level Perspective

7.1.2: Landscape

There is increasing pressure from the landscape to make transport more sustainable, because they have a significant role in global warming and local air pollution. The Dutch government has to adhere to the climate agreement and the RED II (Renewable Energy Directive). Still there are climate groups that are pushing for stricter policy going as far to sue the government (AD, 2019). The inland shipping sector has long been excluded from the discussion, but this is no longer the case. From 2022 onwards inland shipping is included in the RED II, meaning that by 2030 27.1% of the fuel should be renewable (Overheid.nl, 2020). In the Green Deals the inland shipping sector has agreed to progressive GHG emissions reductions (Green Deal, 2019). In 2024 a 20% reduction compared to 2015 needs to be achieved. By 2030 this increases to 40-50% and by 2050 the fleet should be carbon neutral. How this should be achieved is left to the industry, though it is agreed to have at least 150 vessels with a zero-emission powertrains by 2030. This is 3% of the current fleet size (CBS, n.d.-b).

Not only the carbon emissions are getting more attention. The attention to pollutant emissions is increasing as well. For the polluting emissions there are increasingly stringent regulation for new engines, starting with CCR 1 in 2003, CCR2 in 2007 and Stage V in 2019. Engines older than this do not have to adhere to any rules. There is increasing pressure to push for stricter regulation and the support for environmental control zones is increasing. The harbor of Rotterdam sets a requirement of CCR2 certification for all vessels from 2025 (Panteia, 2019). Over 60% of the current fleet does not fulfill this norm. There clearly is an increasing pressure from the landscape to move towards clean and sustainable transport. For a long time the inland shipping sector was excluded, but this is no longer the case and they need to catch up.

7.1.3: Regime

At the regime level it can be argued that there are two distinct regimes: the powertrain regime of the ICE and the fuel supply regime of diesel. Often they are considered as one, but radical changes in the fuel supply can happen without radical changes in the powertrain and vice versa. A majority of the fuels can also be used in both ICE and FC technology (Xing et al., 2021).

The powertrain regime is based on the ICE technology. The ICE regime is dynamically stable with different development pathways. The most used powertrain is the CI engine, with some vessels using SI engines in combination with LNG as a fuel. To cope with the landscape pressure the regime is developing different LTC combustion methods and better aftertreatment systems to increase efficiency and reduce emissions. The fuel production regime is based on fossil diesel. The inland shipping sector is not yet obligated to blend in biofuels, like in road transport. Even though LNG infrastructure is being developed and vessels are increasingly using LNG, it is only a minority and cannot yet be considered part of the regime. The fuel supply regime has a large interest in keeping the status quo of fossil fuels, due to the very large investments in the upstream oil and gas production.

7.1.4: Niche

At the Niche level for the drivetrain the playing field is quite clear. There are only adaptations of the electric drivetrain: battery-electric, diesel-electric or fuel cell-electric. All options depend on the type of energy storage used. As explained in chapter 4 most application are limited to diesel-electric and fuel cell electric. Diesel-electric is a complement to the current ICE regime rather than a substitute. Fuel cell-electric appears to be a promising technology, but the technology is still in development and

it is expected to remain a more expensive option for the next 10-20 years. Fuel cells are highly associated to hydrogen as the most developed fuel cells use hydrogen. However, there are many different fuels than can be used as hydrogen carriers. The fuel is reformed into hydrogen and CO2 before using the hydrogen in the fuel cell. Besides hydrogen fuel cells there are also fuel cells that can directly use fuels like methanol or ammonia (Cheng et al., 2020; Y. Zhao et al., 2019). The introduction of renewable fuels strengthen the ICE regime as it may decouple the association of ICE and GHG emissions. Fuel cell technology also requires renewable fuels, but it already has the image of a sustainable technology.

At the niche level of the fuel supply there is a plethora of options extending beyond the ones discussed in this thesis. Each of the fuels have their own advantages and disadvantages. This creates an incredibly difficult situation in which nobody knows in what options to invest. This is true for the fuel production, transport and distribution as well as the ICE adjustments. As discussed in section 6.3.5, biofuels are the cheapest renewable option until renewable electricity is cheap and abundantly available. It is likely that for the short and medium term multiple fuels will co-exist, because different biofuels prefer different feedstocks. Methanol for example uses wood-based feedstocks, the biodiesels HVO and FAME use waste cooking oils or seeds and ethanol uses grains and crops (Prussi et al., 2020). When looking at the e-fuels the complementarities are greater as all of them require hydrogen, which is the majority of the investment and production costs (TNO, 2020). Therefore, there will be a co-evolution of all e-fuels in the fuel production.

The focus of the sector is on the fuels discussed in chapter 6 with growing attention to methanol. The government policy is technology neutral as they subsidize GHG abatement through the HBEs. This leaves the decision for what fuel to use to the industry. Until a winner arises there will be a lot of uncertainty and actors will be hesitant to invest. As the GHG emission regulation for inland shipping came quite late, they had the possibility to wait and see which fuel would likely be the winner. However, with the inclusion of inland shipping in the RED II and the green deals the pressure is increasing. The SNM framework can be used to help in the selection processes and to create trust in the solution.

7.2: Strategic Niche Management

In SNM the first step to help the niche development is to create an environment free from selection pressures and the competition oriented behavior observed in industries. None of the actors in the EM is able and willing to take the risk on their own, so there needs to be a willingness to cooperate in the initial phases of experimentation and learning. This is done in consortia like: Green Maritime Methanol, Fast Water, Green Pilot, HyMethShip, SUMMETH and SPIRETH. Each of them consists of multiple actors with different positions in the EM. They have investigated required changes in the ship design and in the rules and regulations of methanol as a fuel. They have performed both laboratory testing and some real life pilots.

Up to now these consortia are a good first step towards learning about the technology and its desirability, but most of the work done cannot be categorized as socio-technical experiments. Rather they have been incubating the technology as they mainly focused on technical performance and feasibility (Ceschin, 2014). The Fast Water consortium will start with actual socio-technical experimentation, performing elaborate pilots on multiple vessel types. Their goal is to establish a commercial retrofit for engines between 200 kW – 4 MW, but also demonstrate the complete value chain for bunkering methanol. They want to develop training programs for vessel crew and portside staff and develop rules and regulations for methanol fuel use. They also want to create a business plan for methanol as a fuel (FASTWATER, 2020). Socio-technical experiments like this will help to institutionalize methanol, create acceptance and enhance further development and adoption. The experiments within the consortia are completely shielded from any outside selection pressure as the only goal is to nurture the technology. The consortia publicly share their results and are building towards a collective knowledge base. The local learning of each consortia can be used to extend distant learning that benefits everyone (Rosenkopf & Almeida, 2003). This sharing of knowledge not

only assists learning processes, but it also helps creating and managing expectations of the technology. As more information is published and communicated, more actors may become interested helping the networking process. This in turn can secure key resources and investments in future development of the niche. It can also help to create a positive public opinion contributing to the general acceptance of methanol (Schot & Geels, 2007). The respective trade associations could play a role in facilitating reciprocal learning (Rotmans & Loorbach, 2008).

The experiments gradually shape the niche trajectory as it articulates and stabilizes rules and routines (Raven et al., 2010). This holds true for the processes on the ship and in the ports. It also initiates convergence of the technological trajectory. There is not yet a dominant engine design and different types of engines and retrofits are being tested. Convergence in this trajectory will decrease risk and lower the threshold for investment (Suarez et al., 2015).

Besides the consortia there are also commercial parties developing the methanol niche in the maritime shipping sector. The Stena Germanica was a first-of-its-kind ferry that was converted to methanol in 2015 in cooperation with Methanex Corp, the worlds largest supplier of methanol (Stena Line, 2021). Currently, Methanex Corp. has the largest methanol fleet with 11 methanol powered ocean tankers with 8 more in development (Methanex, n.d.). Competitor Proman, has ordered a third methanol-powered vessels in a joint venture with Stena Bulk (Offshore Energy, n.d.). Even Maersk, an independent transport company, has ordered their first methanol vessel (Lloyd's List, 2021). Despite the fact that these vessels are not inland shipping vessels they do help in nurturing and empowering the methanol niche.

Both inland and maritime shipping share the same infrastructure and a majority of the actors in their respective EMs. Therefore, the development of methanol in marine shipping contributes to methanol as an inland shipping fuel. The methanol suppliers act as product champions of their own product in the transport of their products and others are starting to join. This may lead to a bandwagon effect for both inland and maritime shipping, increasing the number of actors supporting and empowering the niche (Walrave et al., 2018). This niche development and scaling-up further amplifies the institutionalization and optimization of methanol bunkering and onboard methanol handling processes. Next to that, it articulates the expectation that methanol is a feasible shipping fuel.

The maritime shipping sector aims for a fit and conform strategy of empowering methanol. They want to compete on the existing selection pressure starting off with fossil methanol. They focus on the low pollutant emissions of methanol, the ease of handling and its competitive price. They want to gradually increase the share of sustainable methanol in the future. Proman even labelled their newly ordered methanol tankers "Carbon-Neutral-Ready", aiming for carbon neutral operation only by 2040 (Ship & Bunker, 2021). This may work in maritime shipping as the emission regulations are less stringent and no aftertreatment would be needed after retrofitting to methanol. Even in the maritime sector the landscape pressures are great and Maersk is aiming to use sustainable methanol at the start of operation in 2023. This is a strong signal to the industry that they need to switch to renewable fuels. For inland shipping fossil methanol is not likely to be a solution and a stretch and transform strategy is more likely. The selection criteria should change towards renewable fuels as sustainable methanol has an advantage over the other sustainable fuels. For this to happen the subsidies should remain high enough until regulation requires a large share of renewable fuels. Another option would be that final customers demand the use of sustainable fuels to reduce their scope 3 emissions or that the landscape pressure is high enough that the use of fossil fuels becomes unacceptable.

If the incubation and experimentation with methanol generates enough trust and expectations there may be enough socio-technical validity for stakeholders to invest in biomethanol. If this is not the case and methanol does not live up to its expectations the focus should change towards any of the other renewable fuels.

7.3: Innovation Ecosystem Management

If it the uncertainty can be reduced and it is expected that methanol will be a viable fuel there are still the internal challenges to solve. As already discussed earlier the greatest internal challenges are the development of a biomethanol supply and overcoming the lack of incentives for different actors. The focal actor in this EM is most likely the methanol industry, as they have most to gain. Only less than 10% of all methanol is used as fuel (Dalena et al., 2018) and the Dutch inland shipping fuel market is more than 2 times the entire Dutch methanol market (CBS, n.d.-b; Zomer et al., 2020). Thus, inland shipping could greatly expand the methanol market size. As discussed earlier the other actors in the EM do not have very large incentives to invest in methanol and are more neutral towards the specific fuels used. The first barrier that needs to be solved is the establishment of a biomethanol supply. This requires setting up a biomass supply network and investments in new biomass methanol plants.

Setting up a biomass production chain falls within the direct influence of the methanol industry. They need to set-up a biomass supply network or partner with a biomass supplier. Then they need to invest in a biomethanol plant. The biomethanol plants that are completed or under construction are from smaller players in the methanol industry with the exception of BioMCN Europe's largest producers. Nonetheless, the larger producers participate and cofinance biomethanol projects. Proman can even call itself the leading marketer of biomethanol after closing its investment in a large biomethanol plant in Canada (Proman, 2021). They are also one of the main investors in North-C-Methanol, which will be the largest e-methanol plant in the world (F+L Daily, 2020). Thus, the larger companies are starting to focus on sustainable methanol as well.

The second bottleneck is the alignment of the shipyards and engine manufacturers. There are commercial methanol engines for maritime shipping, but not for inland shipping. The same holds true for the experience with retrofits. There is much less experience with retrofitting inland shipping engines than marine engines. The engine manufacturers are certainly capable to produce the engines and if the uncertainty is resolved they are also willing to invest if trust in methanol as an inland shipping fuel is gained. For shipyards the risk is lower as they only need to invest in retrofits and they can set it up relatively quickly. Both the engine manufacturer and the shipyard can wait until the last moment, because they supply the alternatives and there are no serious threats to the ICE in the coming years. The EVP can only be achieved if all actors are able to deliver their share of the value proposition and all bottlenecks are resolved (Adner, 2006). This provides a co-innovation risk as methanol as a fuel is useless without suitable engines. Active management of the ecosystem could reduce the timescale in which this bottleneck is resolved. From the methanol consortia and maritime methanol shipping projects there already is some forms of collaboration and partnerships. It may be helpful if this alliance continued on larger scale inland shipping projects to develop commercial retrofits and new engines. Setting up a common innovation roadmap and committing resources to achieve those goals is a good way to involve partners in a situation with high levels of uncertainty (Williamson & De Meyer, 2012). An example of this is the partnership of energy company Uniper SE, shipping service provider Liberty Pier and the engineering firm Ship Design & Consult GmbH. A medium-term goal of the GMC is to build ships short sea and inland shipping vessels that can use methanol in their engines (Bioenergy International, 2021).

Involvement of the customers may also help to speed up the process. Potential product champions for inland shipping could be liquid bulk vessels that transport methanol on the inland waterways. Not only do they have experience handling methanol, they often have a close, long term partnership with the methanol industry.

Chapter 8: Discussion

This thesis covers a broad range of topics giving rise to multiple limitations in both scope and analyses. These limitations are discussed in this chapter with their implications. The limitations are addressed in the order of the thesis.

8.1: Electrification Frontier

The assessment of which applications cannot be electrified and will still require a high density fuel like diesel of methanol in the foreseeable future is done through analysis of electric pilot cases and energy modelling. This approach gives a clear view of the practical and design implications of switching to an alternative energy source. Nonetheless, it is very limited in scope as there are many aspects that are not taken into consideration. The scope was limited to just the use of the application but this is only a part of the ecosystem as seen in chapter 6 in the case of inland shipping. Especially for electrification there are enormous implications for the infrastructure. It requires the development of a massive charging infrastructure, but it also has implication for the electricity grid as a whole. These developments are briefly discussed, but this is an extensive research topic on its own and of great importance for the feasibility of electrification of these applications.

Next to that, only the technical perspective is taken into account. The environmental and the economic aspects are left out of the discussion. At the environmental side both the GHG emissions and pollutant emissions should be assessed on a life cycle basis, considering the application, the infrastructure and the afterlife. While the operational aspect of batteries electric is unmatched in environmental performance, the production and recycling of batteries is currently contested. The development of a charging infrastructure also brings along a massive demand in rare earth metals, especially if dynamic charging is applied. A thorough analysis of the environmental impact could affect the desirability of electrification. The economic considerations are of major importance, especially since companies are the users in question and their main goal is profit optimization. On the short and medium term this will limit the applications suitable for electrification as the investment cost of electric drivetrains is generally higher. On the long term when the investment costs are expected to decrease the focus may shift towards electrification as the operational costs are lower. If this becomes the case the next point becomes especially relevant.

The current analyses is not only considering the current technology, it also considers the current operating profile of the applications. If the selection criteria change, it may as well change the operating profile to better suit electrification. In combination with developments in autonomation this could lead to smaller and more flexible variants of the applications which are easier to electrify.

Lastly, the analyses makes use of the current state-of-the-art. History shows there is relatively low development in the energy density of batteries. However, there has never been more time and money invested in battery research than is currently being done. If there is a major breakthrough in the energy density the whole basis for the energy storage calculation changes and the results will become more favorable for electrification.

8.2: Engine optimization

The main limitation of the engine optimization approach used is the use of CFD simulations without experimental verification. Each of the elements of the simulations have been verified with experiments individually, but the model as a whole has not been verified in any way. Therefore, it remains the question to what extent the results represent reality. The advantage of simulations is that more information is available to analyze the results. The downside is that all modelling approaches are simplifications and approximations of reality and the results do not always match. One of the trade-offs in simulations is accuracy and computation time. A decision was made to use RANS as the turbulence model, because of its fairly low computational demand compared to the more accurate LES. Where RANS uses time averaged values in determining turbulence, LES solves the larger length scales over time. This results in a qualitative representation of the flow or flame structure. Som et al. (2012) found that LES performs better in capturing the equivalence ratio, temperature and soot

contours. Next to that, it also better predicted the ignition delay which was found to be advanced. If LES would have been used, it could have been combined with a detailed soot model that substantially outperforms the empirical Hiroyaso model (Tang et al., 2018). However, both options drastically increase the computing time of an already computationally expensive simulation. Besides that, the decision to use a rather coarse grid and other simplifications of the modelling approach are likely to have a greater impact on the results.

One of the major simplifications of the simulation approach is simulating just the cylinder processes. This has two implications. Firstly, this implicates that only the gross efficiency can be investigated while the use of PFI methanol may also affect the pumping losses, thus the net efficiency. As the intake temperature is set as one of the parameters the cooling effect of methanol does not have any effect. Secondly, this means that at the start of simulation the in-cylinder mixture is a perfect homogenous distribution. In normal operation methanol is injected into the intake manifold where it mixes with the air and then enters the cylinder through the inlet valves. This causes a flow pattern, or swirl, in the cylinder leading to increased fuel-air mixing, burning rates and heat losses. Gode et al. (2015) found higher efficiencies and lower PM at the cost of higher NOx emissions during their swirl optimization. Sharma et al. (2017) improved the engine efficiency by 7% through intake swirl optimization alone.

Another simplification is the part cycle optimization. This minimizes the computation time and the most important information can be obtained. Still, it disregards the cycle-to-cycle variations and it ignores the gas exchanges over the cycle and therefore the internal EGR as well. Both the internal and external EGR are not taken into account in the analysis, while it is considered one of the important parameters in modern combustion engines. By diluting the mixture with inert species the reactivity of mixture is reduced (Montgomery & Reitz, 2000). This increases the ignition delay and reduces the combustion temperature and the peak pressure (Y. Li et al., 2013). EGR could possibly be used to reduce the MPRR of high MEF operation and decrease ISNOx emissions.

Another element that could change the outcome in experiments is the use of lubrication oil. Methanol in itself does not have good lubricating properties and a methanol compatible lubricant is therefore required. The simulations do not include lubrication oil in the calculation of the PM emissions and Shamun et al. (2017) found that most of the PM emissions when running alcohol fuels come from the lubrication oils and not the fuel.

There are undesirable elements in the used modelling approach and the optimization methodology proved more difficult to apply to dual fuel optimization than for diesel only as discussed in section 5.2. Still, the results provide valuable understanding of the mechanism behind the methanol-diesel dual fuel engine. The exact results may differ slightly in future experiments, but the general trends and relative performance of the diesel benchmark and the dual fuel operation are expected to give valid results.

8.3: Transition Framework

In the transition framework many decisions have been made about the scope and approach of the research. Each of them having different implications.

In the application of the transition framework a sector approach was taken. The information was gathered from public sources, representatives of branch associations and individuals with specific knowledge about specific topics. Individual companies have not been consulted, while they have to it make the decisions. Each individual company has their own strategy, preferences and network. The focus of this transition framework is on methanol compared to the most common alternatives, but as mentioned before there are a plethora options. Each of the options has their own product champions and lobbyists. Every actor in the EM is faced with large uncertainties. Also, the best solution is not always the winning solution in transitions. Public opinion is against ICEs and there is a strong lobby for zero emission technologies. A focus on electrification or hydrogen my be a strategic decision of

the companies from a marketing perspective, while it may not be the best solution from a technical or even economic perspective.

The scope of the research has been fairly limited regarding the feedstock of methanol. The analysis shows that the use of fossil methanol does not provide great opportunities. If it was to be used as a transition to green methanol, through for example blending , it may face resistance. It may be considered part of the carbon lock-in as it promotes the continued use fossil feedstocks. This could overshadow the aim to transition towards renewable methanol. Even if biomethanol is used at the start there could still be resistance. Biomass is expected to play a key role in the energy transition, both for energy and transport, but it is contested as well. First generation biomass competes with food and is already limited in the amount it can contribute to the RED II target (Transport & Environment, 2020). Advanced biomass like wood, which is used in biomass power plants and is the feedstock for methanol, should provide the solution. However, it is also questioned for its sustainability. As discussed in sector 6.3.8 the national supply of biomass is limited and there are many sectors that want to make use of it. A significant share will have to be obtained from international trade which has several problems. The international trade of biomass makes it a commercial product and gives incentive to use land for the production non-food crops in the less wealthy countries (Natuur & Milieu, n.d.). This trend is associated with neo-colonialism as wealthy countries buy up land and resources from less wealthy countries (Okoh, 2015). Woody biomass is also associated with deforestation. Even though certification systems are in place to only use branches and waste wood, there are questions at the effectiveness of these systems to prevent the usage of trees and foster deforestation (Markus, 2019).

Another problem is the international character of the market. The focus of the analysis is mainly based on the Netherlands in a market with a large international focus. The international inland shipping sector is especially difficult to electrify and therefore more likely to adopt methanol as a fuel. Apart from the safety requirements that are set by the CESNI, each individual EU country can set its own policies regarding sustainability and subsidies. It could be that different countries choose different fuels as a solution which would not contribute to a quick adoption of any solution. The amount of subsidy given could be different between countries as well. This could influence the bunkering strategy of ships which is already affected by the limited range compared to diesel. By far the greatest challenge is the uncertainty in which fuels to invest and the fact that this may differ between countries only contributes to this uncertainty.

The assessment of the opportunities and barriers was made for specifically the inland shipping sector. During the analyses it already became clear that there is a significant extend of co-evolution between inland shipping and maritime shipping. For road transport and agricultural machinery the challenges are likely fairly similar. The roadmaps also suggest electrification and biofuels as the solution for the next decade. Which biofuels will be used remains the question in those sectors as well. The challenges may even be smaller in magnitude. In fact there have been countries that have used high blend methanol as an automotive fuel and there are commercial automotive methanol powertrains available.

Chapter 9: Conclusions & Recommendation

The objective of this thesis was to determine the role of methanol as an ICE fuel for heavy duty transport in the energy transition. It did so by analyzing three distinct aspects. Firstly, it was determined for which heavy duty applications methanol provides a solution. Secondly, the performance of a methanol-diesel dual fuel engine is determined and compared to its diesel benchmark. Thirdly, the barriers and opportunities of methanol as fuel are investigated for the inland shipping sector.

9.1: Electrification Frontier

To determine for which heavy duty application methanol provides a solution it was investigated which application cannot be electrified. Electrification is potentially the most efficient way to reduce carbon and pollutant emissions because of the high efficiency and the absence of tail pipe emissions. However, batteries have low energy densities and this is a problem for many heavy duty applications. This electrification limit was investigated by comparing the performance of electric pilot cases to the most common alternatives and by performing energy calculations to compare the size and weight of the energy storage.

From the analysis it can be concluded that a large share of the road transport can be electrified, but that long haul HD trucks will require a high energy density fuel like methanol for the foreseeable future. For the agricultural machinery it is only possible to electrify small tractors and machines with a nominal power up to 50 kW with some limitations in its operating capabilities. Therefore, methanol provides a potential solution the majority of the agricultural machinery. For inland shipping the conclusion is similar. For the foreseeable future electrification in inland shipping is limited to short distance point-to-point shipping. For these applications the weight and size increase of the energy storage is too large for batteries to be a practical solution. There are ways to reduce the required battery size, but this requires enormous investments in infrastructure and this is not expected to be ready in the coming decade. Even with a perfect infrastructure it would still require changes in the operating profile of the applications.

9.2: Engine Performance

CONVERGE CFD simulations of a digital PACCAR MX-13 twin were used to investigate the engine performance. Closed cylinder simulations were performed from IVC to EVO. The performance was optimized through three rounds of DoE with a multi-objective GA optimization after each round. The methanol-diesel dual fuel engine was optimized using four parameters: inlet pressure, SOI, MEF and inlet temperature. A comparison was made with the diesel benchmark that was optimized using the inlet pressure and SOI.

The comparison shows a change in trade-off. During the optimization of the diesel benchmark there was a clear trade-off between GIE and NOx. For the methanol-diesel optimization the limiting factor is mainly is the MPRR. If the MPRR limit can be ignored the GIE increased by 11%, reduced the ISNOx by 28% and almost eliminated ISPM emissions, while all other emissions except of the ISFORM remained within the Stage V limit. If a strict MPRR limit is set the MEF is reduced to just 30%. In that case, the GIE only increased by 1.2% and the ISPM decreased by 43%, while the ISNOx emissions even increased by 19%. Also, the ISUHC, ISCO and ISFORM all breached their emission limits.

It can be concluded that the GIE would increase in the case of a methanol PFI retrofit, but aftertreatment would still be needed. The ISNOx emissions breached the Stage V norm in all cases and in many cases the ISCO, ISUHC and ISFORM emissions breached the norms as well. Both a SCR system and a diesel oxidation catalyst would be required. Other more extensive retrofits like dual direct injection or other more complex retrofits like RCCI may provide an alternative to aftertreatment.

9.3: Methanol Barriers & Opportunities

To determine the barriers and opportunities of methanol as an ICE fuel a value blueprint is made and for each activity the barriers and opportunities are assessed compared to diesel, LNG and hydrogen.

The majority of the EVP does not face any significant barriers. Transport, storage and bunkering can be done with only minor modifications to the current infrastructure. For these actors it is an opportunity because the introduction of methanol would increase their volumes.

For fossil methanol there are few barriers, but the main risk is the lack of opportunities. Fossil methanol is more expensive, has higher investment costs, a lower operating range and a higher carbon footprint than conventional diesel. The opportunities are only apparent for biomethanol. Biomethanol is the cheapest among the assessed renewable fuels and also has the lowest carbon footprint. E-methanol is not a short term option, because it requires very cheap renewable electricity which is not expected to be available in the Netherlands.

Biomethanol appears to be the a good solution, but there currently is only a very small supply, because the production costs are significantly higher than fossil methanol. Biomethanol is only price competitive with the fossil diesel regime with the double counting HBE-subsidy. In order for biomethanol to be a solution, a biomethanol supply chain needs to be established quickly. However, the industry is hesitant because there currently is limited demand for biomethanol due to the higher price. For the engine manufacturers and shipyards there are no barriers in the capabilities, but they are unwilling to invest due to the uncertainty in demand as well. This catch-22 situation is created by the large number of fuel niches that could potentially challenge the regime. As long as there is not a clear winner actor are hesitant to invest.

A way to overcome the uncertainty is to protect and nurture sustainable methanol. Experiments in protected spaces like the consortia are helping to initiate convergence of the technological trajectory of the engine. Experimenting also assists in learning processes and networking processes and it helps creating and managing expectations. If the experiments are deemed successful, methanol will gain trust and socio-technical validity. Besides the consortia, commercial parties should start investing and experimenting as well. Innovation ecosystem theory shows that the EVP can only be delivered if all barriers are resolved. The methanol industry has most to gain and should take initiative to partner with engine manufacturers, shipyards and the companies transporting their product to further increase momentum and reduce uncertainty.

9.4: General Conclusion

This thesis has shown that there is demand for a fuel like sustainable methanol in heavy duty applications, especially in the agricultural machinery and the inland shipping sector. However, the technical and socio-economic analysis shows that it is not a quick solution. Methanol does not provide a quick retrofit alternative for aftertreatment systems and only biomethanol has a clear advantage over the renewable alternatives. The biomethanol supply chain still largely needs to be developed and it cannot compete with fossil diesel without subsidies. Therefore, the role of methanol as fuel in the energy transition starts at the medium term. Nonetheless, sustainable methanol has longer term potential as well using increasingly advanced aftertreatment systems or in fuel cell technology. In order to realize the potential of methanol, investments are required from within the ecosystem by the engine manufacturers and the methanol suppliers. Next to that, the subsidy needs be maintained until the landscape pressure has changed the selection criteria in favor of renewable fuels.

Bibliography

Abma, D., Verbeek, R., Kelderman, B., Hoogvelt, B., & Quispel, M. (2018). Standardized model and cost/benefit assessment for right-size engines and hybrid configurations, (633929).

Acock, A. C. (2011). *A Gentle Introduction to Stata*. *STATA Press*. https://doi.org/10.1016/S0004-3702(98)00053-8

AD. (n.d.). Staat verliest Urgenda-zaak bij Hoge Raad en moet extra CO2-maatregelen nemen | Binnenland | AD.nl. Retrieved May 18, 2021, from https://www.ad.nl/binnenland/staat-verliest-urgenda-zaak-bij-hoge-raad-en-moet-extra-co2-maatregelen-nemen-br~a03abe89/

Adner, R. (2006). Match your innovation strategy to your innovation ecosystem. *Harvard Business Review*, *84*(4).

Adner, R. (2012). *The wide lens : a new strategy for innovation*. *TA - TT -*. New York SE - 278 pages : illustrations ; 24 cm: Portfolio/Penguin. Retrieved from http://catdir.loc.gov/catdir/enhancements/fy1211/2011041760-b.html

Adner, R. (2017). Ecosystem as Structure: An Actionable Construct for Strategy. *Journal of Management*, *43*(1), 39–58. https://doi.org/10.1177/0149206316678451

Adner, R., Oxley, J. E., & Silverman, B. S. (Eds.). (2013). Collaboration and Competition in Business Ecosystems. In *Collaboration and Competition in Business Ecosystems* (Vol. 30, p. iii). Emerald Group Publishing Limited. https://doi.org/10.1108/S0742-3322(2013)0000030018

Alvarado, M. (2017). Insights into the Methanol Industry, *1*(281). Retrieved from www.ihs.com

Álvarez, E., Bravo, M., Jiménez, B., Mourão, A., & Schultes, R. (2018). The Oil and Gas value chain: a focus on oil refining, (November).

American Methanol Institute. (n.d.). Methanol Fact Sheets.

American Methanol Institute, & Malcolm Pirnie Inc. (1999). Evaluation of the fate and transport of methanol in the environment, (January), 1–49.

Amor, R. Ben, & Ghorbel, A. (2018). The risk in Petroleum Supply Chain: A review and typology. *International Journal of Scientific & Engineering Research*, *9*(2). Retrieved from http://www.ijser.org

Ampere Electric-Powered Ferry - Ship Technology. (n.d.). Retrieved March 31, 2020, from https://www.ship-technology.com/projects/norled-zerocat-electric-powered-ferry/

Andersson, K., & Salazar, C. M. (2015). Methanol as a marine fuel report. *FCBI Energy*.

Andersson, Ö. (2012). *Experiment!*

API. (2019). Energy Undestanding our Oil Supply Chain. *Journal of Chemical Information and Modeling*.

Atkinson, C., & Mott, G. (2005). Dynamic Model-Based Calibration Optimization: An Introduction and Application to Diesel Engines, *2005*(724). https://doi.org/10.4271/2005-01-0026

Autio, E., & Thomas, L. D. W. (2014). Innovation ecosystems: Implications for innovation management. *Oxford Handbook of Innovation Management*, (August 2016), 204–228. https://doi.org/10.1093/oxfordhb/9780199694945.013.012

Badra, J., Khaled, F., Tang, M., Pei, Y., Kodavasal, J., Pal, P., … Farooq, A. (2020). Combustion

System Optimization of a Light-Duty GCI Engine Using CFD and Machine Learning. *ASME 2019 Internal Combustion Engine Division Fall Technical Conference, ICEF 2019*, (Ic), 1–22. https://doi.org/10.1115/ICEF2019-7238

Bechtold, R. L., Goodman, M. B., & Timbario, T. A. (2007). *Use of Methanol as a Transportation Fuel*. *Alliance Technical Services Inc.* Retrieved from http://www.ourenergypolicy.org/wp-content/uploads/2012/04/Methanol-Use-in-Transportation.pdf

Beck, M. W., Winkler, D. A., Goyal, H., Sibanda, W., Huang, B., & Zhang, Z. (2018). Opening the black box of neural networks: methods for interpreting neural network models in clinical applications. *Annals of Translational Medicine*, *6*(11), 216–216. https://doi.org/10.21037/atm.2018.05.32

Big Rigs Begin to Trade Diesel for Electric Motors - The New York Times. (n.d.). Retrieved March 29, 2020, from https://www.nytimes.com/2020/03/19/business/electric-semi-trucks-big-rigs.html

Binder, M., Kraussler, M., Kuba, M., & Luisser, M. (2018). *Hydrogen from biomass*. https://doi.org/10.1016/b978-008043947-1/50003-x

Bioenergy International. (2021). Green Methanol Cooperation to develop green methanol for shipping | Bioenergy International. Retrieved May 18, 2021, from https://bioenergyinternational.com/storage-logistics/green-methanol-cooperation-to-develop-green-methanol-for-shipping

BloombergNEF. (2020). No Title. Retrieved March 1, 2021, from https://about.bnef.com/blog/battery-pack-prices-cited-below-100-kwh-for-the-first-time-in-2020-while-market-average-sits-at-137-kwh/

Borisut, P., & Nuchitprasittichai, A. (2019). Methanol Production via CO2 Hydrogenation: Sensitivity Analysis and Simulation—Based Optimization . *Frontiers in Energy Research* . Retrieved from https://www.frontiersin.org/article/10.3389/fenrg.2019.00081

Box, P. O., Delft, A. D., & Wulffers, C. (2011). Environmental and Economic aspects of using LNG as a fuel for shipping in The Netherlands, 1–48.

BP. (2020). Energy Outlook 2020. *BP Energy Outlook 2030, Statistical Review. London: British Petroleum.*, 81. Retrieved from https://www.bp.com/content/dam/bp/business-sites/en/global/corporate/pdfs/energy-economics/energy-outlook/bp-energy-outlook-2020.pdf

Brinkman, N., Wang, M., Weber, T., & Darlingtong, T. (2005). Well-to-Wheels Analysis of Advanced Fuel/Vehicle Systems - A North American Study of Energy Use, Greenhouse Gas Emissions, and Criteria Pollutant Emissions: Appendix B, (May). Retrieved from https://www.energy.gov/sites/prod/files/2014/04/f14/well_to_wheels_analysis_0.pdf%0Ahttp://www.transportation.anl.gov/pdfs/TA/167.pdf

Bromberg, L., & Cheng, W. K. (2010). *Methanol as an alternative transportation fuel in the US: Options for sustainable and/or energy-secure transportation. Sloan Automotive Laboratory Massachusetts Institute of Technology*.

Brynolf, S., Taljegard, M., Grahn, M., & Hansson, J. (2018). Electrofuels for the transport sector: A review of production costs. *Renewable and Sustainable Energy Reviews*, *81*(July 2016), 1887–1905. https://doi.org/10.1016/j.rser.2017.05.288

Cao, W., Zhang, J., & Li, H. (2020). Batteries with high theoretical energy densities. *Energy Storage Materials*, *26*(December 2019), 46–55. https://doi.org/10.1016/j.ensm.2019.12.024

CBS. (n.d.-a). CO2 equivalents. Retrieved February 17, 2021, from https://www.cbs.nl/en-gb/news/2019/37/greenhouse-gas-emissions-down/co2-equivalents

CBS. (n.d.-b). Hoeveel binnenvaartschepen zijn er in Nederland? Retrieved May 3, 2021, from https://www.cbs.nl/nl-nl/visualisaties/verkeer-en-vervoer/vervoermiddelen-en-infrastructuur/binnenvaartschepen

CBS. (n.d.-c). StatLine - Motorbrandstoffen; afzet in petajoule, gewicht en volume. Retrieved March 26, 2021, from https://opendata.cbs.nl/#/CBS/nl/dataset/83406NED/table?dl=28D1F

CBS. (2020). Less coal and more natural gas consumption in 2019. Retrieved March 26, 2021, from https://www.cbs.nl/en-gb/news/2020/20/less-coal-and-more-natural-gas-consumption-in-2019

CBS. (2021). Green electricity production up by 40 percent. Retrieved April 29, 2021, from https://www.cbs.nl/en-gb/news/2021/08/green-electricity-production-up-by-40-percent

CE Delft. (2011). Instruments to reduce pollutant emissions of the existing inland vessel fleet, (November).

CE Delft. (2020). Effects of an EU 55 % GHG reduction target Effects of an EU 55 % GHG reduction target.

Ceschin, F. (2014). How the design of socio-technical experiments can enable radical changes for sustainability. *International Journal of Design*, *8*(3), 1–21.

CESNI. (n.d.). About CESNI - Comité Européen pour l'Élaboration de Standards dans le domaine de la Navigation Intérieure. Retrieved January 5, 2021, from https://www.cesni.eu/en/about-cesni/

CESNI. (2020). Vergadering van CESNI op 30 april 2020. Retrieved January 10, 2021, from https://www.cesni.eu/nl/actualites/vergadering-van-cesni-op-30-april-2020/

Chakarov, D. (2011). Methanol replacing hydrogen gas as the fuel of the future. Retrieved from https://www.nordicenergy.org/article/methanol-replacing-hydrogen-gas-as-the-fuel-of-the-future/

Chang, Y., Jia, M., Li, Y., & Xie, M. (2015). Application of the Optimized Decoupling Methodology for the Construction of a Skeletal Primary Reference Fuel Mechanism Focusing on Engine-Relevant Conditions. *Frontiers in Mechanical Engineering*, *1*(September), 1–14. https://doi.org/10.3389/fmech.2015.00011

Cheng, Y., Zhang, J., Lu, S., & Jiang, S. P. (2020). Significantly enhanced performance of direct methanol fuel cells at elevated temperatures. *Journal of Power Sources*, *450*(September 2019), 227620. https://doi.org/10.1016/j.jpowsour.2019.227620

Clausen, L. R., Houbak, N., & Elmegaard, B. (2010). Technoeconomic analysis of a methanol plant based on gasification of biomass and electrolysis of water. *Energy*, *35*(5), 2338–2347. https://doi.org/10.1016/j.energy.2010.02.034

Cluzel, C. (2020). Fuels Roadmap for 2020 and beyond - implications for future strategy.

Coenen, L., Moodysson, J., & Martin, H. (2015). *Path Renewal in Old Industrial Regions: Possibilities and Limitations for Regional Innovation Policy*. *Regional Studies* (Vol. 49). Taylor & Francis. https://doi.org/10.1080/00343404.2014.979321

Colban, W. F., Miles, P. C., & Oh, S. (2007). Effect of intake pressure on performance and emissions in an automotive diesel engine operating in low temperature combustion regimes. *SAE Technical Papers*. https://doi.org/10.4271/2007-01-4063

CORDIS. (2019). Final Report Summary - FABRIC (FeAsiBility analysis and development of on-Road chargIng solutions for future electric vehiCles). Retrieved February 28, 2021, from https://cordis.europa.eu/project/id/605405/reporting

Costa, M., Bianchi, G. M., Forte, C., & Cazzoli, G. (2014). A numerical methodology for the multi-objective optimization of the DI diesel engine combustion. *Energy Procedia*, *45*, 711–720. https://doi.org/10.1016/j.egypro.2014.01.076

Curran, S. J., Wagner, R. M., Graves, R. L., Keller, M., & Green, J. B. (2014). Well-to-wheel analysis of direct and indirect use of natural gas in passenger vehicles. *Energy*, *75*, 194–203. https://doi.org/10.1016/j.energy.2014.07.035

Daag, P. van der. (2013). Improving eco-performance and quality of fossil LNG (in shipping) - Options for Amsterdam. *Holland Innovation Team*. Retrieved from https://www.hollandinnovationteam.nl/images/Small-mid scale LNG Victoria Plaza.pdf

Dalena, F., Senatore, A., Marino, A., Gordano, A., Basile, M., & Basile, A. (2018). *Methanol Production and Applications: An Overview*. *Methanol: Science and Engineering*. Elsevier B.V. https://doi.org/10.1016/B978-0-444-63903-5.00001-7

Dan Meszler, Delgado, O., Rodríguez, F., & Muncrief, R. (2018). European heavy-duty vehicles: Cost-effectiveness of fuel-efficiency technologies for long-haul tractor-trailers in the 2025-2030 timeframe. *The ICCT White Paper*, (January).

De Laat, P. (2020). Overview of Hydrogen Projects in the Netherlands - TKI Nieuw Gas, 89. Retrieved from https://www.topsectorenergie.nl/sites/default/files/uploads/TKI Gas/publicaties/Overview Hydrogen projects in the Netherlands versie 1mei2020.pdf

Deen, G., Nooijen, P., & Been, J. (2020). *Breakthrough LNG deployment in Inland Waterway Transport Activity 2 . 3 Evaluation report pilot test MTS Argonon*.

Di Blasio, G., Viscardi, M., & Beatrice, C. (2015). DoE Method for Operating Parameter Optimization of a Dual-Fuel BioEthanol/Diesel Light Duty Engine. *Journal of Fuels*, *2015*, 1–14. https://doi.org/10.1155/2015/674705

Dierickx, J., Beyen, J., Block, R., Hamrouni, M., Huyskens, P., Meichelböck, C., & Verhelst, S. (2018). Strategies for introducing methanol as an alternative fuel for shipping. *Transport Research Arena*, 1–10.

Dierickx, J., Sileghem, L., & Verhelst, S. (2019). Efficiency and Emissions of a High Speed Marine Diesel Engine converted to Dual-Fuel Operation with Methanol. In *Cimac* (pp. 1–14).

DieselNet. (n.d.). Emission Standards EU: Nonroad Engines. Retrieved from https://dieselnet.com/standards/eu/nonroad.php

DNV GL. (2019). Comparison of Alternative Marine Fuels. Retrieved from https://sea-lng.org/wp-content/uploads/2019/09/19-09-16_Alternative-Marine-Fuels-Study_final_report.pdf

Dominković, D. F., Bačeković, I., Pedersen, A. S., & Krajačić, G. (2018). The future of transportation in sustainable energy systems: Opportunities and barriers in a clean energy transition. *Renewable and Sustainable Energy Reviews*, *82*(July 2017), 1823–1838. https://doi.org/10.1016/j.rser.2017.06.117

Doyle, A. (2020). CRI successfully demonstrates chemical storage with renewable methanol - News - The Chemical Engineer. Retrieved January 4, 2021, from https://www.thechemicalengineer.com/news/cri-successfully-demonstrates-chemical-storage-

with-renewable-methanol/

DST. (2019). Fact sheet nº 3 After-treatment.

Du, J., Noguchi, R., & Ahamed, T. (2018). Feasibility Study of Motor Powered Agricultural Tractors Based on Physical and Mechanical Properties of Energy Sources. *Agricultural Information Research*, *27*(2), 14–27. https://doi.org/10.3173/air.27.14

Dutch Government. (2018). Brandstofstickers. Retrieved April 26, 2020, from https://www.rijksoverheid.nl/onderwerpen/auto/brandstofstickers

Dutch Government. (2019). *Climate Agreement*. https://doi.org/10.1016/J.ENG.2016.04.009

Duurzaam Bedrijfsleven. (2017). BioMCN Delfzijl steekt € 1,2 mln in biomethanol uit CO2. Retrieved January 4, 2021, from https://www.duurzaambedrijfsleven.nl/industrie/22321/biomcn-delfzijl-steekt-12-mln-in-biomethanol-uit-co2

Duurzaam Bedrijfsleven. (2018). DNV GL: 'Elektrische scheepvaart ligt ver in de toekomst.' Retrieved April 28, 2020, from https://www.duurzaambedrijfsleven.nl/logistiek/27751/dnv-gl-elektrische-scheepvaart-ligt-nog-ver-in-de-toekomst

e-Mobility | Freightliner Trucks. (n.d.). Retrieved March 29, 2020, from https://freightliner.com/e-mobility/

E4tech. (2018). Master plan for CO2-reduction in the Dutch shipping sector – Biofuels for Shipping, (May). Retrieved from www.platformduurzamebiobrandstoffen.nl

E4tech. (2019). H2 Emission Potential Literature Review, (22), 40pp.

Earl, T., Mathieu, L., Cornelis, S., Kenny, S., Ambel, C. C., & Nix, J. (2018). Analysis of long haul battery electric trucks in EU. *8th Commercial Vehicle Workshop*, (May), 17–18.

EFIP. (2019). Green Inland Shipping event 16 October 2019 showed the most innovative solutions in inland navigation at the CO2 neutral Port of Brussels. Retrieved April 28, 2020, from https://www.inlandports.eu/news/press-releases/green-inland-shipping-event-16-october-2019-showed

Eisenbach, S., Ettenhuber, C., Schiereck, D., & Flotow, P. von. (2011). Beginning Consolidation in the Renewable Energy Industry and Bidders' M & A-Success. *Technology and Investment*, *02*(02), 81–91. https://doi.org/10.4236/ti.2011.22009

Elektrische & hybride trucks - DAF Trucks N.V. (n.d.). Retrieved March 28, 2020, from https://www.daf.com/nl-nl/over-daf/innovatie/elektrische-en-hybride-trucks

Elgas. (2019). LNG - What is LNG? Liquefied Natural Gas (Methane) Uses & Properties. Retrieved April 28, 2020, from https://www.elgas.com.au/blog/493-what-is-lng-liquefied-natural-gas-methane

Elgowainy, A., Wang, M., Joseck, F., & Ward, J. (2017). *Life-Cycle Analysis of Fuels and Vehicle Technologies*. *Encyclopedia of Sustainable Technologies* (Vol. 1). Elsevier. https://doi.org/10.1016/B978-0-12-409548-9.10078-8

Ellis, J. (2017). Methanol as an alternative fuel? In *Washington Methanol Policy Forum*.

Ellis, J., & Tanneberger, K. (2015). Study on the use of ethyl and methyl alcohol as alternative fuels in shipping, *46*(0), 8–31.

ERTRAC, EPoSS, & ETIP SNET. (2017). European Roadmap Electrification of Road Transport Status: final for publication, (June), 48. Retrieved from https://www.ertrac.org/uploads/images/ERTRAC_ElectrificationRoadmap2017.pdf

Etherington, D. (2021). Elon Musk says Tesla Semi is ready for production, but limited by battery cell output. Retrieved January 29, 2021, from https://techcrunch.com/2021/01/27/elon-musk-says-tesla-semi-is-ready-for-production-but-limited-by-battery-cell-output/?guccounter=1&guce_referrer=aHR0cHM6Ly93d3cuZ29vZ2xlLmNvbS8&guce_referrer_sig=AQAAAKVAFbE78aYZU3CGKP3uYYDGzGzhUeWDmwEf03ZYf9tMXbyQtOyweq

ETIP Bioenergy. (n.d.). Conversion of MSW and cellulosic materials to methanol/ethanol via gasification and synthesis. Retrieved January 3, 2021, from https://www.etipbioenergy.eu/value-chains/conversion-technologies/advanced-technologies/sugar-to-alcohols/conversion-of-msw-and-cellulosic-materials-to-methanol-ethanol-via-gasification-and-synthesis

European Biofuels Technology Platform. (2016). Biofuel Fact Sheet. *Biofuel Fact Sheet*.

European Commission. (2017). Electrification of the Transport System: Studies and Reports, 1–49. Retrieved from ec.europa.eu/newsroom/horizon2020/document.cfm?doc_id=46372

European Environmental Agency. (2019). Emissions of air pollutants from transport. Retrieved from https://www.eea.europa.eu/data-and-maps/indicators/transport-emissions-of-air-pollutants-8/transport-emissions-of-air-pollutants-8

European Technology and Innovation Platform. (2018). *STRATEGIC RESEARCH AND INNOVATION AGENDA 2018*. *The New Urban Area Development*. https://doi.org/10.1007/978-3-662-44958-5_8

Extractives Hub. (n.d.). Petroleum Industry Overview, 1–29.

F+L Daily. (2020). Proman to build world's largest green methanol plant in North Sea - F&L Asia. Retrieved May 18, 2021, from https://www.fuelsandlubes.com/flo-article/proman-to-build-worlds-largest-green-methanol-plant-in-north-sea/?web=1&wdLOR=cB9823CD3-69E5-43DF-8569-27AD800ECAD3

Fang, K., Li, Z., Shenton, A., Fuente, D., & Gao, B. (2015). Black Box Dynamic Modeling of a Gasoline Engine for Constrained Model-Based Fuel Economy Optimization. *SAE Technical Paper 2015-01-1618*, 3–10. https://doi.org/10.4271/2015-01-1618

Farmers Weekly. (2018). Buying a tractor? How to make sense of engine statistics - Farmers Weekly. Retrieved February 1, 2021, from https://www.fwi.co.uk/machinery/tractors/buying-a-tractor-how-to-make-sense-of-engine-statistics

FASTWATER. (2020). FASTWATER consortium fast tracks commercial pathway to climate neutral methanol as marine fuel, (860251).

Friedrich, R. J. (1982). In Defense of Multiplicative Terms in Multiple Regression Equations. *American Journal OfPolitical Science*, *26*(4), 797–833.

Frontier Economics. (2018). *INTERNATIONAL ASPECTS OF A POWER-TO-X ROADMAP - A report prepared for the World Energy Council Germany*. Retrieved from www.weltenergierat.de

Fuel Cells and Hydrogen Joint Undertaking (FCH). (2019). *Hydrogen Roadmap Europe - a Sustainable Pathway for the European Energy Transition*. https://doi.org/10.2843/249013

Futurism. (2017, December 5). China Has Launched the World's First All-Electric Cargo Ship. Retrieved April 28, 2020, from https://futurism.com/china-launched-worlds-first-all-electric-

cargo-ship

Gebart, R. (n.d.). Advanced biofuels and chemicals from black liquor (and renewable electricity).

Geels, F. W. (2002). Technological transitions as evolutionary reconfiguration processes: A multi-level perspective and a case-study. *Research Policy*, *31*(8–9), 1257–1274. https://doi.org/10.1016/S0048-7333(02)00062-8

Geels, F. W. (2004). From sectoral systems of innovation to socio-technical systems: Insights about dynamics and change from sociology and institutional theory. *Research Policy*, *33*(6–7), 897–920. https://doi.org/10.1016/j.respol.2004.01.015

Geertsma, C. (E) dr. ir., & Krijgsman, ir. M. (2019). Alternative fuels and power systems to reduce environmental impact of support vessels. *Proceedings of Marine Electrical and Control Systems Safety Conference (MECSS)*, *1*. https://doi.org/10.24868/issn.2515-8198.2019.003

Giers, M., Jaworska, L., & Ludmiła, L. (2020). *GLOBAL HYDROGEN MARKET*. https://doi.org/10.1016/b978-0-12-819460-7.00004-9

Gigler, J., & Weeda, M. (2018). *Outlines of a Hydrogen Roadmap*. *TKI Nieuw Gas*. Retrieved from https://www.topsectorenergie.nl/sites/default/files/uploads/TKI Gas/publicaties/20180514 Roadmap Hydrogen TKI Nieuw Gas May 2018.pdf

Giglio, E., Vitale, G., Lanzini, A., & Santarelli, M. (2021). Integration between biomass gasification and high-temperature electrolysis for synthetic methane production. *Biomass and Bioenergy*, *148*, 106017. https://doi.org/10.1016/j.biombioe.2021.106017

GMM consortium partners. (2021). Green Maritime Methanol : WP 5 - System Design for Short Sea Shipping Table of Contents.

Gode, R., Goswami, A., Barman, J., & Lakhlani, H. (2015). Impact of swirl on NOx and soot emission by optimizing helical inlet port of 4 valve direct injection diesel engine. *SAE Technical Papers*, (September). https://doi.org/10.4271/2015-26-0091

Government of the Netherlands. (n.d.). Inland Shipping | Freight transport. Retrieved January 5, 2021, from https://www.government.nl/topics/freight-transportation/inland-shipping

Grahn, M. (2020). E-fuels : the big picture , focusing on the role of electro-methanol.

Grand View Research. (2019). Methanol Market Size, Share, Analysis | Industry Research Report, 2025. Retrieved January 4, 2021, from https://www.grandviewresearch.com/industry-analysis/methanol-market

Green Deal. (2019). Green Deal on Maritime and Inland Shipping and Ports, 1–21. Retrieved from www.greendeals.nl/green-deals/green-deal-zeevaart-binnenvaart-en-havens

GreenBiz. (2020). 8 electric truck and van companies to watch in 2020. Retrieved March 29, 2020, from https://www.greenbiz.com/article/8-electric-truck-and-van-companies-watch-2020

Greenport. (2020a). LNG now available at 93 ports. Retrieved December 21, 2020, from https://www.greenport.com/news101/lng/lng-now-available-in-93-ports

Greenport. (2020b). Research says ports embracing methanol. Retrieved December 14, 2020, from https://www.greenport.com/news101/energy-and-technology/research-indicates-ports-embracing-methanol

GSI. (n.d.). The World's First Thousand DWT Pure Electric Boat Launched. Retrieved April 28, 2020,

from http://gsi.cssc.net.cn/en/component_news/news_detail.php?id=41

Han, J., Somers, L. M. T., Cracknell, R., Joedicke, A., Wardle, R., & Mohan, V. R. R. (2020). Experimental investigation of ethanol/diesel dual-fuel combustion in a heavy-duty diesel engine. *Fuel*, *275*(2020), 117867. https://doi.org/10.1016/j.fuel.2020.117867

Hansson, J., Brynolf, S., Fridell, E., & Lehtveer, M. (2020). The potential role of ammonia as marine fuel-based on energy systems modeling and multi-criteria decision analysis. *Sustainability (Switzerland)*, *12*(8), 10–14. https://doi.org/10.3390/SU12083265

Hansson, J., Månsson, S., Brynolf, S., & Grahn, M. (2019). Alternative marine fuels: Prospects based on multi-criteria decision analysis involving Swedish stakeholders. *Biomass and Bioenergy*, *126*(October 2018), 159–173. https://doi.org/10.1016/j.biombioe.2019.05.008

Harmsen, J., Nesterova, N., Bekdemir, C., & Van Kranenburg, K. (2020). Green Maritime Methanol WP2 Initiation and Benchmark analysis. Retrieved from www.tno.nl

Harney, B. M. (1975). Methanol from Coal-A Step Toward Energy Self-Sufficiency. *Energy Sources*, *2*(3), 233–249. https://doi.org/10.1080/00908317508945951

Hjelkrem, O. A., Arnesen, P., Aarseth Bø, T., & Sondell, R. S. (2020). Estimation of tank-to-wheel efficiency functions based on type approval data. *Applied Energy*, *276*(June), 115463. https://doi.org/10.1016/j.apenergy.2020.115463

Hoekman, S. K., & Robbins, C. (2012). Review of the effects of biodiesel on NOx emissions. *Fuel Processing Technology*, *96*, 237–249. https://doi.org/10.1016/j.fuproc.2011.12.036

Horvath, S., Fasihi, M., & Breyer, C. (2018). Techno-economic analysis of a decarbonized shipping sector: Technology suggestions for a fleet in 2030 and 2040. *Energy Conversion and Management*, *164*(February), 230–241. https://doi.org/10.1016/j.enconman.2018.02.098

House, K. Z., Baclig, A. C., Ranjan, M., Van Nierop, E. A., Wilcox, J., & Herzog, H. J. (2011). Economic and energetic analysis of capturing CO2from ambient air. *Proceedings of the National Academy of Sciences of the United States of America*, *108*(51), 20428–20433. https://doi.org/10.1073/pnas.1012253108

Hunter, C., & Penev, M. (2019). Market Segmentation Analysis of Medium and Heavy Duty Trucks with a Fuel Cell Emphasis Fuel Cell M / HD Vehicle Market Segmentation, 1–6. Retrieved from https://www.hydrogen.energy.gov/pdfs/review19/sa169_hunter_2019_o.pdf

IBISWorld. (n.d.). The 10 Global Biggest Industries by Revenue - 2020 | IBISWorld. Retrieved December 29, 2020, from https://www.ibisworld.com/global/industry-trends/biggest-industries-by-revenue/

Ibrahim, F., Wan Mahmood, W. M. F., Abdullah, S., & Mansor, M. R. A. (2017). Comparison of Simple and Detailed Soot Models in the Study of Soot Formation in a Compression Ignition Diesel Engine. *SAE Technical Papers*, *2017-March*(March). https://doi.org/10.4271/2017-01-1006

ICIS. (2020). IMO issues guidelines for low carbon marine fuels, benefiting methanol. Retrieved February 7, 2021, from https://www.icis.com/explore/resources/news/2020/11/09/10572618/imo-issues-guidelines-for-low-carbon-marine-fuels-benefiting-methanol

Inland Navigation Europe. (2018). Freight by water goes electric. Retrieved April 28, 2020, from http://www.inlandnavigation.eu/news/innovation/freight-by-water-goes-electric/

International Energy Agency. (2015). *Technology Roadmap*. *SpringerReference*.

https://doi.org/10.1007/springerreference_7300

International transport forum. (2011). PERMISSIBLE MAXIMUM WEIGHTS OF TRUCKS IN EUROPE (in tonnes), *44*(August), 12–13.

IRENA, & Methanol Institute. (2021). *Innovation Outlook: Renewable Methanol*. *International Renewable Energy Agency, Abu Dhabi*. Retrieved from https://www.methanol.org/wp-content/uploads/2020/04/IRENA_Innovation_Renewable_Methanol_2021.pdf

Jadun, P., McMillan, C., Stenberg, D., Muratori, M., Vimmerstedt, L., & Mai, T. (2017). Electrification Futures Study : End-Use Electric Technology Cost and. *National Renewable Energy Lab*, 109. Retrieved from www.nrel.gov/publications.%0Ahttps://www.nrel.gov/docs/fy18osti/70485.pdf

Kemp, R., Schot, J., & Hoogma, R. (1998). Regime shifts to sustainability through processes of niche formation: The approach of strategic niche management. *Technology Analysis and Strategic Management*, *10*(2), 175–198. https://doi.org/10.1080/09537329808524310

Kemper, A. (2010). Business in the Canadian Context ADMS 1010 - Week 9 Oil in Canada. Retrieved from https://www.slideserve.com/bessie/week-9-oil-in-canada

Khajepour, A., Fallah, S., & Goodarzi, A. (2014). Introduction to Vehicle Propulsion and Powertrain Technologies, (May), 1–46.

Khandelwal, M., van Dril, T. (2020). Decarbonisation options for the Dutch biofuels industry | PBL Planbureau voor de Leefomgeving. *The Hague, 2020, PBL Publication Number: 3887*, (April), 67.

King, S. L. (1999). NEURAL NETWORKS VS. MULTIPLE LINEAR REGRESSION FOR ESTIMATING PREVIOUS DIAMETER.

Kokjohn, S. L., Hanson, R. M., Splitter, D. A., & Reitz, R. D. (2011). Fuel reactivity controlled compression ignition (RCCI): A pathway to controlled high-efficiency clean combustion. *International Journal of Engine Research*, *12*(3), 209–226. https://doi.org/10.1177/1468087411401548

Korberg, A. D., Brynolf, S., Grahn, M., & Skov, I. R. (2021). Techno-economic assessment of advanced fuels and propulsion systems in future fossil-free ships. *Renewable and Sustainable Energy Reviews*, *142*(February), 110861. https://doi.org/10.1016/j.rser.2021.110861

Krishnan, S. R., Srinivasan, K. K., Singh, S., Bell, S. R., Midkiff, K. C., Gong, W., … Willi, M. (2004). Strategies for reduced NO x emissions in pilot-ignited natural gas engines. *Journal of Engineering for Gas Turbines and Power*, *126*(3), 665–671. https://doi.org/10.1115/1.1760530

Krishnan, Sundar Rajan, Srinivasan, K. K., & Raihan, M. S. (2016). The effect of injection parameters and boost pressure on diesel-propane dual fuel low temperature combustion in a single-cylinder research engine. *Fuel*, *184*, 490–502. https://doi.org/10.1016/j.fuel.2016.07.042

Kruyt, B. (2019). *Varen op batterijen Nut en noodzaak*.

Lajunen, A., Sainio, P., Laurila, L., Pippuri-Mäkeläinen, J., & Tammi, K. (2018). Overview of powertrain electrification and future scenarios for non-road mobile machinery. *Energies*, *11*(5), 1–22. https://doi.org/10.3390/en11051184

Lambert, F. (2020). Tesla is working with mysterious third-parties to deploy Megacharger network for electric semi trucks. Retrieved December 7, 2020, from https://electrek.co/2020/10/22/tesla-mysterious-third-parties-megacharger-network-electric-semi-trucks/

Lappas, A., & Heracleous, E. (2011). *Production of biofuels via Fischer-Tropsch synthesis: Biomass-to-liquids*. *Handbook of Biofuels Production: Processes and Technologies*. Woodhead Publishing Limited. https://doi.org/10.1533/9780857090492.3.493

Lele, A., Soni, K., Narayanaswamy, K., & Krishnasamy, A. (2019). Experimental and modeling investigation of no formation mechanism for biodiesel and its blend with methanol. *SAE Technical Papers*, *2019-April*(April), 1–13. https://doi.org/10.4271/2019-01-0217

Li, J., Han, Z., Shen, C., & Lee, C. F. (2014). A study on biodiesel NOx emission control with the reduced chemical kinetics model. *Journal of Engineering for Gas Turbines and Power*, *136*(10), 1–7. https://doi.org/10.1115/1.4027358

Li, Y., Jia, M., Chang, Y., Fan, W., Xie, M., & Wang, T. (2015). Evaluation of the necessity of exhaust gas recirculation employment for a methanol/diesel reactivity controlled compression ignition engine operated at medium loads. *Energy Conversion and Management*, *101*, 40–51. https://doi.org/10.1016/j.enconman.2015.05.041

Li, Y., Jia, M., Chang, Y., Liu, Y., Xie, M., Wang, T., & Zhou, L. (2013). Parametric study and optimization of a RCCI (reactivity controlled compression ignition) engine fueled with methanol and diesel. *Energy*, *65*, 319–332. https://doi.org/10.1016/j.energy.2013.11.059

Li, Y., Jia, M., Xu, L., & Bai, X. S. (2019). Multiple-objective optimization of methanol/diesel dual-fuel engine at low loads: A comparison of reactivity controlled compression ignition (RCCI) and direct dual fuel stratification (DDFS) strategies. *Fuel*, *262*(September 2019), 116673. https://doi.org/10.1016/j.fuel.2019.116673

Liquefied Gas Carrier. (n.d.). Potential hazards of a large liquefied natural gas spill during marine transportation. Retrieved March 17, 2021, from http://www.liquefiedgascarrier.com/LNG-spill-risk.html

Liu, J., Yao, A., & Yao, C. (2015). Effects of diesel injection pressure on the performance and emissions of a HD common-rail diesel engine fueled with diesel/methanol dual fuel. *Fuel*, *140*, 192–200. https://doi.org/10.1016/j.fuel.2014.09.109

Lloyd's List. (2021). Maersk claims progress in carbon neutral methanol hunt :: Lloyd's List. Retrieved May 18, 2021, from https://lloydslist.maritimeintelligence.informa.com/LL1136363/Maersk-claims-progress-in-carbon-neutral-methanol-hunt

LNG Masterplan Consortium. (2015). *LNG Masterplan for Rhine-Main-Danube Sub-activity 2.4 Technical Evidence & Safety & Risk Assessment Deliverable 2.4.4 Emergency and incident response study*.

Lundgren, C. A., Xu, K., Jow, T. R., Allen, J., & Zhang, S. S. (2017). Lithium-Ion Batteries and Materials BT - Springer Handbook of Electrochemical Energy. In C. Breitkopf & K. Swider-Lyons (Eds.) (pp. 449–494). Berlin, Heidelberg: Springer Berlin Heidelberg. https://doi.org/10.1007/978-3-662-46657-5_15

Malins, C. (2017). What role is there for electrofuel technologies in European transport's low carbon future? *Cerulogy*, (November), 1–86.

MAN Diesel & Turbo. (2014). Using Methanol Fuel in the MAN B&W ME-LGI Series, 1–16. Retrieved from https://www.mandieselturbo.com/docs/default-source/shopwaredocuments/using-methanol-fuel-in-the-man-b-w-me-lgi-series.pdf

Mansor, W. N. W. (2014). Dual Fuel Engine Combustion and Emissions – an Experimental

Investigation coupled with computer simulation. *PhD Thesis*, *1*.

Mareev, I., Becker, J., & Sauer, D. U. (2018). Battery dimensioning and life cycle costs analysis for a heavy-duty truck considering the requirements of long-haul transportation. *Energies*, *11*(1). https://doi.org/10.3390/en11010055

Maritiem Kennis Centrum, TNO, & TU Delft. (2018). Methanol as an alternative fuel for vessels, 24. Retrieved from https://platformduurzamebiobrandstoffen.nl/wp-content/uploads/2018/02/2018_MKC_TNO-TU-Delft_Methanol-as-an-alternative-fuel-for-vessels.pdf

Markus, N. (2019). Biomassa ligt onder vuur. Is dat terecht? | Trouw. Retrieved June 16, 2021, from https://www.trouw.nl/nieuws/biomassa-ligt-onder-vuur-is-dat-terecht~b5a7253f/

Mathieu, L. (2020). Recharge EU: how many charge points will Europe and its Member States need in the 2020s. *Transport and Environment*, 68.

McGill, R., Remley, W., & Winther, K. (2013). *Alternative fuels for marine applications*. https://doi.org/10.1016/j.fuel.2019.03.082

Methanex. (n.d.). Shipping Industry To Welcome New, Lower Emission, Methanol Dual-Fuel Vessels | Methanex Corporation. Retrieved May 18, 2021, from https://www.methanex.com/news/shipping-industry-welcome-new-lower-emission-methanol-dual-fuel-vessels

Methanol Institute. (n.d.). *Methanol Production*.

Methanol Institute. (2013). Safe Handling of Methnol, 149. Retrieved from http://www.methanol.org/wp-content/uploads/2016/06/Methanol-Safe-Handling-Manual-Final-English.pdf

Ministry of Economic Affairs. (2015). Biomassa 2030, 32. Retrieved from https://www.rijksoverheid.nl/documenten/rapporten/2015/12/01/biomassa-2030

Ministry of Infrastructure and Water Management. (2003). 103(49) Guidelines for on-board NOx verification procedure - direct measurement and monitoring method. Retrieved January 20, 2021, from https://puc.overheid.nl/nsi/doc/PUC_2110_14/1/

Moirangthem, K. (2016). *Alternative Fuels for Marine and Inland Waterways*. *European Commission - Joint Research Centre Technical Reports*. https://doi.org/10.2790/227559

Montgomery, D. T., & Reitz, R. D. (2000). Optimization of Heavy-Duty Diesel Engine Operating Parameters Using A Response Surface Method, (724). https://doi.org/10.4271/2000-01-1962

Moraga, J. L., & Mulder, M. (2018). *Electrification of heating and transport A scenario analysis of the Netherlands up to 2050*. Retrieved from http://www.rug.nl/ceer/http://www.rug.nl/feb/Nettelbosje2,9747AEGroningen

Mordor Intelligence. (2019). Methanol Market | Growth, Trends, and Forecast (2020 - 2025). Retrieved January 4, 2021, from https://www.mordorintelligence.com/industry-reports/methanol-market

MTZ Equipment Ltd. (2019). Electric drive tractor.

Mulder, M., Perey, P., & Moraga, J. L. (2019). *Outlook for a Dutch hydrogen market*. *CEER Policy Papers*. Retrieved from https://www.rug.nl/news/2019/03/groene-waterstof-alleen-rendabel-bij-hoge-gasprijzen-en-streng-klimaatbeleid

Myers, R. H. (1990). *Classical and modern regression with applications* (Vol. 2). Duxbury press Belmont, CA.

Natuur & Milieu. (n.d.). Is biomassa een duurzame oplossing? | Natuur & Milieu. Retrieved June 16, 2021, from https://www.natuurenmilieu.nl/themas/grondstoffen/projecten-grondstoffen/biomassa/is-biomassa-een-duurzame-oplossing/

Natuur & Milieu. (2018). Biomassavisie 2018, (november).

NEa. (n.d.). Renewable energy units | General - Energy for Transport | Dutch Emissions Authority. Retrieved March 17, 2021, from https://www.emissionsauthority.nl/topics/general---energy-for-transport/renewable-energy-units

New Atlas. (2016, December 6). John Deere's electric tractor: A vision of zero emissions farming. Retrieved April 27, 2020, from https://newatlas.com/john-deere-electric-tractor-sesam/46812/

Nieuwe Oogst. (2019, March 28). Trekker zonder diesel snel te koop. Retrieved April 27, 2020, from https://www.nieuweoogst.nl/nieuws/2019/03/28/trekker-zonder-diesel-snel-te-koop

Nikola Corp | Nikola Motor. (n.d.). Retrieved March 29, 2020, from https://nikolamotor.com/motor

NPS Diesel. (2020). NPS Diesel en Vink Diesel introduceren MARINE POWERED BY DAF: "Schoner is niet duurder" - NPS Diesel. Retrieved July 16, 2021, from https://www.npsdiesel.com/nieuws/nps-diesel-en-vink-diesel-introduceren-marine-powered-by-daf-schoner-is-niet-duurder/

Nylund, N.-O., & Erkkilä, K. (2005). Heavy-duty truck emission and fuel consumption: Simulating real-world driving in laboratory conditions. *Proceeding of the 2005 DEER Conference*, 1–23.

Offshore Energy. (n.d.). Proman Stena Bulk JV orders 3rd methanol-powered tanker - Offshore Energy. Retrieved May 18, 2021, from https://www.offshore-energy.biz/proman-stena-bulk-jv-orders-3rd-methanol-powered-tanker/

Okoh, A. I. S. (2015). GREENHOUSE GAS REDUCTION SCHEMES AND THE RE-COLONIZATION OF NATURE IN AFRICA. *Journal of Good Governance and Sustainable Development in Africa*, *2*(4). Retrieved from http://www.rcmss.com

Osborne, J., & Waters, E. (2002). Four assumptions of multiple regression that researchers should always test. *Practical Assessment, Research & Evaluation*, *8*(2), 1–9.

Otten, M. B. J., & Afman, M. R. (2015). Emissiekentallen elektriciteit - Kentallen voor grijze en 'niet-geoormerkte stroom' inclusief upstream-emissies, 1–8.

Overheid.nl. (2020). Consultatie REDII besluit energie vervoer kalenderjaren 2022 2030. Retrieved April 3, 2021, from https://www.internetconsultatie.nl/redii_besluit_energie_vervoer_kalenderjaren_2022_2030

Pal, P., Probst, D., Pei, Y., Zhang, Y., Traver, M., Cleary, D., & Som, S. (2017). Numerical Investigation of a Gasoline-Like Fuel in a Heavy-Duty Compression Ignition Engine Using Global Sensitivity Analysis. *SAE International Journal of Fuels and Lubricants*, *10*(1), 56–68. https://doi.org/10.4271/2017-01-0578

Panteia. (2013). CONTRIBUTION TO IMPACT ASSESSMENT of measures for reducing emissions of inland navigation. Retrieved from http://ec.europa.eu/transport/sites/transport/files/modes/inland/studies/doc/2013-06-03-contribution-to-impact-assessment-of-measures-for-reducing-emissions-of-inland-navigation.pdf

Panteia. (2019). Op weg naar een klimaatneutrale binnenvaart per 2050: Transitie- en Rekenmodel binnenvaart.

PBL. (2018). 14 Elektriciteit. In *Analyse van het Voorstel voor Hoofdpunten van het Klimaatakkoord* (pp. 217–236).

Petrov, N., & Trendafilov, K. (2011). Determining agricultural machinery lifetime by using economic indicators, *9*(4), 26–29.

PGW. (2015). Safety Data Sheet : Liquefied Natural Gas (LNG), 1–11.

Planbureau voor de Leefomgeving. (2020). Klimaat- en Energieverkenning 2020, 184.

Plasun, R. (1999). Optimization of VLSI Semiconductor Devices. Retrieved August 4, 2021, from https://www.iue.tuwien.ac.at/phd/plasun/node32.html

Polat, S., Yücesu, H. S., Uyumaz, A., Kannan, K., & Shahbakhti, M. (2020). An experimental investigation on combustion and performance characteristics of supercharged HCCI operation in low compression ratio engine setting. *Applied Thermal Engineering*, *180*(August). https://doi.org/10.1016/j.applthermaleng.2020.115858

Port-Liner. (n.d.). Portliner EC52. Retrieved April 28, 2020, from https://www.portliner.nl/ships/ec52

Port-Liner, & Ports and the City. (n.d.). *Port-Liner Introduction*. Retrieved from https://www.portsandthecity.nl/static/files/tinymce/uploads/Port- Liner Introduction by Hen van Haar .pdf

Probst, D. M., Raju, M., Senecal, P. K., Kodavasal, J., Pal, P., Som, S., … Pei, Y. (2019). Evaluating optimization strategies for engine simulations using machine learning emulators. *Journal of Engineering for Gas Turbines and Power*, *141*(9). https://doi.org/10.1115/1.4043964

Proman. (2021). Proman closes its investment in Québec's first carbon-recycling and biofuels plant and will lead bio-methanol marketing - Proman. Retrieved May 18, 2021, from https://www.proman.org/news/proman-closes-its-investment-in-quebecs-first-carbon-recycling-and-biofuels-plant-and-will-lead-bio-methanol-marketing/

Prussi, M., Yugo, M., De Prada, L., Padella, M., & Edwards, M. (2020). *JEC Well-To-Wheels report v5*. https://doi.org/10.2760/100379

Prussi, M., Yugo, M., De Prada, L., Padella, M., Edwards, R., & Lonza, L. (2020). *JEC Well-to-Tank report v5*. Publications Office of the European Union, Luxembourg. https://doi.org/10.2760/959137

Qi, D. H., Jia, C. C., & Feng, Y. M. (2014). Combustion and emissions behaviour for methanol-gasoline blended fuels in a multipoint electronic fuel injection engine. *International Journal of Sustainable Energy*, *33*(5), 985–999. https://doi.org/10.1080/14786451.2013.774004

Quartz. (2017, November 23). China's first all-electric cargo ship is going to be used to transport coal. Retrieved April 28, 2020, from https://qz.com/1137026/chinas-first-all-electric-cargo-ship-is-going-to-be-used-to-transport-coal/

Raven, R., Van Den Bosch, S., & Weterings, R. (2010). Transitions and strategic niche management: Towards a competence kit for practitioners. *International Journal of Technology Management*, *51*(1), 57–74. https://doi.org/10.1504/IJTM.2010.033128

Roldán, J. A. (n.d.). Should inland freighters use hydrogen? Retrieved April 28, 2020, from https://www.ingenieroemprendedor.com/english/blog/should-inland-freighters-use-hydrogen/

Rosenkopf, L., & Almeida, P. (2003). Overcoming local search through alliances and mobility. *Management Science*, *49*(6), 751–766. https://doi.org/10.1287/mnsc.49.6.751.16026

Rotmans, J., & Loorbach, D. (2008). Transition management: reflexive governance of societal complexity through searching, learning and experimenting.

Sawant, P., & Bari, S. (2018). Effects of Variable Intake Valve Timings and Valve Lift on the Performance and Fuel Efficiency of an Internal Combustion Engine, 1–11. https://doi.org/10.4271/2018-01-0376.Abstract

Schootstra, S. (2018). Vrachtboot met Powerbank - Energie & Transitie. Retrieved April 28, 2020, from https://siebeschootstra.nl/vrachtboot-met-powerbank/

Schot, J., & Geels, F. W. (2007). Niches in evolutionary theories of technical change: A critical survey of the literature. *Journal of Evolutionary Economics*, *17*(5), 605–622. https://doi.org/10.1007/s00191-007-0057-5

Schot, J., & Geels, F. W. (2008). Strategic niche management and sustainable innovation journeys: Theory, findings, research agenda, and policy. *Technology Analysis and Strategic Management*, *20*(5), 537–554. https://doi.org/10.1080/09537320802292651

Schröder, J., Müller-Langer, F., Aakko-Saksa, P., Winther, K., Baumgarten, W., & Lindgren, M. (2020). Methanol as Motor Fuel, 60. Retrieved from https://www.iea-amf.org/app/webroot/files/file/Annex%0AReports/AMF_Annex_56.pdf

Sdanghi, G., Maranzana, G., Celzard, A., & Fierro, V. (2020). Towards non-mechanical hybrid hydrogen compression for decentralized hydrogen facilities. *Energies*, *13*(12). https://doi.org/10.3390/en13123145

See The BYD Class 8 Electric Truck In Motion: Video. (n.d.). Retrieved April 7, 2020, from https://insideevs.com/news/375749/byd-class-8-electric-truck-in-motion/

Semi | Tesla Nederland. (n.d.). Retrieved March 29, 2020, from https://www.tesla.com/nl_NL/semi?redirect=no

Sendo Shipping. (n.d.). Sendo Liner: Het schip van de toekomst.

Shahabuddin, M., Krishna, B. B., Bhaskar, T., & Perkins, G. (2020). Advances in the thermo-chemical production of hydrogen from biomass and residual wastes: Summary of recent techno-economic analyses. *Bioresource Technology*, *299*(December 2019), 122557. https://doi.org/10.1016/j.biortech.2019.122557

Shamun, S., Novakovic, M., Malmborg, V. B., Preger, C., Shen, M., Messing, M. E., … Tunestäl, P. (2017). Detailed characterization of particulate matter in alcohol exhaust emissions. *COMODIA 2017 - 9th International Conference on Modeling and Diagnostics for Advanved Engine Systems*. https://doi.org/10.1299/jmsesdm.2017.9.b304

Sharma, V. K., Mohan, M., & Mouli, C. (2017). Effect of intake swirl on the performance of single cylinder direct injection diesel engine. *IOP Conference Series: Materials Science and Engineering*, *263*(6). https://doi.org/10.1088/1757-899X/263/6/062077

Ship & Bunker. (2021). First Proman Stena Methanol-Fuelled Ship to Launch Next Year - Ship & Bunker. Retrieved May 18, 2021, from https://shipandbunker.com/news/world/510648-first-proman-stena-methanol-fuelled-ship-to-launch-next-year

Ship Technology. (2017). A decade to autonomous cargo ships? Retrieved April 28, 2020, from https://www.ship-technology.com/features/featurea-decade-to-autonomous-cargo-ships-5838573/

Ship Technology. (2019). Ellen E-ferry: world first a glimpse of the future of ferries. Retrieved March 31, 2020, from https://www.ship-technology.com/features/ellen-e-ferry/

Simić, A. (2014). Energy efficiency of inland waterway self-propelled cargo ships. *RINA, Royal Institution of Naval Architects - Influence of EEDI on Ship Design 2014*, (September 2014), 50–58. https://doi.org/10.13140/RG.2.1.1548.7200

Smil, V. (2020). Germany's Energiewende, 20 Years Later. Retrieved March 6, 2021, from https://spectrum.ieee.org/energy/renewables/germanys-energiewende-20-years-later

Smith, A., & Raven, R. (2011). What is protective space? Reconsidering niches in transitions to sustainability. *Research Policy*, *41*(6), 1025–1036. https://doi.org/10.1016/j.respol.2011.12.012

Som, S., Senecal, P. K., & Pomraning, E. (2012). Comparison of RANS and LES turbulence models against constant volume diesel experiments. *24th Annual Conference on Liquid Atomization and Spray Systems, ILASS Americas*, *Di*(May), 1–11.

SPB. (2016). PROMINENT - D1.1 List of operational profiles and fleet families.

Spoof-Tuomi, K., & Niemi, S. (2020). Environmental and Economic Evaluation of Fuel Choices for Short Sea Shipping. *Clean Technologies*, *2*(1), 34–52. https://doi.org/10.3390/cleantechnol2010004

Statista. (n.d.). • Industrial prices for electricity in the Netherlands 1995-2019 | Statista. Retrieved March 17, 2021, from https://www.statista.com/statistics/596254/electricity-industry-price-netherlands/

Štefančič, N. S. (n.d.). Mapping out renewable methanol around the world - MefCO_2. Retrieved January 4, 2021, from http://www.mefco2.eu/news/mapping-out-renewable-methanol-around-the-world.php

Stena Line. (2021). The world´s first methanol ferry – StenaLine.com. Retrieved May 18, 2021, from https://www.stenaline.com/media/stories/the-worlds-first-methanol-ferry/

Suarez, F., Grodal, S., & Gotsopoulos, A. (2015). PERFECT TIMING? DOMINANT CATEGORY, DOMINANT DESIGN, AND THE WINDOW OF OPPORTUNITY FOR FIRM ENTRY. *Strategic Management Journal*, *36*(3), 437–448. https://doi.org/10.1002/smj

Sutton, H. (2011). Analysing the Calue Chain for the Petroleum Industry. Retrieved from https://www.slideshare.net/sherifshicko/value-chain-petrol-dieselfinal-draft

Tang, M., Pei, Y., Zhang, Y., Traver, M., Cleary, D., Luo, Z., … Lee, S. Y. (2018). Numerical investigation of fuel effects on soot emissions at heavy-duty diesel engine conditions. *ASME 2018 Internal Combustion Engine Division Fall Technical Conference, ICEF 2018*, *2*, 1–16. https://doi.org/10.1115/ICEF2018-9696

Tcvetkov, P., Cherepovitsyn, A., & Fedoseev, S. (2019). Public perception of carbon capture and storage: A state-of-the-art overview. *Heliyon*, *5*(12), e02845. https://doi.org/10.1016/j.heliyon.2019.e02845

Teoh, Y. H., Masjuki, H. H., Kalam, M. A., & How, H. G. (2015). Effect of injection timing and EGR on engine-out-responses of a common-rail diesel engine fueled with neat biodiesel. *RSC Advances*, *5*(116), 96080–96096. https://doi.org/10.1039/c5ra14831f

Tesla Semi production version will have closer to 600 miles of range, says Elon Musk - Electrek. (n.d.). Retrieved March 29, 2020, from https://electrek.co/2018/05/02/tesla-semi-production-version-range-increase-elon-musk/#

The Next Web. (2020). Say hello to Ellen, the electric ferry with 57 times the battery capacity of a Tesla. Retrieved April 1, 2020, from https://thenextweb.com/world/2020/01/16/ellen-electric-passenger-ferry-battery-57-times-capacity-than-tesla/

TIAX LLC. (2007). *Full fuel cycle assessment: Well-to-wheels energy inputs, emissions, and water impacts*. Retrieved from http://scholar.google.com/scholar?hl=en&btnG=Search&q=intitle:Full+fuel+cycle+assessment:+well-to-wheels+energy+inputs,+emissions,+and+water+impacts#1

TNO. (2020). Power-2-Fuel Cost Analysis. Retrieved from www.smartport.nl

Tordo, S., Tracy, B., & Arfaa, N. (2011). *National Oil Companies and Value Creation*. *World Bank Working Paper Series* (Vol. Number 218).

TORQ — Neuron EV. (n.d.). Retrieved March 29, 2020, from https://www.neuronev.co/torq

Tosun, E., Aydin, K., & Bilgili, M. (2016). Comparison of linear regression and artificial neural network model of a diesel engine fueled with biodiesel-alcohol mixtures. *Alexandria Engineering Journal*, *55*(4), 3081–3089. https://doi.org/10.1016/j.aej.2016.08.011

Transport & Environment. (2020). RED II and advanced biofuels Recommendations about Annex IX of the Renewable Energy Directive and its implementation at national level, (May), 1–21.

Tremel, A. (2018). *Electricity-based Fuels*. *SpringerBriefs in Applied Sciences and Technology*.

Tremel, A., Wasserscheid, P., Baldauf, M., & Hammer, T. (2015). Techno-economic analysis for the synthesis of liquid and gaseous fuels based on hydrogen production via electrolysis. *International Journal of Hydrogen Energy*, *40*(35), 11457–11464. https://doi.org/10.1016/j.ijhydene.2015.01.097

TRUCK - BYD USA. (n.d.). Retrieved March 28, 2020, from https://en.byd.com/truck/

Tuominen, T. (2016). Potential of Methanol in Dual Fuel Combustion, 75.

Turcksin, L., Macharis, C., Lebeau, K., Boureima, F., Mierlo, J. Van, Bram, S., … Pelkmans, L. (2011). A multi-actor multi-criteria framework to assess the stakeholder support for different biofuel options : The case of Belgium. *Energy Policy*, *39*(1), 200–214. https://doi.org/10.1016/j.enpol.2010.09.033

U.S. Energy Information Administration. (2020). Annual Energy Outlook 2020 - Industry. Retrieved from https://www.eia.gov/outlooks/aeo/pdf/AEO2020 Industrial.pdf

Upham, P., Kivimaa, P., Mickwitz, P., & Åstrand, K. (2014). Climate policy innovation: a sociotechnical transitions perspective. *Environmental Politics*, *23*(5), 774–794. https://doi.org/10.1080/09644016.2014.923632

US Office of Energy Efficiency & Renewable Energy. (2010). Fact #620: April 26, 2010 Class 8 Truck Tractor Weight by Component. Retrieved March 27, 2020, from https://www.energy.gov/eere/vehicles/fact-620-april-26-2010-class-8-truck-tractor-weight-component

Van Driel, H., & Schot, J. (2005). Radical innovation as a multilevel process: Introducing floating grain elevators in the port of rotterdam. *Technology and Culture*, *46*(1), 51–76. https://doi.org/10.1353/tech.2005.0011

Vancoillie, J., Demuynck, J., Sileghem, L., Van De Ginste, M., & Verhelst, S. (2012). Comparison of the renewable transportation fuels, hydrogen and methanol formed from hydrogen, with gasoline

- Engine efficiency study. *International Journal of Hydrogen Energy*, *37*(12), 9914–9924. https://doi.org/10.1016/j.ijhydene.2012.03.145

Verardi, V., & Croux, C. (2009). Robust Regression in Stata. *The Stata Journal*, *9*(3), 439–453. https://doi.org/10.1177/1536867X0900900306

Verbeek, R., Hart, P. 't, Pruyn, J., & Bergsma, J. (2020). Final Report : Assessment of alternative fuels for seagoing vessels using Heavy Fuel Oil, 1–39.

Verenigde Naties, & Economische Commissie. (2015). Europese overeenkomst voor het internationale vervoer van gevaarlijke goederen over de weg (ADR) Bijlagen Ministerie van Infrastructuur en Milieu.

Verhees, B., Raven, R., Veraart, F., Smith, A., & Kern, F. (2012). Interrogating Protective Space : Shielding , Nurturing and Empowering Dutch Solar PV, *201204*(2012).

Verhelst, S., Turner, J. W., Sileghem, L., & Vancoillie, J. (2019). Methanol as a fuel for internal combustion engines. *Progress in Energy and Combustion Science*, *70*(January), 43–88. https://doi.org/10.1016/j.pecs.2018.10.001

VIV. (2019, October 11). Port-Liner krijgt flow-batterijen. Retrieved April 28, 2020, from https://www.verbrandingsmotor.nl/port-liner-krijgt-flow-batterijen/6834

VMS Insight. (2019). *Het effect van elektrisch aangedreven trucks en bussen op het aftersales businessmodel*.

Volvo FL Electric. (n.d.). Retrieved March 29, 2020, from https://www.volvotrucks.nl/nl-nl/trucks/trucks/volvo-fl/volvo-fl-electric.html

Volvo Trucks Unveils Electric Truck, Readies Commercialization. (n.d.). Retrieved March 29, 2020, from https://www.trucks.com/2019/09/13/volvo-unveils-vnr-electric-truck/

Vopak. (n.d.). Vopak stores a wide variety of liquid bulk products and gasses. Retrieved from 18-01-2021

Walrave, B., Talmar, M., Podoynitsyna, K. S., Romme, A. G. L., & Verbong, G. P. J. (2018). A multi-level perspective on innovation ecosystems for path-breaking innovation. *Technological Forecasting and Social Change*, *136*(April 2017), 103–113. https://doi.org/10.1016/j.techfore.2017.04.011

Wang, C., Li, Y., Xu, C., Badawy, T., Sahu, A., & Jiang, C. (2019). Methanol as an octane booster for gasoline fuels. *Fuel*, *248*(February), 76–84. https://doi.org/10.1016/j.fuel.2019.02.128

Wang, H., Gan, H., Wang, G., & Zhong, G. (2020). Emission and Performance Optimization of Marine Four-Stroke Dual-Fuel Engine Based on Response Surface Methodology. *Mathematical Problems in Engineering*, *2020*. https://doi.org/10.1155/2020/5268314

Wang, S., & Notteboom, T. (2014). The Adoption of Liquefied Natural Gas as a Ship Fuel : A Systematic Review of Perspectives and Challenges. *Transport Reviews*, *0*(0), 1–26. https://doi.org/10.1080/01441647.2014.981884

Wang, X., & Song, C. (2020). Carbon Capture From Flue Gas and the Atmosphere: A Perspective. *Frontiers in Energy Research*, *8*(December 2020). https://doi.org/10.3389/fenrg.2020.560849

Wang, Z., Liu, H., & Reitz, R. D. (2017). Knocking combustion in spark-ignition engines. *Progress in Energy and Combustion Science*, *61*, 78–112. https://doi.org/10.1016/j.pecs.2017.03.004

WaterstofNet. (2020, April 9). H2-Share's first hydrogen-powered rigid truck hits the road in the Netherlands. Retrieved April 25, 2020, from https://www.waterstofnet.eu/nl/nieuws/h2-share-s-first-hydrogen-powered-rigid-truck-hits-the-road-in-the-netherlands

Weeda, M., & Segers, R. (2020). The Dutch hydrogen balance, and the current and future representation of hydrogen in the energy statistics, 33.

Willems, R. C. (2020). *Designed Experiments for Efficient Engines*. Technische Universiteit Eindhoven.

Williamson, P. J., & De Meyer, A. (2012). Ecosystem advantage: How to successfully harness the power of partners. *California Management Review*, *55*(1), 24–46. https://doi.org/10.1525/cmr.2012.55.1.24

World Bank Group. (2019). *BALANCING PETROLEUM POLICY TOWARD VALUE, SUSTAINABILITY, AND SECURITY*. https://doi.org/10.1596/978-1-4648-1384-9

World Biogas Association. (2017). Anaerobic Digestion Market report The Netherlands. Retrieved from http://www.worldbiogasassociation.org/wp-content/uploads/2017/07/WBA-netherlands-4ppa4_v1.pdf

World Nuclear Association. (2018, August). Heat values of various fuels. Retrieved April 25, 2020, from https://www.world-nuclear.org/information-library/facts-and-figures/heat-values-of-various-fuels.aspx

Xing, H., Stuart, C., Spence, S., & Chen, H. (2021). Fuel cell power systems for maritime applications: Progress and perspectives. *Sustainability (Switzerland)*, *13*(3), 1–34. https://doi.org/10.3390/su13031213

Yao, M., Chen, Z., Zheng, Z., Zhang, B., & Xing, Y. (2006). Study on the controlling strategies of homogeneous charge compression ignition combustion with fuel of dimethyl ether and methanol. *Fuel*, *85*(14–15), 2046–2056. https://doi.org/10.1016/j.fuel.2006.03.016

YARA. (n.d.). Yara Birkeland press kit. Retrieved April 28, 2020, from https://www.yara.com/news-and-media/press-kits/yara-birkeland-press-kit/

Yi, Q., Gong, M. H., Huang, Y., Feng, J., Hao, Y. H., Zhang, J. L., & Li, W. Y. (2016). Process development of coke oven gas to methanol integrated with CO2 recycle for satisfactory techno-economic performance. *Energy*, *112*, 618–628. https://doi.org/10.1016/j.energy.2016.06.111

Zahra, S. A., & Nambisan, S. (2012). Entrepreneurship and strategic thinking in business ecosystems. *Business Horizons*, *55*(3), 219–229. https://doi.org/10.1016/j.bushor.2011.12.004

Zhang, J., Meerman, H., Benders, R., & Faaij, A. (2020). Comprehensive review of current natural gas liquefaction processes on technical and economic performance. *Applied Thermal Engineering*, *166*(November 2019), 114736. https://doi.org/10.1016/j.applthermaleng.2019.114736

Zhang, W., Yang, J., Zhang, W., & Ma, F. (2019). Research on regenerative braking of pure electric mining dump truck. *World Electric Vehicle Journal*, *10*(2). https://doi.org/10.3390/wevj10020039

Zhao, K. (2019). A Brief Review of China's Methanol Vehicle Pilot and Policy, (March), 1–10. Retrieved from http://www.miit.gov.cn/n1146295/n1652858/n1652930/n3757016/c6684042/content.html

Zhao, Y., Setzler, B. P., Wang, J., Nash, J., Wang, T., Xu, B., & Yan, Y. (2019). An Efficient Direct Ammonia Fuel Cell for Affordable Carbon-Neutral Transportation. *Joule*, *3*(10), 2472–2484.

https://doi.org/10.1016/j.joule.2019.07.005

Zomer, G., Finner, S., Harmsen, J., Vredeveldt, L., & Lieshout, P. van. (2020). Green Maritime Methanol Operation aspects and the fuel supply chain, 1–14.

Appendix A: Overview Electric Pilot Cases

A1.1: Electric Truck Pilot Cases

Currently, there are multiple trucks available or in development, those of pilots with information publicly available are mentioned.

A1.1.1: DAF trucks

DAF trucks is working on the development of two types of electric trucks, the LF and the CF electric for light and heavy distribution applications in cities. Next to that, they are developing a hybrid version of the CF truck for middle ranges which can drive electrically in the urban environment ("Elektrische & hybride trucks - DAF Trucks N.V.," n.d.).

The LF Electric is a 19-ton truck with a 195kW, 250kW peak power, engine with a battery capacity of 222kWh. The expected driving range comes down to 220km with full load.

The CF Electric is a heavy duty tractor with a gross combined weight of 37 ton. The electric motor can provide 210 kW, 240 kW peak, and it can achieve a range of 100 km with its 170 kWh battery pack.

The CF hybrid has a 330 kW diesel engine with 75 kW, 130 kW peak, electric engine. It uses a 85 kWh battery pack with this it can drive 30-50 km fully electric and it can be fully charged in 30 minutes.

A1.1.2: Daimler Freightliner

Daimler is expecting the eCascadia and the eM2 106 to start production late 2021 (GreenBiz, 2020). The eCascadia, a heavy duty 36 ton tractor, is expected to have a range of 400 km using a 550 kWh battery pack to power its 544 kW electric engine. It should be able to charge 80% in 90 minutes. The eM2 106 is a medium duty truck for local distribution, pick-up and delivery and last mile logistic applications. It has a 370 km range with its 325 kWh battery, expecting to recharge 80% in 60 minutes and it is providing its power using a 353 kW electric engine ("e-Mobility | Freightliner Trucks," n.d.).

A1.1.3: Tesla

One of the most ambitious and most discussed announcements of electric trucks is the Tesla Semi. In 2017 Elon Musk announced the Tesla Semi, a heavy duty 40 ton truck, which is expected to start production late 2020 after a postponement of 1.5 years ("Tesla Semi production version will have closer to 600 miles of range, says Elon Musk - Electrek," n.d.). It is expected to have range of 475 km or 800 km depending on the version, claiming it will have a TCO lower than that of Diesel trucks and its premium will be paid back in 2 years ("Semi | Tesla Nederland," n.d.). The latest announcements even state ranges up to 950km ("Tesla Semi production version will have closer to 600 miles of range, says Elon Musk - Electrek," n.d.). It also claims to use less than 125 kWh per 100 miles ("Semi | Tesla Nederland," n.d.), suggesting a battery pack of 600 kWh or 1 MWh and it is mentioned that with its mega chargers it could charge 643 km in just 30 minutes. The announcements are received with scepticism as it would drastically outperform competitors on price and performance and not many specifications have been released which indicate how it can be achieved. An example of one of the problems is the charging time as it would require a staggering charging power of 1.5 MW.

A1.1.4: Volvo

Volvo has also developed a zero-emission 16 ton truck, the FL electric, which is designed for regional transport ("Volvo FL Electric," n.d.). Its production is expected at the end of 2020. The FL Electric has a range up to 300 km and is powered by a 165 kW, 200 kW peak, electric engine. The truck can be equipped with up to 6 battery packs of 50 kWh each.

Next to the FL electric, Volvo is also working on the VNR electric a heavy duty electric truck that should be available at the end of 2020, however the specifications of this truck are not yet announced ("Volvo Trucks Unveils Electric Truck, Readies Commercialization," n.d.).

A1.1.5: BYD

The Chinese company BYD is one of the world's largest EV companies, producing a variety of electric vehicles from passenger cars, to 11 different types of commercial vehicles. It is offering a heavy duty truck as well with the Class 8 TT Day Cab ("See The BYD Class 8 Electric Truck In Motion: Video," n.d.; "TRUCK - BYD USA," n.d.). It has a 360 kW electric engine, using a 435 kWh battery. With this it has a range of 200 km and it has a gross combined weight rating (GCWR) of 40 ton.

A1.1.6: Others

Besides these large and well known automotive producers, there are also start-ups like Neuron EV working on the development of an electric truck ("TORQ — Neuron EV," n.d.) or on fuel cell electric trucks like Nikola ("Nikola Corp | Nikola Motor," n.d.).

A1.2.1: Overview Specifications Electric and Diesel Trucks

Table A.1: Overview of electric and diesel truck specifications

Brand	Type	Drivetrain	Power	Battery [kWh]	Max Power [kW]	Range [km]	Tank [L]	Max weight [Ton]
DAF	LF Electric	Electric	195	222	250	220		19
DAF	CF Electric	Electric	210	170	240	100		37
MAN	eTruck	Electric	264	185	264	200		26
Daimler	eCascadia	Electric	544	550	544	400		36
Daimler	eM2 106	Electric	353	325	353	370		12
Tesla	Semi	Electric		1000		800		40
Volvo	FL Electric	Electric	130	300	185	300		16
Volvo	FE Electric	Electric	260	300	740	200		27
BYD	T9	Electric		350	-	200		28
BYD	T7	Electric	150	175	150	200		11
BYD	T5	Electric		150	-	250		7.3
BYD	Class 8 TT Day Cab	Electric	360	435	360	200		40
DAF	CF Hybrid	Hybrid	75	85	130	50		40
DAF	LF FA city min	Diesel	115		115		110	12
DAF	LF FA city max	Diesel	127		127		185	12
DAF	LF FA 12t distribution min	Diesel	135		135		925	12
DAF	LF FA 12t distribution max	Diesel	194		194		925	12
DAF	LF 230 FT	Diesel	217		217		170	21
DAF	CF Low Deck-trekker min	Diesel	270		270		1215	50
DAF	CF Low Deck-trekker max	Diesel	390		390		1215	78
DAF	CF 450 MX11	Diesel	330		330		430	50
DAF	CF 530 MX-13	Diesel	390		390		430	50
DAF	XF Low Deck-trekker min	Diesel	315		315		1215	50
DAF	XF Low Deck-trekker max	Diesel	390		390		1215	50
DAF	XF FAR - Lange afstand	Diesel	390		390		1435	50
DAF	XF 430 FTM	Diesel					1215	78
DAF	XF 450 FTN	Diesel					1215	60
Mercedes-Benz	actros	Diesel	175		175		990	18
Mercedes-Benz	actros	Diesel	390		390		1260	26
Volvo	FH AT2612F	Diesel	375		375		1480	100
Volvo	FH AT2412F	Diesel	375		375		900	44

A2.1: Electric Tractor Pilot Cases

In the tractor market the trend towards electrification is slowly becoming visible as there are currently 2 battery electric tractors running of which the specifications are published. The John Deere Concept SESAM, a concept that rebuild a traditional 6R into an electric tractor (New Atlas, 2016), and the Fendt Vario e100 that is expected to be commercialised at the end of the year (Nieuwe Oogst, 2019).

A2.1.1: John Deere Concept SESAM

The tractor is a modification of the 6R, a 82-184 kW tractor. It was modified using a 130 kW electric engine with a 150 kWh battery. It can work in the field for 4 hours before it needs to be recharged and it has a similar maximum weight as the 6R which is around the 10450 kg.

A2.1.2: Fendt E100 Vario

This electric tractor has a 50 kW, 150 kW peak, engine. With its 100 kWh battery it has an operating time of 5 hours and it has a maximum weight of 4500 kg.

Far more tractors are heading towards hybrid concepts, as it allows the diesel engine to operate at its optimal operating point and electric engines have a rather constant efficiency over its operating curve as can be seen in figure 3.1. MTZ Equipment Ltd. (2019) found that hybridisation could reduce fuel consumption up to 15% on the field and 30% on the road for its MTZ 3623 model. This model uses a 270 kW engine to charge the battery. Unfortunately, most electric and hybrid tractors are still in development and have not yet released all specifications.

A2.2: Overview Specification Electric and Diesel Tractors

Table A.2: Overview of electric and diesel tractor specifications

Brand	Type	Drivetrain	Peak Power	Battery [kWh]	max weight [Ton]	Tank [L]	Fuel use [g/kWh]
Fendt	e100 Vario	electric	150	100	4500	-	-
John Deere	Concept Sesam	electric	300	130	10450	-	-
Belarus	3023	hybrid	220	-	-	-	-
Belarus	3622	hybrid	270	-	-	-	-
STEYR	STEYR Konzept	hybrid	-	-	-	-	-
MTZ	MTZ 3623	hybrid	270	-	20000	500	-
MTZ	ET-450	hybrid	335	-	-	-	-
Kirovets	-	hybrid	340	-	-	-	-
BELARUS	3522	diesel	264	-	12300	650	220
BELARUS	4522	diesel	343	-	14785	650	-
BELARUS	MSU-622	diesel	46	-	3440	94	-
BELARUS	952.6	diesel	70	-	5325	140	-
BELARUS	1523.6	diesel	112	-	6780	200	-
BELARUS	1523	diesel	148	-	9000		227
BELARUS	1822B.3	diesel	132	-	10000		250
BELARUS	2022.6	diesel	148	-	7400	300	-
MTZ	MTZ 920	diesel	63	-	4300	135	-
MTZ	MTZ 2022	diesel	158	-	10000	420	-
MTZ	MTZ K744 Kirovets	diesel	324	-	19200	800	205
John Deere	5075E	diesel	55	-	5100	82	-
John Deere	6120M	diesel	140	-	10450	205	-
John Deere	9620R	diesel	670	-	27000	1490	-
Fendt	211 F Vario S3	diesel	82	-	4500	76	212
Fendt	314 Vario Gen4	diesel	112	-	8500	210	-
Fendt	516 Vario S4	diesel	120	-	10500	298	-
Fendt	1050 Vario Gen2	diesel	380	-	23000	800	-
Fendt	1165 MT S4	diesel	475	-	27000	1000	-
Fendt	828 Vario S4	diesel	211	-	16000	505	192

A3: Electric Inland Shipping Pilot Cases

A3.1: Pilot Cases

The electrification in shipping has started with ferries which have fixed routes and do not have to travel very long distances without stopping, as they stop frequently at set places. So, ferries have the opportunity to recharge the batteries very often which makes them a great candidate for electrification. There are a handful of electric ferries with just a few of them releasing details. Two of these are described below.

A3.1.1: Ampere
An electric ferry that began operation in 2015. It operates on a 5.7 km crossing 34 times a day. It is 80m long and can accommodate 120 cars and 360 passengers. It uses two 450 kW engines for propulsion and with its 1000 kWh battery weighing 10 ton it can run its operation at over 18 km/h ("Ampere Electric-Powered Ferry - Ship Technology," n.d.).

A3.1.2: Ellen
This 60m ferry, launched in 2019, has a range of 38 km and operates on a 20 km route transporting 31 cars or 5 trucks and up to 198 passengers with a total weight of 650 tonnes (The Next Web, 2020). It sails with a speed up to 28.7 km/h using its combined propulsion power of 1.5 MW. The ferry requires 4.3 MWh battery capacity, which are fully charged in the morning. During the day it is six times partly recharged in the harbour and then fully charged again during the night (Ship Technology, 2019).

For inland cargo vessels the challenge is larger since it often requires ships to operate over a larger distances without chances to recharge frequently. Desktop research therefore could only find a few cases in which full battery electric inland shipping barges were being developed or piloted.

A3.1.3: Guangzhou Shipyard International Company Ltd
This barge ship was the world's first all-electric cargo ship launched in November 2017 in Guangzhou China. It is a 70.5 m long vessel that can travel 80 km with a maximum speed of 12.8 km/h (Futurism, 2017). The 2000 deadweight tonnage (DWT) ship has a battery capacity of 2400 kWh to power its two electric engines of 160 kW each (GSI, n.d.). The ship is charged during its unloading time of 2 hours after each journey. Huang Jialin, chairman of the ship's design firm Hangzhou Modern Ship Design & Research Co., expects the battery to last about 5 years and sees the stability of the power system as one of the main challenges for long-haul vessels (Quartz, 2017).

A3.1.4: YARA Birkeland
The YARA Birkeland is an electric cargo vessel due to set sailing in 2020. The ship has a length of 80 m with a DWT of 3200 ton or a load of 120 twenty-foot equivalent unit containers (TEU). It has a sailing speed of 13 km/h and a top speed of 24 km/h. This is made possible by two main thrusters of 1200 kW each (YARA, n.d.). With its 7 MWh battery capacity it is able to sail for 120 km (Ship Technology, 2017).

A3.1.5: Port-liner EC52 & EC110
Port-liner is a company developing two fully electric ships. After a delay due to the change from lithium-ion batteries to vanadium redox flow-batteries the ships are expected to become operational half of 2020 (VIV, 2019). The EC52 is a 52m long ship that can carry either 1000 DWT or 36 TEU (Port-Liner, n.d.). It uses one 20 foot container to sail for up to 15 hours and it is stated that the cargo capacity is increased by 8% since no engine room is required.

The EC110 is a 110m long ship able to sail up to 35 hours using four of those containers (Inland Navigation Europe, 2018). These four containers have a capacity of around 7 MWh which allows it to sail up to 230 km on low current rivers, which is enough to sail the distance between Antwerp and Rotterdam (Port-Liner & Ports and the City, n.d.). The EC110 is capable of shipping 280 TEU or 7000 DWT.

Appendix B: Diesel Benchmark Simulation results

Table B.1 shows the most important results of the diesel benchmark simulations. Run 351 and 352 are the control runs for checking the GA optimization results. Contact the author if there is interest in the source data.

Table B.1: Diesel benchmark simulation results. The green boxes obey the emission limits.

Run	PINLET	SOI	CAD10	CAD50	CAD90	λ	PPRR	GIE	COMBL	HEATL	EXHAUSTL	ISNOX	ISUHC	ISPM	ISCO	ISFORM
	Mpa	CAD ATDC	ATDC	ATDC	ATDC		Bar/CAD					g/kWh	g/kWh	g/kWh	g/kWh	mg/kWh
101	0.2000	-10.00	-6.79	-3.30	3.82	3.82	13.9	46.16%	0.95%	22.35%	30.53%	20.45	0.0039	0.005	0.294	0.83
102	0.2500	-5.00	-2.39	1.84	8.53	4.77	13.2	47.56%	0.71%	20.39%	31.34%	15.89	0.0146	0.016	0.283	1.85
103	0.2500	-15.00	-8.78	-8.50	-4.39	4.77	111.6	42.18%	0.94%	27.69%	29.19%	26.06	0.0157	0.002	0.413	5.09
104	0.1500	-5.00	-1.59	2.14	12.34	2.86	17.2	46.14%	0.60%	20.89%	32.37%	13.88	0.0038	0.006	0.227	0.83
105	0.1500	-15.00	-7.79	-7.40	-3.20	2.86	84.8	41.34%	1.00%	29.53%	28.13%	29.28	0.0046	0.001	0.011	3.49
201	0.2000	-4.00	-1.19	3.10	11.14	3.82	12.3	47.05%	0.65%	20.15%	32.15%	14.26	0.0143	0.012	0.321	2.91
202	0.1500	-2.00	1.40	5.20	15.90	2.86	14.9	46.12%	0.50%	19.74%	33.63%	11.08	0.0071	0.009	0.278	1.62
203	0.1500	-6.00	-2.50	1.20	11.13	2.86	18.7	46.03%	0.64%	21.39%	31.94%	15.02	0.0036	0.005	0.224	0.82
204	0.2500	-2.00	0.61	4.82	11.91	4.77	11.6	47.50%	0.61%	19.49%	32.40%	12.82	0.0198	0.028	0.314	2.93
205	0.2500	-6.00	-3.40	0.74	7.40	4.77	13.4	47.47%	0.76%	20.73%	31.04%	17.14	0.0115	0.015	0.275	1.65
301	0.2500	0.00	2.60	6.84	14.12	4.77	10.6	47.26%	0.56%	18.96%	33.22%	11.14	0.0378	0.023	0.361	5.44
302	0.1500	0.00	3.51	7.22	18.21	2.86	14.4	45.80%	0.46%	19.15%	34.59%	9.66	0.0101	0.010	0.366	2.18
303	0.1500	2.00	5.70	9.10	20.34	2.86	14.5	45.28%	0.42%	18.62%	35.68%	8.21	0.0094	0.011	0.512	2.67
304	0.2500	2.00	4.71	8.91	16.31	4.77	9.0	46.86%	0.52%	18.37%	34.25%	9.78	0.0486	0.025	0.444	8.59
305	0.2000	1.00	3.90	8.21	16.71	3.82	9.8	46.49%	0.52%	18.73%	34.26%	10.23	0.0261	0.018	0.487	5.24
351	0.2500	-3.59	-0.99	3.22	10.14	4.77	12.5	47.57%	0.66%	19.98%	31.79%	14.29	0.0220	0.0178	0.287	2.40
352	0.1754	2.00	5.20	9.20	18.72	3.35	10.0	45.84%	0.48%	18.59%	35.09%	9.29	0.0212	0.0153	0.586	5.14
											Stage V norm	1.8	0.19	0.015	3.5	12.8*

Appendix C: Diesel Benchmark Regressions Models

Table C.1 to C.7 show regression models for the first cycle diesel benchmark optimization. Table C.8 to C.14 show the regression models for the second cycle diesel benchmark optimization. Table C.15 to C.22 show the regression models for the third cycle diesel benchmark optimization.

Table C.1: GIE regression model for the first cycle diesel benchmark optimization.

Linear regression

GIE	Coef.	St.Err.	t-value	p-value	[95% Conf	Interval]	Sig
PINLET	.113	.029	3.88	.161	-.257	.482	
SOI	-.01	.003	-3.74	.166	-.043	.023	
SOI2	-.001	0	-5.72	.11	-.002	.001	
Constant	.416	.012	33.69	.019	.259	.572	**

R-squared	0.997	Number of obs	5.000
F-test	118.011	Prob > F	0.068

*** p<.01, ** p<.05, * p<.1

Table C.2: ISNOX regression model for the first cycle diesel benchmark optimization.

Linear regression

ISNOX	Coef.	St.Err.	t-value	p-value	[95% Conf	Interval]	Sig
PINLET	46.148	16.572	2.78	.219	-164.415	256.711	
SOI	-2.323	.306	-7.60	.083	-6.206	1.559	*
PINLET#SOI	5.222	1.482	3.52	.176	-13.611	24.055	
Constant	-.904	3.412	-0.26	.835	-44.262	42.453	

R-squared	0.997	Number of obs	5.000
F-test	103.589	Prob > F	0.072

*** p<.01, ** p<.05, * p<.1

Table C.3: ISUHC regression model for the first cycle diesel benchmark optimization.

Linear regression

ISUHC	Coef.	St.Err.	t-value	p-value	[95% Conf	Interval]	Sig
PINLET	.11	.036	3.03	.094	-.046	.266	*
SOI	0.0001	0	-0.27	.815	-.002	.001	
Constant	-.014	.008	-1.74	.224	-.05	.021	

R-squared	0.822	Number of obs	5.000
F-test	4.624	Prob > F	0.178

*** p<.01, ** p<.05, * p<.1

Table C.4: ISPM regression model for the first cycle diesel benchmark optimization.

Linear regression

ISPM	Coef.	St.Err.	t-value	p-value	[95% Conf	Interval]	Sig
PINLET	.146	.015	9.77	.065	-.044	.336	*
SOI	-.001	0	-2.97	.207	-.004	.003	
PINLET#SOI	.009	.001	6.65	.095	-.008	.026	*
Constant	-.014	.003	-4.42	.142	-.053	.026	

R-squared	0.997	Number of obs	5.000
F-test	107.726	Prob > F	0.071

*** p<.01, ** p<.05, * p<.1

Table C.5: ISCO regression model for the first cycle diesel benchmark optimization.

Linear regression

ISCO	Coef.	St.Err.	t-value	p-value	[95% Conf	Interval]	Sig
PINLET	-1.166	1.201	-0.97	.509	-16.424	14.091	
SOI	.073	.022	3.32	.186	-.208	.355	
PINLET#SOI	-.345	.107	-3.22	.192	-1.71	1.019	

Constant	.522	.247	2.11	.281	-2.619	3.664

R-squared	0.967	Number of obs	5.000
F-test	9.718	Prob > F	0.231

*** p<.01, ** p<.05, * p<.1

Table C.6: ISFORM regression model for the first cycle diesel benchmark optimization.

Linear regression

ISFORM	Coef.	St.Err.	t-value	p-value	[95% Conf	Interval]	Sig
PINLET	13.149	12.691	1.04	.409	-41.455	67.754	
SOI	-.295	.127	-2.32	.146	-.841	.251	
Constant	-3.159	2.894	-1.09	.389	-15.611	9.293	

R-squared	0.764	Number of obs	5.000
F-test	3.233	Prob > F	0.236

*** p<.01, ** p<.05, * p<.1

Table C.7: MPRR regression model for the first cycle diesel benchmark optimization.

Linear regression

MPRR	Coef.	St.Err.	t-value	p-value	[95% Conf	Interval]	Sig
PINLET	113.827	292.043	0.39	.734	-1142.732	1370.385	
SOI	-8.3	2.92	-2.84	.105	-20.866	4.265	
Constant	-57.641	66.596	-0.87	.478	-344.181	228.898	

R-squared	0.804	Number of obs	5.000
F-test	4.115	Prob > F	0.196

*** p<.01, ** p<.05, * p<.1

Table C.8: GIE regression model for the second cycle diesel benchmark optimization.

Linear regression

GIE	Coef.	St.Err.	t-value	p-value	[95% Conf	Interval]	Sig
PINLET	.141	.006	25.38	0	.124	.159	***
SOI	-.004	.001	-3.04	.056	-.008	0	*
SOI2	-0.0005	0	-3.17	.05	-.001	0	*
Constant	.434	.002	181.99	0	.427	.442	***

R-squared	0.995	Number of obs	7.000
F-test	218.228	Prob > F	0.001

*** p<.01, ** p<.05, * p<.1

Table C.9: ISNOX regression model for the second cycle diesel benchmark optimization.

Linear regression

ISNOX	Coef.	St.Err.	t-value	p-value	[95% Conf	Interval]	Sig
PINLET	19.536	1.563	12.50	0	15.197	23.875	***
SOI	-1.014	.046	-22.11	0	-1.141	-.886	***
Constant	6.046	.376	16.07	0	5.002	7.091	***

R-squared	0.994	Number of obs	7.000
F-test	322.542	Prob > F	0.000

*** p<.01, ** p<.05, * p<.1

Table C.10: ISUHC regression model for the second cycle diesel benchmark optimization.

Linear regression

ISUHC	Coef.	St.Err.	t-value	p-value	[95% Conf	Interval]	Sig
PINLET	.105	.017	6.03	.004	.057	.153	***
SOI	.002	.001	2.98	.041	0	.003	**
Constant	-.004	.004	-0.91	.416	-.015	.008	

R-squared	0.919	Number of obs	7.000

F-test	22.629	Prob > F	0.007

*** p<.01, ** p<.05, * p<.1

Table C.11: ISPM regression model for the second cycle diesel benchmark optimization.

Linear regression

ISPM	Coef.	St.Err.	t-value	p-value	[95% Conf	Interval]	Sig
PINLET	.245	.03	8.10	.004	.149	.341	***
SOI	-.003	.001	-2.29	.106	-.007	.001	
PINLET#SOI	.026	.006	4.05	.027	.006	.047	**
Constant	-.027	.006	-4.29	.023	-.046	-.007	**

R-squared	0.985	Number of obs	7.000
F-test	67.673	Prob > F	0.003

*** p<.01, ** p<.05, * p<.1

Table C.12: ISCO regression model for the second cycle diesel benchmark optimization.

Linear regression

ISCO	Coef.	St.Err.	t-value	p-value	[95% Conf	Interval]	Sig
PINLET	.477	.195	2.44	.071	-.065	1.018	*
SOI	.013	.006	2.25	.088	-.003	.029	*
Constant	.235	.047	4.99	.008	.104	.365	***

R-squared	0.734	Number of obs	7.000
F-test	5.516	Prob > F	0.071

*** p<.01, ** p<.05, * p<.1

Table C.13: ISFORM regression model for the second cycle diesel benchmark optimization.

Linear regression

ISFORM	Coef.	St.Err.	t-value	p-value	[95% Conf	Interval]	Sig
PINLET	10.577	4.694	2.25	.087	-2.456	23.61	*
SOI	.291	.138	2.11	.102	-.092	.673	
Constant	.932	1.13	0.82	.456	-2.205	4.069	

R-squared	0.705	Number of obs	7.000
F-test	4.768	Prob > F	0.087

*** p<.01, ** p<.05, * p<.1

Table C.14: MPRR regression model for the second cycle diesel benchmark optimization.

Linear regression

MPRR	Coef.	St.Err.	t-value	p-value	[95% Conf	Interval]	Sig
PINLET	-404.759	97.799	-4.14	.026	-715.998	-93.521	**
SOI	-.682	.135	-5.04	.015	-1.113	-.251	**
PINLET2	906.232	244.225	3.71	.034	128.998	1683.467	**
Constant	54.306	9.354	5.81	.01	24.536	84.076	**

R-squared	0.977	Number of obs	7.000
F-test	42.161	Prob > F	0.006

*** p<.01, ** p<.05, * p<.1

Table C.15: GIE regression model for the third cycle diesel benchmark optimization.

Linear regression

GIE	Coef.	St.Err.	t-value	p-value	[95% Conf	Interval]	Sig
PINLET	.146	.005	27.84	0	.134	.158	***
SOI	-.002	0	-10.46	0	-.002	-.001	***
SOI2	0.0003	0	-6.67	0	0	0	***
Constant	.437	.001	396.96	0	.434	.439	***

R-squared	0.991	Number of obs	12.000
F-test	306.949	Prob > F	0.000

*** p<.01, ** p<.05, * p<.1

Table C.16: ISNOX regression model for the third cycle diesel benchmark optimization.

Linear regression

ISNOX	Coef.	St.Err.	t-value	p-value	[95% Conf	Interval]	Sig
PINLET	17.816	2.096	8.50	0	13.075	22.557	***
SOI	-.872	.033	-26.70	0	-.946	-.798	***
Constant	7.046	.435	16.19	0	6.061	8.031	***

R-squared	0.989	Number of obs	12.000
F-test	392.496	Prob > F	0.000

*** p<.01, ** p<.05, * p<.1

Table C.17: ISUHC regression model for the third cycle diesel benchmark optimization.

Linear regression

ISUHC	Coef.	St.Err.	t-value	p-value	[95% Conf	Interval]	Sig
PINLET	.279	.026	10.95	0	.22	.338	***
SOI	-.005	.001	-3.40	.009	-.008	-.002	***
PINLET#SOI	.038	.007	5.46	.001	.022	.053	***
Constant	-.033	.005	-6.31	0	-.045	-.021	***

R-squared	0.960	Number of obs	12.000
F-test	64.348	Prob > F	0.000

*** p<.01, ** p<.05, * p<.1

Table C.18: ISPM regression model for the third cycle diesel benchmark optimization.

Linear regression

ISPM	Coef.	St.Err.	t-value	p-value	[95% Conf	Interval]	Sig
PINLET	.131	.016	7.94	0	.094	.168	***
SOI	.001	0	4.32	.002	.001	.002	***
Constant	-.009	.003	-2.64	.027	-.017	-.001	**

R-squared	0.901	Number of obs	12.000
F-test	40.881	Prob > F	0.000

*** p<.01, ** p<.05, * p<.1

Table C.20: ISCO regression model for the third cycle diesel benchmark optimization.

Linear regression

ISCO	Coef.	St.Err.	t-value	p-value	[95% Conf	Interval]	Sig
PINLET	.14	.253	0.55	.595	-.443	.724	
SOI	.044	.009	4.94	.001	.023	.064	***
SOI2	.004	.002	1.95	.087	-.001	.008	*
Constant	.355	.053	6.68	0	.233	.478	***

R-squared	0.874	Number of obs	12.000
F-test	18.488	Prob > F	0.001

*** p<.01, ** p<.05, * p<.1

Table C.21: ISFORM regression model for the third cycle diesel benchmark optimization.

Linear regression

ISFORM	Coef.	St.Err.	t-value	p-value	[95% Conf	Interval]	Sig
PINLET	37.566	6.089	6.17	0	23.525	51.607	***
SOI	-.633	.337	-1.88	.097	-1.409	.143	*
PINLET#SOI	5.852	1.639	3.57	.007	2.072	9.631	***
Constant	-3.333	1.248	-2.67	.028	-6.212	-.455	**

R-squared	0.916	Number of obs	12.000
F-test	29.154	Prob > F	0.000

*** p<.01, ** p<.05, * p<.1

Table C.22: MPRR regression model for the third cycle diesel benchmark optimization.

Linear regression

MPRR	Coef.	St.Err.	t-value	p-value	[95% Conf	Interval]	Sig
PINLET	-412.84	66.542	-6.20	0	-566.287	-259.393	***
SOI	-.535	.053	-10.12	0	-.657	-.413	***
PINLET2	922.274	166.141	5.55	.001	539.152	1305.397	***
Constant	55.931	6.348	8.81	0	41.292	70.57	***

R-squared	0.975	Number of obs	12.000
F-test	104.495	Prob > F	0.000

*** *p<.01*, ** *p<.05*, * *p<.1*

Appendix D: Dual Fuel Simulation Results

Table D.1 and table D.2 show the most important results of the methanol-diesel dual fuel simulations. Runs 250, 251, 252 and 351 are control runs for checking the GA optimization results. Runs 253 to 257 are test runs to see what inlet temperatures should be used for the third optimization cycle. Contact the author if there is interest in the source data.

Table D.1: Dual fuel simulation results for run 101 to 257. The green boxes obey the emission limits.

Run	PINLET	SOI	MEF	TINLET	CAD10	CAD50	CAD90	λ	MPRR	GIE	COMBL	HEATL	EXHAUSTL	ISNOX	ISUHC	ISPM	ISCO	ISFORM
	Mpa	CAD ATDC		K	ATDC	ATDC	ATDC		Bar/CAD					g/kWh	g/kWh	g/kWh	g/kWh	mg/kWh
101	0.2	-15	50.0%	400	-7.8	-7.3	-4.9	5.3	77.7	44.67%	2.70%	19.78%	32.85%	15.03	0.625	0.0002	16.4	144.5
102	0.15	-25	25.0%	400	-6.5	-6.0	-5.3	2.6	77.1	40.58%	0.86%	29.77%	28.79%	14.87	0.128	0.0004	2.0	29.3
103	0.25	-25	25.0%	400	-8.4	-7.8	-5.8	4.4	48.2	42.33%	2.79%	25.55%	29.32%	5.47	0.566	0.0016	21.1	117.0
104	0.15	-5	25.0%	400	-1.6	0.2	8.2	2.6	28.3	46.54%	2.26%	18.12%	33.08%	15.66	0.594	0.0016	11.8	96.4
105	0.25	-5	25.0%	400	-2.7	0.1	6.8	4.4	15.9	47.09%	4.41%	16.91%	31.58%	15.62	0.967	0.0095	27.4	189.9
106	0.15	-25	75.0%	400	-3.4	-2.5	-2.1	7.8	71.0	46.41%	0.28%	19.20%	34.10%	4.50	0.010	0.0000	0.5	2.5
107	0.25	-25	75.0%	400	-6.6	-4.8	-1.3	13.1	31.2	50.17%	1.65%	12.71%	35.47%	0.65	0.114	0.0004	11.2	31.6
108	0.15	-5	75.0%	400	-1.7	-1.3	-0.8	7.8	89.1	43.11%	0.60%	26.63%	29.67%	9.51	0.007	0.0000	2.1	2.4
109	0.25	-5	75.0%	400	-3.5	-2.8	2.3	13.1	48.5	49.22%	3.78%	13.07%	33.94%	7.50	0.580	0.0006	24.2	134.7
151	0.25	-3	75.0%	400	-3.5	-1.7	3.9	13.1	24.8	50.41%	3.34%	12.10%	34.16%	6.47	0.479	0.0015	20.9	104.5
201	0.2	-5	30.0%	400	-4.3	-3.0	-1.6	3.8	18.3	48.64%	3.88%	16.41%	31.07%	15.27	0.851	0.0043	22.8	146.9
202	0.28	-5	30.0%	400	-3.0	-0.4	6.0	5.3	17.2	46.81%	5.62%	16.43%	31.14%	14.82	1.081	0.0102	37.0	216.1
203	0.2	-2	30.0%	400	-0.9	1.7	9.3	3.8	23.9	46.99%	4.17%	16.06%	32.78%	13.45	1.038	0.0066	26.0	166.8
204	0.28	-2	30.0%	400	-1.2	2.4	9.2	5.3	15.3	46.60%	5.97%	16.04%	31.39%	12.17	1.320	0.0138	40.0	254.2
205	0.2	-5	60.0%	400	-2.7	-1.8	3.3	6.6	40.6	49.10%	2.45%	14.19%	34.25%	11.30	0.645	0.0008	13.5	141.5
206	0.28	-5	60.0%	400	-3.6	-2.4	3.3	9.2	34.2	46.42%	8.61%	13.44%	31.53%	11.07	1.098	0.0032	61.4	222.5
207	0.2	-2	60.0%	400	-2.4	0.1	6.0	6.6	16.8	49.59%	2.69%	13.51%	34.21%	9.00	0.892	0.0022	15.0	168.8
208	0.28	-2	60.0%	400	-3.6	-0.3	5.6	9.2	15.3	46.65%	9.22%	12.48%	31.65%	9.42	1.137	0.0052	66.0	209.2
209	0.24	-3.5	45.0%	400	-2.4	-0.2	6.6	5.8	19.6	46.98%	6.55%	14.38%	32.09%	12.09	1.149	0.0060	44.4	190.3
350	1.67	-3	75.5%	400	-1.6	-0.4	5.4	3.3	28.7	50.76%	0.46%	12.53%	36.25%	6.66	0.150	0.0003	1.0	29.3
251	0.15	0	75.0%	400	-1.1	0.0	4.1	7.8	32.6	49.94%	0.43%	13.56%	36.06%	7.24	0.137	0.0002	0.7	26.6
252	0.15	1	75.0%	400	-1.1	0.0	5.1	7.8	32.6	50.18%	0.42%	13.08%	36.32%	6.65	0.173	0.0002	0.7	33.1
253	0.15	-3	75.0%	350	2.4	4.9	12.3	3.4	27.1	47.52%	7.91%	8.09%	36.48%	3.74	9.632	0.0003	38.7	1655.8
254	0.25	-4	60.0%	375	-1.6	0.7	5.0	9.9	17.5	46.18%	11.71%	10.11%	32.01%	9.61	2.497	0.0025	83.2	298.2
255	0.25	-2	60.0%	375	0.3	2.2	6.7	9.9	17.2	45.83%	12.40%	9.64%	32.13%	8.64	2.799	0.0030	88.8	323.1
256	0.2	-2	60.0%	390	-0.3	0.9	6.5	6.7	31.1	48.92%	4.77%	12.02%	34.28%	9.44	1.527	0.0016	29.3	193.4
257	0.2	0	30.0%	380	2.8	5.2	12.6	4.0	14.0	47.11%	5.33%	13.41%	34.14%	10.26	1.899	0.0072	34.1	322.2
											Stage V norm			1.8	0.19	0.015	3.5	12.8

Table d.2: Dual fuel simulation results for run 301 to 351. The green boxes obey the emission limits.

Run	PINLET	SOI	MEF	TINLET	CAD10	CAD50	CAD90	λ	MPRR	GIE	COMBL	HEATL	EXHAUSTL	ISNOX	ISUHC	ISPM	ISCO	ISFORM
	Mpa	CAD ATDC		K	ATDC	ATDC	ATDC		Bar/CAD					g/kWh	g/kWh	g/kWh	g/kWh	mg/kWh
301	0.16	-4	30.0%	365	-0.2	1.8	8.7	3.4	20.5	47.62%	4.11%	14.27%	34.00%	11.45	1.609	0.0025	24.7	243.9
302	0.16	-1	60.0%	365	3.0	4.5	8.4	3.5	30.3	47.89%	6.23%	10.39%	35.50%	8.57	2.813	0.0005	38.7	268.3
303	0.22	-4	60.0%	365	-1.2	1.5	5.7	4.8	19.8	46.59%	11.08%	9.37%	32.96%	8.61	3.113	0.0017	76.6	313.1
304	0.22	-1	30.0%	365	1.9	4.7	12.1	4.7	12.1	46.60%	7.48%	12.71%	33.22%	9.86	9.377	0.0105	35.9	2440.4
305	0.16	-4	60.0%	385	-0.4	0.5	3.2	3.3	43.7	48.27%	2.07%	15.61%	34.04%	11.00	1.155	0.0003	10.2	177.7
306	0.16	-1	30.0%	385	2.3	4.2	11.7	3.2	19.6	47.17%	3.56%	14.78%	34.50%	11.01	1.354	0.0031	21.3	188.1
307	0.22	-4	30.0%	385	-1.4	1.2	8.1	4.4	15.3	47.43%	5.14%	14.77%	32.67%	13.27	1.446	0.0072	32.4	243.8
308	0.22	-1	60.0%	385	0.5	1.9	7.4	4.5	28.7	47.26%	8.66%	10.85%	33.22%	8.76	2.077	0.0028	59.1	240.9
309	0.19	-2.5	45.0%	375	0.5	2.5	8.7	4.0	15.8	47.54%	6.51%	12.03%	33.92%	9.92	2.106	0.0030	42.3	250.3
350	0.177	1	25.0%	400	2.0	6.1	14.1	4.5	15.1	46.38%	3.44%	16.39%	33.78%	11.01	1.113	0.0087	21.3	181.1
											Stage V norm			1.8	0.19	0.015	3.5	12.8

Appendix E: Regression models Dual Fuel Optimization

Table E.1 to E.7 show the regression models for the second cycle methanol-diesel dual fuel optimization. The first cycle was optimized without regression models and GA optimization, as the optimization direction was very clear. The third round optimization regression models are discussed in section 5.2.

Table E.1: GIE regression model for the second cycle dual fuel optimization.

Linear regression

GIE	Coef.	St.Err.	t-value	p-value	[95% Conf	Interval]	Sig
PINLET	3.245	.908	3.57	.005	1.222	5.268	***
MEF	.013	.019	0.67	.52	-.03	.055	
PINLET2	-7.231	2.061	-3.51	.006	-11.823	-2.639	***
Constant	.119	.097	1.22	.249	-.097	.334	
R-squared		0.579	Number of obs			14.000	
F-test		4.584	Prob > F			0.029	

*** p<.01, ** p<.05, * p<.1

Table E.2: ISNOX regression model for the second cycle dual fuel optimization.

Linear regression

ISNOX	Coef.	St.Err.	t-value	p-value	[95% Conf	Interval]	Sig
PINLET	-5.706	3.824	-1.49	.167	-14.226	2.814	
SOI	-.636	.127	-5.00	.001	-.919	-.353	***
MEF	-14.161	.867	-16.34	0	-16.092	-12.23	***
Constant	17.381	1.19	14.60	0	14.728	20.033	***
R-squared		0.968	Number of obs			14.000	
F-test		100.480	Prob > F			0.000	

*** p<.01, ** p<.05, * p<.1

Table E.3: ISUHC regression model for the second cycle dual fuel optimization.

Linear regression

ISUHC	Coef.	St.Err.	t-value	p-value	[95% Conf	Interval]	Sig
PINLET	4.603	.968	4.76	.001	2.447	6.759	***
SOI	.077	.032	2.39	.038	.005	.148	**
MEF	-.972	.219	-4.43	.001	-1.461	-.483	***
Constant	.561	.301	1.86	.092	-.11	1.232	*
R-squared		0.845	Number of obs			14.000	
F-test		18.135	Prob > F			0.000	

*** p<.01, ** p<.05, * p<.1

Table E.4: ISPM regression model for the second cycle dual fuel optimization.

Linear regression

ISPM	Coef.	St.Err.	t-value	p-value	[95% Conf	Interval]	Sig
PINLET	.124	.011	11.19	0	.099	.15	***
SOI	.001	0	4.24	.002	0	.001	***
MEF	.021	.005	4.40	.002	.01	.032	***
PINLET#MEF	-.162	.021	-7.60	0	-.21	-.114	***
Constant	-.014	.003	-5.19	.001	-.02	-.008	***
R-squared		0.979	Number of obs			14.000	
F-test		103.487	Prob > F			0.000	

*** p<.01, ** p<.05, * p<.1

Table E.5: ISCO regression model for the second cycle dual fuel optimization.

Linear regression

ISCO	Coef.	St.Err.	t-value	p-value	[95% Conf	Interval]	Sig
PINLET	314.773	74.153	4.24	.002	149.549	479.997	***
SOI	1.381	2.464	0.56	.588	-4.109	6.87	
MEF	-7.984	16.809	-0.48	.645	-45.437	29.469	
Constant	-33.447	23.085	-1.45	.178	-84.882	17.989	
R-squared		0.673	Number of obs			14.000	
F-test		6.873	Prob > F			0.009	

*** *p<.01, ** p<.05, * p<.1*

Table E.6: ISFORM regression model for the second cycle dual fuel optimization.

Linear regression

ISFORM	Coef.	St.Err.	t-value	p-value	[95% Conf	Interval]	Sig
PINLET	947.735	106.164	8.93	0	707.575	1187.896	***
SOI	4.262	3.595	1.19	.266	-3.869	12.394	
MEF	773.31	212.239	3.64	.005	293.193	1253.428	***
MEF2	-922.636	212.949	-4.33	.002	-1404.359	-440.913	***
Constant	-164.594	53.911	-3.05	.014	-286.548	-42.639	**
R-squared		0.952	Number of obs			14.000	
F-test		44.963	Prob > F			0.000	

*** *p<.01, ** p<.05, * p<.1*

Table E.7: GIE regression model for the second cycle dual fuel optimization.

Linear regression

MPRR	Coef.	St.Err.	t-value	p-value	[95% Conf	Interval]	Sig
PINLET	-172.913	52.23	-3.31	.009	-291.065	-54.76	***
SOI	10.823	4.819	2.25	.051	-.078	21.724	*
MEF	-82.044	41.766	-1.96	.081	-176.526	12.438	*
SOI#MEF	-33.987	9.618	-3.53	.006	-55.744	-12.229	***
Constant	86.598	24.316	3.56	.006	31.59	141.605	***
R-squared		0.877	Number of obs			14.000	
F-test		16.067	Prob > F			0.000	

*** *p<.01, ** p<.05, * p<.1*

Appendix F: Overview Fuel Costs Sources

Figure 6.5 in section 6.3.5 is based on the minimum and maximum prices of tables F.1 to F.11. All fuels are calculated back to €/GJ using an exchange rate of 1.20 US$/€.

Table F.1: Expected E-fuel prices (Brynolf, Taljegard, Grahn, & Hansson, 2018)

	Min €/GJ	Max €/GJ
e-LNG	27.8	80.6
e-methanol	27.8	72.2
e-diesel	30.6	94.4

Table F.2: Expected E-fuel production costs (Grahn, 2020)

	€/GJ	
Fossil fuels	11.1	38.9
Bio methane	11.1	50.0
Biomethanol	22.2	33.3
Biodiesel	13.9	58.3

Table F.3: Biomethanol price (Maritiem Kennis Centrum et al., 2018)

	€/ton	€/GJ
Biomethanol	1100	51.88679

Table F.4: Biofuel and natural gas prices (Khandelwal, M., van Dril, 2020)

	Min €/GJ	Min €/GJ
Biodiesel	18.3	22.5
Biomethanol	12.5	20.8
Natural gas	3.9	

Table F.5: E-fuel prices (Tremel, Wasserscheid, Baldauf, & Hammer, 2015)

	€/kWh	€/GJ
E-methanol	0.175	48.61
E-diesel	0.195	54.17
E-methane	0.169	46.94

Table F.6: Fossil fuel prices and biofuel production costs (E4tech, 2018)

	€/GJ	Min €/GJ	Max €/GJ
Price	LNG	5	6
	EN590	10	18
Production costs	Biodiesel	14	29
	Biomethanol	16	25
	Bio-LNG	12	35

Table F.7: Prices fossil, bio and E-methanol (Zomer et al., 2020)

	Min €/GJ	Max €/GJ
Grey Methanol	9	22
Biomethanol	11	33
E-methanol	27	68

Table F.8: Prices fossil and biofuels (Verbeek et al., 2020)

Fuel	Min €/GJ	Max €/GJ
MGO	9.6	19.2
Biodiesel	14	39
Fossil LNG	9.2	12.9
BioLNG	11.6	35
Fossil Methanol	13.6	19
BioMethanol	15	25

Table F.9: E-fuel prices (TNO, 2020)

Fuel	Min €/GJ	Max €/GJ
E-H2	10	22
E-methanol	18	52
E-LNG	17	41
E-diesel	20	48

Table F.10: Fossil and biohydrogen prices (Giers, Jaworska, & Ludmiła, 2020)

	Min €/GJ	Max €/GJ
Grey hydrogen	13.17	16.08
Green hydrogen	31.17	38.08

Table F.11: Biohydrogen prices (Shahabuddin, Krishna, Bhaskar, & Perkins, 2020)

	Min €/GJ	Max €/GJ
Biomass based hydrogen	15.97	33.33

Appendix G: Overview Drivetrain Costs Sources

Table 6.4 in section 6.3.6 is based on tables G.1 to G.8. To convert prices an exchange rate of 1.20 US$/€ is used.

Table G.1: Aftertreatment costs according to CE Delft (2011)

	Min €/kW	Max €/kW	Installation costs
SCR	20	65	50k
DPF	40	110	
Total 750 kW engine	126.67	241.67	

Table G.2: Aftertreatment costs according to DST (2019)

	€/kW	Installation costs
SCR + DPF	100	45k
Total 750 kW engine	160	

Table G.3: Engine and fuel storage prices (Horvath et al., 2018).

	Engine [€/kW]	Storage [€/kWh]
MGO ICE	538	0.083
MeOH ICE	554	0.139
LNG ICE	781	0.305
H2 ICE	781	0.831
MGO FC	2650	0.083
LNG FC	2650	0.139
MeOH FC	2650	0.305
H2 FC	1692	0.831

Table G.4: Engine retrofit costs for alternative fuels (K. Andersson & Salazar, 2015)

Retrofit	€/kW
Methanol	250
LNG	1000

Table G.5: Engine costs and engine retrofit costs (E4tech, 2018)

	€/kW
Retrofit	
Retrofit Methanol	350
New Methanol	270
New LNG	2-3x Methanol engine costs

Table G.6: Engine costs and engine retrofit costs (Ellis & Tanneberger, 2015)

	€/kW
Retrofit Methanol	326.67
Retrofit LNG	553.33
New Methanol	679.17
New LNG	1062.50

Table G.7: Engine costs (TNO, 2020)

	Engine costs €/kW
MGO	636
Methanol	655
LNG	923
H2	2000

Table G.8: Engine costs and storage costs (Verbeek et al., 2020)

	Engine costs €/kW	Storage €/GJ
MGO	636	27
Methanol	655	45
LNG	923	100